Clay linked Gels

Mechanical Enhancement of Hydrogels by Incorporation of Clay Minerals

Dissertation

zur Erlangung des akademischen Grades

Doktor der Naturwissenschaften – Dr. rer. nat.

an der Fakultät für Biologie, Chemie und Geowissenschaften der Universität Bayreuth

vorgelegt von

Manuela Stirner

aus Passau

Bayreuth, 2014

Die vorliegende Arbeit wurde n der Zeit von Oktober 2009 bis August 2013 in Bayreuth am Lehrstuhl für Anorganische Chemie I unter Betreuung von Herrn Professor Dr. Josef Breu angefertigt.

Vollständiger Abdruck der von der Fakultät für Biologie, Chemie und Geowissenschaften der Universität Bayreuth genehmigten Dissertation zur Erlangung des akademischen Grades eines Doktors der Naturwissenschaften (Dr. rer. nat.).

Dissertation eingereicht am: 01.04.2014

Zulassung durch die Promotionskommission: 30.04.2014

Wissenschaftliches Kolloquium: 01.07.2014

Amtierender Dekan: Prof. Dr. Rhett Kempe

Prüfungsausschuss:

Prof. Dr. Josef Breu (Erstgutachter)

Prof. Dr. Axel Müller (Zweitgutachter)

Prof. Dr. Jürgen Senker (Vorsitz)

Prof. Dr. Matthias Karg

“An investment in knowledge pays the best interest.”

Benjamin Franklin

To my parents Christine and Franz

Summary

Superabsorbent polymers are found in numerous industrial applications due to their outstanding swelling ability for water. Besides swelling capacity, the performance of absorbent gel materials (AGM) is critically determined by the gel strength in the swollen state. If the gel strength of the hydrogel is low, it is easily deformable, which allows the occurrence of gel blocking. Gel blocking hampers homogeneous swelling of the AGM and limits the effective total capacity. The primarily swollen particles gain volume upon swelling and built up a sealing layer that avoids wetting of the lower AGM layers. For application of AGM in hygiene products it is therefore highly desirable to minimize gel blocking while not sacrificing any swelling capacity. In order to strengthen AGM particles, either the gel strength of the bulk polymer may be improved or the surface of AGM particles may be stiffened by additional crosslinking, which results in core – shell particles.

This work explores the incorporation of stiff inorganic fillers - clay minerals - into the AGM matrix in order to improve the gel strength of bulk AGM or Young's -modulus of surface shells of AGM particles. Enhancement of the gel strength and Young's -modulus is thus achieved by designing AGM composites. The high ionic strength in combination with low pH of the partially neutralized acrylic acid mixtures used to polymerize AGM represents the major obstacle on the way to such AGM composites. Clays tend to agglomerate in such environments and resulting agglomerates might even weaken the gels. In order to exploit the full potential of clay minerals as fillers in AGM matrices it is essential to first disperse the clay platelets homogeneously in the suspension of the partially neutralized monomers.

We were able to obtain stable suspensions of clay minerals by modifying them with a commercial cationic dentrimer, ODD. ODD carries an ethylene glycol brush on a poly (ethylene imine) core and is electrostatically bound to the clay surface by intrinsic protonation. A successful dispersion of modified clays allowed to explore the influence of critical parameters like the aspect ratio of the clay platelets on the mechanical performance of the AGM composites by comparing synthetic lithium hectorite (aspect ratio ≈ 10000) and montmorillonite PGV® (aspect ratio ≈ 30).

While the hydrogels could be reinforced by incorporating the different fillers, the tradeoff between swelling capacity and gel strength of the AGM in fully swollen state could be improved only with montmorillonite PGV®, however not with lithium hectorite. Interestingly, for the high aspect ratio lithium hectorite a crossing of the trade off curve could be observed with better performance of the AGM at low swelling (< 5.5 g/g), whereas the PGV® AGM composites showed superior properties at any swelling degree compared to the reference.

With the core – shell approach high swelling capacity and high gel strength are spatially separated. While the core of the particle provides the high swelling ability, the shell will grant pressure resistance of shape reducing gel blocking. To optimize this concept, mechanical strengthening of the shell has to be achieved while preserving maximum flexibility expressed by a high stress at break beyond certain threshold values for strain (> 400 %) and Young's -modulus (> 100 kPa). Moreover, core and shell have to be kept chemically compatible. We considered commercial bulk AGM for the core, while the shell should be built up by an AGM composite material incorporating different clay minerals as filler. The type of clay, the filler content, the amount of organic crosslinker, the acrylic acid content, and the degree of neutralization were varied to optimize the mechanical properties of the composite shells. For the large aspect ratio lithium hectorite both strain at break and Young's -modulus were found to be below the threshold values. For composites of modified montmorillonite PGV®, however, a significant improvement in performance of the shells could be achieved. For the best composite shells 800 % strain at break in combination with 600 kPa stress at break and a Young's -modulus of 140 kPA were observed.

Zusammenfassung

Superabsorbierende Polymere finden auf Grund ihrer herausragenden Quellfähigkeit in zahlreichen industriellen Produkten Anwendung. Neben der Quellfähigkeit ist die Effizienz absorbierender Gel – Materialien (AGM) entscheidend von der Stärke des Gels im vollständig gequollenen Zustand abhängig. Ist die Gelstärke gering, ist das Hydrogel leicht verformbar, was das Auftreten von „gel blocking“ ermöglicht. Gel blocking verhindert ein homogenes Quellen des AGM und beschränkt dessen effektive maximale Kapazität. Die zuerst gequollenen Partikel gewinnen während des Quellens an Volumen und bilden eine versiegelnde Schicht aus, welche das Durchnässen der unteren AGM Schichten verhindert. Für die Anwendung von AGM in Hygieneartikeln ist es deshalb höchst erstrebenswert den gel blocking Effekt zu minimieren ohne dabei an Quellkapazität einzubüßen. Um AGM zu verstärken kann entweder die Stärke des bulk Polymers verbessert werden oder die Oberfläche der AGM Partikel durch zusätzliche Quervernetzung versteift werden woraus Kern – Schale Partikel resultieren.

Diese Arbeit erforscht die Einlagerung steifer anorganischer Füllstoffe – Schichtsilicate – in die AGM Matrix, um die Gelstärke bulk AGM oder den Youngschen -Modul von oberflächlichen Schalen von AGM Partikeln zu verbessern. Eine Erhöhung der Gelstärke und des Youngschen -Moduls wird also durch das Design von AGM Kompositen erreicht. Die hohe Ionenstärke in Kombination mit dem niedrigen pH Wert der teil-neutralisierten Acrylsäuremischungen, welche zur Polymerisation von AGM verwendet werden, stellen das größte Hindernis auf dem Weg zu solchen AGM Kompositen dar. Schichtsilicate tendieren unter derartigen Umständen dazu, zu agglomerieren und resultierende Agglomerate könnten das Gel sogar schwächen. Um das volle Potential von Schichtsilicaten als Füllstoff in AGM Matrizen ausnutzen zu können, ist es essenziell die Schichtsilicat Plättchen zunächst homogen in der Suspension von teil-neutralisierten Monomeren zu dispergieren.

Wir waren in der Lage stabile Suspensionen von Schichtsilicaten zu erhalten, indem diese mit einem kommerziellen kationischen Dentrimer, ODD, modifiziert wurden. ODD weist eine Ethylenglykol Bürste gebunden an einen Polyethylenimin – Kern auf und wird elektrostatisch an die Schichtsilicat Oberfläche durch intrinsische Protonierung gebunden. Das erfolgreiche Dispergieren der modifizierten Schichtsilicate ermöglichte eine

Untersuchung des Einflusses von kritischen Parametern wie des Aspektverhältnisses auf das mechanische Verhalten der AGM Komposite, wobei der synthetische Lithium Hectorit (Aspektverhältnis ≈ 10000) mit Montmorillonite PGV® (Aspektverhältnis ≈ 30) verglichen wurde.

Während die Hydrogele durch die Einlagerung der verschiedenen Füllstoffe verstärkt werden konnten, konnte der Tradeoff aus Quellkapazität und Gelstärke des AGM im vollständig gequollenen Zustand nur mit Montmorillonit PGV® verbessert werden, jedoch nicht mit Lithium Hectorit . Interessanterweise wurde für den Lithium Hectorit mit hohem Aspektverhältnis ein Überkreuzen der Tradeoff Kurve beobachtet, wobei nur bei einem geringem Quellgrad (< 5.5 g/g) des AGM eine Verbesserung erreicht wurde. Dahingegen zeigte das PGV® AGM Komposit bei jedem Quellgrad bessere Eigenschaften im Vergleich zur Referenz.

Durch den Kern – Schale Ansatz werden hohe Quellkapazität und hohe Gelstärke räumlich voneinander getrennt. Während der Kern des Partikels die hohe Quellkapazität bereitstellt, garantiert die Schale mechanische Stärke welche das gel blocking reduziert. Um dieses Konzept zu optimieren muss eine mechanische Verstärkung der Schale erreicht werden, wobei eine maximale Flexibilität erhalten bleiben soll, was durch eine hohe Reißspannung oberhalb bestimmter Grenzwerte für Dehnung (> 400%) und Youngscher -Modul (> 100 kPa) wiedergegeben wird. Außerdem müssen Kern und Schale chemisch kompatibel sein. Wir haben kommerzielles bulk AGM für den Kern in Betracht gezogen, während die Schale aus einem AGM Komposit, welches verschiedene Schichtsilicate als Füllstoff enthielt, aufgebaut werden sollte. Die Art des Schichtsilicats, der Schichtsilicat Gehalt, die Menge an organischem Quervernetzer, der Acrylsäuregehalt und der Neutralisationsgrad wurden variiert um die mechanischen Eigenschaften der Komposit Schalen zu optimieren. Für Lithium Hectorite mit hohem Aspektverhältnis lagen sowohl die Reißdehnung als auch der Youngsche-Modul unter den Grenzwerten. Für Komposite des modifizierten Montmorillonite PGV® jedoch konnte eine signifikante Verbesserung des Verhaltens der Schale erreicht werden. Für die besten Komposit Schalen wurden 800 % Reißdehnung in Kombination mit 600 kPa Reißspannung und einem Youngschen -Modul von 140 kPa beobachtet.

Contents

List of abbreviations:

AA	Acrylic acid
AGM	Absorbent gel material
AllylODD	Modifier ODD functionalized with Allyl glycidyl ether
DN	Degree of neutralization
EDTA	Ethylene diamine tetra acetate
KPS	Potassium persulfate
LiHec	Nanocomposite containing lithium hectorite
MBAA	Methylene bis acrylamide
PDADMAC	Poly diallyldimethylammoniumchloride
PGV	Nanocomposite containing montmorillonite PGV®
PXRD	Powder X-ray diffraction
PZC	Point of zero charge
PZNPC	Point of zero net proton charge
PZSE	Point of zero salt effect
Ref	Reference sample
rpm	Revolutions per minute
SAP	Super absorbent polymer
TEMED	Tetra methyl ethylene diamine
VLRH	Very low rubber hardness

1 Introduction

1.1 Hydrogels

1.1.1 Definition

Hydrogels are hydrophilic polymer networks. The crosslinked polymer chains are natural or synthetic polymers, which, due to their hydrophilic nature, swell in water without dissolving. Upon swelling, the polymer network maintains its three-dimensional structure and retains a significant fraction of water within its structure. For superabsorbent materials, the absorption of water can reach more than thousand times of the dry material's weight.

Hydrogels may be classified regarding the type of hydrophilic group which is responsible for the swelling behavior. Consequently hydrogels can be divided into five groups:

- Non-ionic
- Cationic
- Anionic
- Amphoteric (anionic and cationic monomers)
- Zwitterionic (monomers have both anionic and cationic groups)

The swelling behavior of absorbent materials is judged regarding swelling in water and in saline or other salt solutions. Non-ionic polymers do not show any difference in their swelling behavior in water or salt solutions. The driving force for swelling in this case is dipolar interactions. In all other cases, where the polymer carries ionic subunits, swelling is driven by osmotic pressure. Amphoteric and zwitterionic hydrogels exhibit a higher absorption for salt solutions than for pure water. Additional water is included into the gel structure by hydration of the free counterions which are associated to the charged polymer. The free counterions also induce ionic repulsion. Consequently anionic and cationic hydrogels swell more in pure water, whereas in salt solutions the polymer chains are partially collapsed. Out of these five different groups of hydrogels only non-ionic and

anionic polymers are used in commercial applications due to monomer availability and more important due to their performance.[1]

1.1.2 Commercial applications of hydrogels

Hydrogels attract commercial attention in several fields of applications. Many applications for hydrogels can be found in the area of biomedicine as they can be polymerized under mild conditions, for example via photopolymerization, and as they are biodegradable. Furthermore, hydrogels are sensitive towards external stimuli and show response to their environment. The response mechanism is based on the chemical structure of the polymer. In biomedical applications, the response to pH, temperature, and ionic composition are of most importance.[2] The stimuli-responsive changes in the structural network of the hydrogels make them suitable as drug-delivery systems.[3-5] Furthermore, the mechanical properties of hydrogels, in particular the elastic modulus and the deformability, can be tailored to address the specific field of utilization. Gong et al. synthesized very strong hydrogels with double network structures in order to serve as articular cartilage.[6] Additional to the physical properties, also mass transport properties and biological interaction requirements are to be considered if hydrogels are chosen to provide a scaffold as space filling material or in tissue engineering, like bone tissue engineering or muscle growth.[7-9] Besides biomedical applications, environmentally responsive hydrogels are used as pumps and valves, for example in microfluidic channels which can be regulated by swelling and deswelling of pH responsive hydrogels.[10] The response to external stimuli can furthermore be utilized to construct sensors, for instance pH or ionic strength sensors or chemical sensors.[11,12] Hydrogels are also used for metal particle preparation and in miniature biofuel cells.[13,14]

In addition to the mentioned more academic examples, large quantities of hydrogels also find use in applications where the stimuli-response plays a minor role. In agriculture and in hygiene products such as disposable diapers the high water or saline absorption and the ability of retaining the liquid are the features that attract attention to (superabsorbent) hydrogels. In agriculture hydrogels are used for water storage to slow down wilting of plants and for controlled release of fertilizer or pesticides.[15]

1.2 Hydrogel nanocomposites

In the last decades, nanocomposites of polymers have gained more and more importance also in industrial applications. By incorporating inorganic materials into polymer matrices, the polymer's chemical properties are retained to a good deal while at the same time remarkable improvements in physical properties can be obtained. Consequently, nanocomposites of hydrogels have also been explored and numerous applications are reported in several fields of applications, conserving the hydrogels' outstanding stimuli responsive behavior and combining it with additional features. As mentioned above, the use of hydrogels is widespread in biomedicine. Electro-sensitive hydrogels used for drug delivery show material fatigue after several on- off switching cycles. The fatigue problem can be overcome by incorporating clay nanoparticles into the hydrogel.[16] Besides for drugs, hydrogels can also serve as scaffold for metal particles. For instance, silver nanoparticles, which display antimicrobial activity and show poor binding characteristics with surfaces, can be embedded in hydrogel networks. The resulting nanocomposite opens new doors towards antibacterial applications.[17] Silica containing nanocomposite hydrogels are used as intra-ocular lenses.[18] Hydrogel nanocomposites also occur in several health care products, such as wound dressings. In this case clay minerals are used in order to strengthen the hydrogel and make it more elastic.[19] Another example for metal containing hydrogel nanocomposites can be found in microfluidic valves. Particles with distinct and strong optical absorption profiles, e.g. gold particles, are entrapped in the hydrogel and allow external control of swelling behavior and hence valve operation with light of specific wavelength as stimulus.[20] Further fields of applications of nanocomposite hydrogels are dye adsorption and catalysis.[21,22]

1.3 Superabsorbent polymers (SAP)

A superabsorbent polymer per definition is a hydrogel that in dry state is able to take up 10 times or more of a fluid as compared to its own weight. While taking up the liquid and increasing its volume the hydrogel retains its original form. Due to their excellent swelling ability SAP are applied in agriculture and horticulture and in healthcare products like disposable diapers and napkins.[1,23]

SAP can be distinguished between natural SAP and synthetic SAP. Natural SAP can be based on polysaccharides like chitin, cellulose, starch and natural gums. These polysaccharides can be transformed into SAP either by graft copolymerization with suitable vinyl monomers in the presence of a crosslinker or by direct crosslinking. Furthermore, there are poly (amino acid) based natural SAP. These SAP contain polypeptides as main part of their structure which are obtained from soybeans or fish.[24] Examples for synthetic SAP are poly (acryl amide), poly (ethylene oxide), poly (acrylo nitrile), or poly (2-hydroxyethyl methacrylate). The most established synthetic SAP are poly acrylates, especially poly (acrylic acid). Poly (acrylic acid) hydrogels can reach a maximum swelling of more than 99 wt% water.[25] In industrial environment SAP are often referred to as absorbent gel material (AGM). This synonym is used in the remaining part of this thesis.

1.3.1 Defining the performance of AGM

As pointed out above, AGM are of importance in industrial applications due to their excellent swelling properties. To be more precise, the performance of AGM encompasses three aspects to be considered:

- Swelling capacity
- Absorption rate
- Gel bed permeability and gel strength of the swollen gel

In other words, AGM have to be able to take up high amounts of liquids in a reasonable timeframe and retain this liquid without being easily deformed. Low deformability and hence high gel strength of the swollen AGM is necessary to preserve high gel bed permeability.

In an ideal hydrogel, the crosslinking points would be homogenously distributed and the gel strength of the gel would increase with the number of crosslinking points. Given constant osmotic pressure, the maximum capacity would be determined by fully stretched chains between the crosslinking points and would linearly decrease with the number of crosslinking points. To optimize capacity, soft gels would be the choice.

In health care products and in agricultural applications, the gel strength should, however, be high enough to avoid major deformation or even mashing of the hydrogel.[26] In order

to exploit the full capacity of the AGM, high gel bed permeability is desirable and the so called “gel blocking” has to be avoided. Therefore, a minimum pressure resistance of shape represented by the gel strength is required.

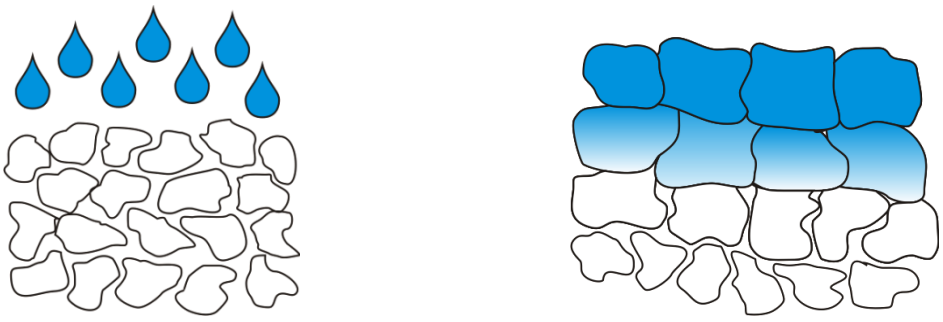

Fig. 1. Schematic description of the gel blocking process

When the liquid reaches the AGM grains, the dry particles start to swell. Upon swelling, the AGM particles grow in size. Gel bed permeability depends on the pores and interconnecting channels in between the swollen AGM particles, which means on the gel’s wet porosity.[27] The softer the swollen material, the more easily the gaps and channels in between the swollen grains (wet porosity) will be closed if pressure is applied, e.g. by a baby’s weight. A dense swollen AGM layer is built up (i.e. wet porosity drops drastically) and blocks further influx of more liquid (Fig. 1, right). The adjacent layers of dry AGM cannot be reached by the liquid directly anymore, but can only be swollen via transfer of the liquid from swollen particle to dry particle. Swelling of the lower layers of AGM then is a diffusion controlled process. A gradient of highly swollen particles, which form the sealing layer, to barely or even non-swollen particles in the lower layers is developed. This gradient persists if the liquid supply is stopped before the fully swollen state for all AGM particles is reached.[28]

In health care products gel blocking is thus highly undesired. High efficiency of the AGM grains is only achieved if the extraordinary swelling capacity of all AGM grains present can be fully exploited. Therefore, the incoming liquid needs to reach all dry particles without hindrance in order to achieve complete uptake of the liquid in the fastest way. Fast liquid uptake is only possible if all AGM particles can be reached by the liquid quickly and diffusion controlled swelling can be avoided.

Consequently, for the performance of specific AGM not only the swelling capacity but also the gel strength is essential. Crosslinking levels must be chosen that show a reduced capacity in order to provide a threshold gel strength (Fig. 2).

The mechanical properties of AGM critically depend on the structure of the polymer, in particular on the number and the distribution of crosslinking points in the network, which are determined by the chosen method for crosslinking. Especially the distribution is influenced by the method of polymerization.

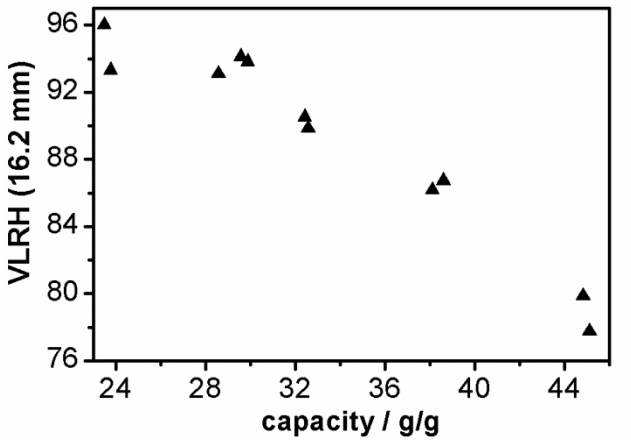

Fig. 2. Trade off line of partially neutralized poly (acrylic acid) AGM with varying number of crosslinking points

The gel strength in Fig. 2 is reflected by the values derived from VLRH measurements. Details about the method and the determination of the maximum swelling capacity are given in section 3.4. The number of crosslinking points has been systematically varied by increasing concentrations of crosslinker while keeping all other reaction conditions constant during polymerization. The dependency of gel strength and capacity on the crosslinking level is clearly visible. High crosslinker amounts cause high gel strength. However, the maximum swelling capacity of the hydrogel is comparably low. With decreasing crosslinking level, the gel strength of the AGM decreases, while at the same time the maximum swelling increases. In order to further enhance the properties of the hydrogel and surpass the trade off line resulting from the variation of crosslinker content, one has to influence and change the structure of the polymer network.

Various methods for crosslinking were explored that influence the distribution of crosslinking points. Irradiation of a polymer chain leads to excitation and radical formation whereupon a crosslinked structure develops.[29] Another and more common possibility of network formation is via chemical reaction. The polymer network is formed through free radical crosslinking polymerization. The free radical polymerization can either be done in solution or in inverse suspension. Inverse suspension polymerization allows easier handling of the gel product. Furthermore, heat removal from the exothermic

polymerization process is more efficient and the particle size of the product is easier definable and more homogeneous compared to solution polymerization. Drawbacks however are the higher complexity of the process and the additional ingredients which need to be recycled.

Free radical crosslinking polymerization offers several options to tune the final polymer structure and consequently the polymers properties. Important polymerization variables are: [30]

- Monomer type and concentration
- Crosslinker type and concentration
- Initiator type and concentration
- Polymerization temperature
- Specific solvent

Chen and Zhao give an overview how the above mentioned polymerization conditions influence the structure of the polymer and hence the polymer´s properties for the example of a poly acrylate superabsorbent and its water absorbency.[31] Increasing the monomer concentration results in an increase of the kinetic chain length and an increase of the crosslinking efficiency. A denser polymer network is obtained, which is less swellable and the water absorbency decreases. A reduction of the water absorbency is also obtained with increasing crosslinker concentration. An increase of the initiator concentration causes an increase of the water absorbency. The network gets less homogenous and contains more chain ends, which have higher swelling ratios. This effect also appears if the polymerization temperature is increased. Increasing the reaction temperature decreases the half life time of the initiator. The number of free radicals per time is increased and hence the consequence is comparable to an increase of the initiator amount.

Free radical crosslinking polymerizations lead to inhomogeneous gel structures. This is due to the fact that the crosslinker exhibits at least two functional groups and hence the reactivity of the crosslinker is higher than the one of the monomers. As a consequence, the crosslinker molecules are incorporated into the growing polymer chains more rapidly than the monomer molecules so that the final network exhibits a crosslinking density distribution with higher crosslinked regions formed in early stages of the polymerization and less crosslinked regions formed in later stages of the polymerization.[32] At the

beginning of the polymerization, when conversion rates are low, a considerable part of the crosslinker has already reacted at both double bonds. Furthermore, a strong tendency towards cyclization relative to intermolecular crosslinking is found at early stages of the polymerization. As at the beginning of the polymerization only few polymer chains are found in the monomer mixture, the probability of a free radical at the end of one growing chain to meet a double bond of another chain and hence intermolecular crosslinking is low.[33]

The gel strength however is a bulk value averaged over the total gel volume. The gel includes areas of high crosslinking resulting in high gel strength and low swelling capacity and areas of low crosslinking resulting in low gel strength and high swelling capacity. In volumes with low crosslinking density the gel strength is still below what is needed to minimize gel blocking. Moreover, the heterogeneities in crosslinking density hamper the effective swelling capacity. Consequently, the experimentally measured trade off line (Fig. 2) between capacity and gel strength is below what could be expected for an ideal homogenous network. Factors influencing the quality of a polymer network are discussed in the next section.

1.3.2 Enhancing the performance of AGM – Optimizing gel strength without sacrificing swelling capacity

In order to enhance the performance of AGM, higher gel strength needs to be achieved without reducing the maximum swelling capacity. The objective of this thesis was to achieve this goal for an AGM based on poly (acrylic acid) by applying platy clay fillers. The fillers are envisaged to improve the performance of hydrogels by several mechanisms:

- Homogenization of the polymer network
- Incorporation of stiff, reinforcing fillers
- Attachment of a composite shell with high mechanical strength

1.3.2.1 Homogenization of the polymer network

As mentioned, optimum swelling ability and gel strength are found in an ideal network where all crosslinking points are uniformly distributed and no irregularities occur. The

hydrogel in this case is able to swell uniformly in every dimension until every single polymer chain in between two crosslinking points is maximally stressed (Fig. 3, I).

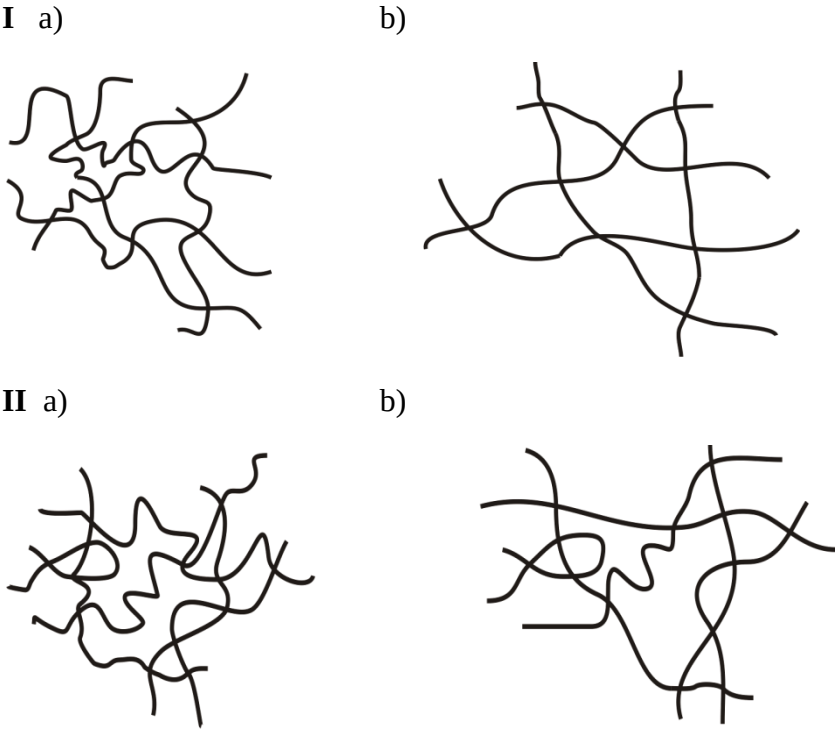

Fig. 3. Hydrogel polymer network:
I) homogeneous distribution of crosslinking points, a) non-swollen, b) fully swollen
II) inhomogeneous distribution of crosslinking points, a) non-swollen b) fully swollen

If, however, the polymer network is not ideal, the length of the polymer chains between two crosslink points varies. Consequently, some polymer chains within the network are still coiled also in fully swollen state and not stretched (Fig. 3, II b)). Furthermore, inhomogeneously polymerized polymer networks contain irregularities like loops, entanglements, loose chain ends (dangling chains), or linear non-crosslinked and hence extractable polymer chains. These irregularities restrict the maximum swelling capacity and a part of the network's swelling potential is lost. Also the optimum mechanical performance of the hydrogel is not reached, as stress in not transferred to the whole polymer network. The spatial inhomogeneities of the hydrogel are depending on the crosslinking density and increase with increasing crosslinker amount, as the extent of network imperfections, which means regions of high or low concentration of crosslinking points, increase.[34]

Consequently, swelling ability as well as mechanical properties of the AGM can be improved by homogenizing the polymer network.

Haraguchi et al. prepared AGM composites consisting of poly (*N*-isopropyl acrylamide) and Laponite® XLG. They observed a stabilizing effect of the *N*-isopropyl acrylamide monomer on a Laponite® dispersion and conclude that the monomers surround the clay platelets.[35,36] Furthermore, they show that initiation of the polymerization occurs only at the clay surface and all resulting polymer chains are attached to clay surfaces by ionic or polar interactions. The clay platelet thus acts as multifunctional crosslinking agent with a much smaller number of crosslinking points than comparable AGM with the same quantity of an organic crosslinker. Moreover, these crosslinking points are homogeneously distributed with only few structural inhomogeneities. The chain length in between the crosslinking points is equal throughout the AGM composite and large in comparison to organically crosslinked gels, which leads to higher deformability of the sample.[35,37]

1.3.2.2 Reinforcement by stiff fillers with high aspect ratio

The incorporation of filler material into AGM was studied intensively in the past years. Fillers of different geometries, like spherical nanoparticles, fibers or platelets were integrated into divers AGM systems in order to strengthen the material or improve the liquid uptake. As an example for spherical nanoparticles incorporated into AGM, metal nanoparticles or zeolithes can be mentioned.[38,39] Imogolite fibers were used by Shikinaka et al. to enhance the properties of their poly (acyl amide) AGM.[40] Among the platelet shaped fillers used for the enhancement of AGM qualities, clay minerals of different kinds are widely spread. Natural AGM as well as synthetic AGM were used for the synthesis of nanocomposites including clay minerals like mica, kaolin, attapulgite, and montmorillonite.[41-45] However, the studies on the mentioned AGM composites incorporating clay minerals mainly focused on swelling capacity. The quality of the dispersion of the clay minerals used as fillers was not further investigated and discussed. The quality of the dispersion of the clay mineral and a homogenous distribution is a key factor on the way to improving AGM's swelling properties and gel strength. Therefore, enhancement of both swelling capacity and gel strength can be expected when addressing the optimization of the clay dispersion in the polymer matrix.

The focus of this work was set on clay minerals as filler material, as they feature high moduli and much higher aspect ratios as compared to fibers or spherical particles.[46]

Reinforcement of a rubbery matrix by incorporation of fillers was already described in 1944 by Smallwood.[47] Smallwood characterizes the implementation of a rigid spherical particle into a rubbery matrix. The composites exhibit complete adhesion between filler and matrix. The volume loading of the filler is low and spherical particles are completely dispersed. The mentioned conditions lead to the Einstein – Smallwood equation:

$$E = E_m\,(1 + 2.5\,\Phi) \qquad (1)$$

E is the modulus of the composite; E_m is the modulus of the rubbery matrix and Φ is the volume fraction of the filler. The constant of 2.5 is derived from the spherical shape of the filler particles. The enforcement is only depending on the shape of the filler and its volume fraction, whereas the filler size is not of importance in this idealized case. In real systems, none of the made assumptions is perfectly fulfilled, for which reason many authors generalized and expanded the equation.

Rao and Pochan described the molecular mechanics of the reinforcing effect with the help of the Mooney's theory.[48] Originally, Mooney's theory studied the influence of spherical particles on the viscosity of a concentrated colloidal fluid. It can be expanded to polymer matrices and non-spherical fillers. In case the modulus of the filler is much higher than the modulus of the matrix, the increase of the modulus of the composite material can be described by a modified Mooney equation:

$$ln\frac{E}{E_m} = \frac{k_E * \Phi_f}{1 - \frac{\Phi_f}{\Phi_{f-max}}} \qquad (2)$$

with E being the modulus of the nanocomposite, E_m the modulus of the matrix, k_E the Einstein coefficient, Φ_f the volume fraction of the filler and $\Phi_{f\text{-}max}$ as the maximum volume fraction possible for the filler. The Einstein coefficient k_E is defined by the interaction between filler and matrix as well as the aspect ratio of the filler. The value of k_E is the higher the stronger the interactions between filler and matrix are and the higher the aspect ratio of the filler is.

Another theory concerning the enhancing effect of filler materials on the mechanical properties of a polymer was developed by Halpin and Tsai.[49] The theory is based on early works by Hill and Hermans.[50,51] Hill assumed a composite cylinder model in which an embedded phase consists of cylindrical fibers which are continuous and perfectly aligned. Hermans generalizes the model and considers a single fiber which is surrounded by a cylinder of pure matrix. This cylinder is embedded in an infinite body that exhibits the properties of the composite. Halpin and Tsai reduced the findings of Hermans to a simpler analytical form and extended it to a variety of reinforcement geometries, including also discontinuous filler reinforcement. The resulting Halpin-Tsai equations enable the calculation of the effect of volume fraction of the filler, the relative moduli of the components, and the geometry of the filler on the modulus of the composite.

A general form of the Halpin-Tsai equation is expressed as follows:

$$\frac{P}{P_m} = \frac{1 + \eta\zeta\Phi}{\eta\Phi} \tag{3}$$

where

$$\eta = \frac{\frac{P_f}{P_m} - 1}{\frac{P_f}{P_m} + \zeta} \tag{4}$$

P represents one of the three different composite moduli, which are plain strain bulk modulus, transverse shear modulus and longitudinal shear modulus, P_m is the corresponding matrix modulus and P_f the corresponding fiber modulus. Φ is the volume fraction of the fiber and ζ is a measure for the reinforcement geometry, which depends on loading conditions.

As described above, incorporation of clay minerals can be used to enhance mechanical properties of polymers, such as tensile properties or impact resistance and ductility. Also several other properties of polymers are affected by the incorporation of clay minerals. To be mentioned are thermal properties and fire retardancy, electrical and electrochemical properties, and gas – and water – permeation. Furthermore, polymer crystallization and

degradation can be influenced.[52] Like stated before, the focus in this work is the mechanical enhancement of AGM by incorporation of clay minerals.

1.3.2.3 Attachment of a shell

Alternatively to improving the gel strength of bulk AGM, gel blocking can be minimized by attaching a stiff, permeable shell to a softer particle core. Attaching a shell around the AGM particle would lead to an enhancement of the pressure resistance of shape of the particle. The swelling capacity would be barely influenced as the shell amounts only a small part of the total volume of the particle. The strong elastic shell surrounding the soft core with high capacity forces the particle shape to a sphere upon swelling. Thereby, wet porosity and hence gel bed permeability will be improved compared to AGM without surface treatment. Ideally, the shell should resist the tension created upon swelling and not crack. In practice, cracking of the shell might occur due to its non-uniform thickness. However, this cracking should be limited and open the complete swelling capacity to incoming saline without allowing the soft core to escape. The core – shell approach requires a shell material expandable far beyond the reversible part of the stress-strain curve. It is the stress and strain at break, hence the point when the shell starts breaking, which determines performance improvement. Precisely, a threshold value of 400 % of strain at break has to be overcome in combination with a high Young's -modulus and hence high stress at break. The threshold is determined by the requirement of sufficient swelling capacity of the core and high gel bed permeability. In case the shell is very strong at low strain at break, the tension created upon swelling of the core will not extend it sufficiently. Consequently, the swelling capacity will be intrinsically limited by the small volume of the swollen particle. In case the shell is soft and breaks below 300 – 400 % of strain, the AGM particle will be easily deformable and gel bed permeability will decrease tremendously.

A method already applied commercially is surface crosslinking. In this process, multifunctional compounds which are capable of reacting with active groups (e.g. carboxyl groups) of the AGM are deposited for example by spraying on the dry AGM grains. Heat treatment initiates the crosslinking process.[53] The technique of surface crosslinking was applied in literature for both pure AGM as well as for AGM composites.[53-55]

The shell rupture of such surface crosslinked AGM particles is illustrated in Fig. 4.

Fig. 4. Shell rupture of surface crosslinked AGM particles (typical particle size ~500 μm)
left: beginning of shell rupture, right: ruptured shell of fully swollen AGM particles

Due to the low elasticity of the shell created by surface crosslinking of the AGM particle, shell rupture begins already at comparably low swelling degrees of the core. With increasing rupture of the shell its mechanically enhancing effect on the AGM particle gets lost. In order to avoid gel blocking, a highly elastic shell is desirable which postpones shell rupture to higher swelling degrees of the core.

Alternatively to shell crosslinking, an additional layer of a stiffer polymer may be applied as a shell on AGM particles. This method is, however, only described in the literature for poly (*N*-isopropyl acrylamide). This core was coated for example with *N*-(3-aminopropyl) methacrylamide, copolymers of poly (*N*-isopropylacrylamide) and acrylic acid or with 3-Acrylamidophenylboronic acid via solution polymerization.[56-58]. However, the focus of these studies was on adjusting the responsive swelling or deswelling behavior of the hydrogel and its sensitivity towards the environment, for instance in order to control drug release. Less attention was given to the task of strengthening the hydrogel.

Generally, with core and shell differing in chemistry delaminating of the two phases during swelling might be a possible problem to keep an eye on.

1.4 Challenges concerning the synthesis of clay nanocomposites of AGM

Aiming to incorporate clay minerals in AGM, several aspects have to be considered. As mentioned above, the AGM investigated in this work was based on poly (acrylic acid). The polymer was either synthesized as crosslinked poly (acrylic acid) or pre-neutralized to 75 mol% with NaOH. Hence, the monomer mixture exhibits an acidic pH in both cases and high ionic strength, especially in the DN 75 case.

Clays tend to agglomerate in such environments. Resulting agglomerates might even weaken the gels as they exhibit lower aspect ratios than single clay platelets and hence less reinforcement can be achieved. In order to exploit the full potential of clay minerals as fillers in AGM matrices it is essential to first disperse the clay platelets homogeneously in the suspension of the monomers.[59-61]

1.4.1 Structure of clay minerals

Due to the particular structural features of clay minerals, it is extremely difficult under the given conditions of low pH < 7 and high ionic strength to obtain a homogeneous suspension of clay minerals which is at least stable on the time scale of processing and polymerization.

Clay minerals are composed of tetrahedral and octahedral sheets. The tetrahedral sheet is built up by silicon cations which are tetrahedrally coordinated by oxygen. Each SiO_4 tetrahedron shares three of its corner oxygen atoms with adjacent tetrahedra, forming a two-dimensional network which in ideal case exhibits a hexagonal structure. The forth oxygen atom is part of the contiguous octahedral layer consisting of cations octahedrally coordinated by oxygen. The octahedra, which are connected via edges, are completed by hydroxyl groups situated above the center of the hexagonal gaps presented by the tetrahedral layer. The clay mineral is called dioctahedral if two thirds of the centers of all octahedra of the octahedral layer are occupied. In case all centers of the octahedra are occupied, the clay mineral is called trioctahedral. Furthermore, clay minerals can be distinguished between 1:1 clay minerals which are built up of one tetrahedral and one octahedral sheet and 2:1 clay minerals consisting of two tetrahedral sheets and one octahedral sheet.[62] The clay minerals utilized in this work are 2:1 clays.

2:1 Clay minerals show bi-functional character. The basal plane of these clay minerals exhibits a permanent negative charge due to isomorphic substitution of cations within the octahedral and/or tetrahedral layers by cations with lower valence.[63] Contrary to the permanent nature of the charge of the basal plane, the charge of the clay edge is depending on the pH of the suspension medium. The edges of clay minerals possess hydroxyl groups. The acidity of these hydroxyl groups is depending on the type of cations within the tetrahedral and octahedral sheet. In general, the edge charge is positive in acidic suspension media and negative in basic suspension media.

1.4.2 House of cards agglomeration due to acidic polymerization medium

Like stated before, the monomer mixture at both degrees of neutralization is acidic. Consequently, the edges of the clay mineral would be positively charged if the clay was dispersed in the monomer mixture. The positively charged edges are attracted by the negatively charged basal planes and the so called “house of cards” structures are formed (Fig. 5).

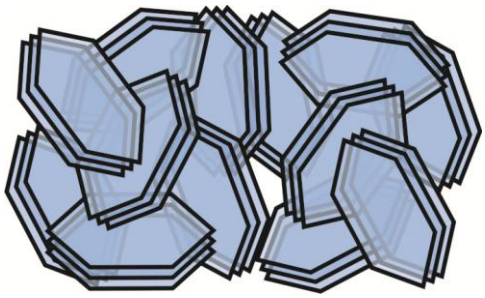

Fig. 5. House of cards structure of clay tactoids

The clay tactoids agglomerate and a homogeneous distribution of the clay in the monomer mixture is no longer warranted. Since for particles of lower aspect ratio the specific edge surface is higher, the problem of house of cards agglomeration is expected to be worst with clays like Laponite®.

In order to avoid the formation of house of cards structures, either the charge of the clay edge needs to be neutralized by modification or the sign of the charge of the basal plane needs to be reversed (“Umladen”) .

1.4.3 Acid activation of clays

If clays are kept at pH values below the point of zero charge, the edges not only start carrying a positive charge, the clay also acts as solid buffer system. Consequently, the octahedral layers start to dissolve as soluble complexes in the suspension medium. This process is well known as acid activation used to produce bleaching earths with high surface area. The degree of dissolution is highly dependent on the basic nature of the octahedral cations, the temperature and the reaction time. Furthermore, clay particles with small diameters offer more exposed specific edge surface and therefore react more quickly. Laponite® consists of small particles (< 20 nm) and contains basic octahedral cations (Li, Mg) and will therefore be most quickly dissolved. Contrary to this, montmorillonite PGV® carries rather acidic Fe and Al cations and comes in larger particles and will be dissolved comparatively slow.

For this reason we did not attempt to produce any Laponite® based AGM composites but rather concentrated efforts on montmorillonite PGV® and synthetic lithium hectorite showing particle diameters of > 10 µm.

1.4.4 Lamellar agglomeration due to high ionic strength

A third obstacle on the way to homogenous and stable clay suspensions in the monomer mixture is the high ionic strength. High ionic strength leads to the formation of lamellar agglomerates (Fig. 6).

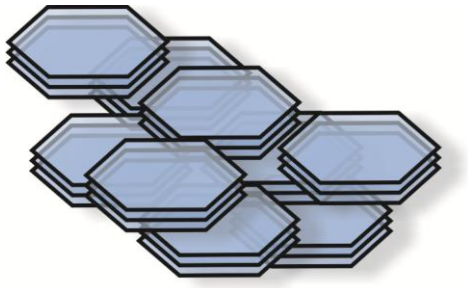

Fig. 6. Lamellar agglomerates of clay tactoids

In general, clay dispersions in electrolyte free environment like deionized water are stabilized via repulsive forces between the electric double layers on the surface of the clay tactoids. With increasing electrolyte concentration, the thickness of the electronic double layer decreases and hence the electronic repulsion decreases.[64] If the thickness of the

electronic double layer falls below a certain limit, the attractive van der Waals forces between the clay tactoids dominate the repulsive force and the clay tactoids coagulate and trigger formation of lamellar agglomerates. The tendency toward the formation of lamellar agglomerates increases with increasing diameter of the clay mineral since the absolute area of parallel overlap and hence the absolute attractive force between parallel platelets increases with diameter.

The formation of lamellar agglomerates can be avoided by adding steric stabilization of the clay tactoids with the help of suitable modifiers.

2 Objective

The objective of this work is improving the performance of AGM for their application in hygiene products. The most important features of AGM in these applications are high maximum swelling capacity and pressure resistance of shape, represented by the gel strength. The material does not only have to absorb large amounts of liquids, it also needs to retain its shape in order to prevent gel blocking, which would restrict the liquid uptake dramatically.

As pointed out, in commercial AGM maximum swelling capacity and gel strength are manipulated by changing the portion of organic crosslinker in the polymerization process. The higher the amount of crosslinker, the lower is the maximum swelling capacity, and the higher is the gel strength. Most frequently, commercial products are crosslinked with amounts between 0.1 and 0.5 mol% in respect to the monomer. However, the crosslinking points in AGM networks that contain organic crosslinkers and which are polymerized via free radical crosslinking polymerization are inhomogeneously distributed, as previously discussed in section 1.3.1.

The AGM investigated in this work consisted of poly (acrylic acid), which was either applied in non-neutralized condition or neutralized to 75 % with sodium hydroxide. Consequently, the pH of the monomer mixture in any case was acidic. The amount of acrylic acid in the polymerization mixture was 15 wt% of the total mass or higher. This means, the monomer mixture possessed a high ionic strength.

We attempted to strengthen the AGM without restricting its extraordinary swelling ability by two approaches. First, clay minerals were incorporated into the bulk polymer network. By this mean, a homogeneous distribution of crosslinking points should be provided and the gel strength of the material should be enhanced. In a second approach, clay-linked gel formulas were envisaged to serve as shell elastomers in a core-shell context. Taking commercial AGM as core, the composition of the shell had to be optimized to maximize the mechanical strength, in particular Young’s -modulus and strain at break. Two different clay minerals with different aspect ratios were chosen for these investigations.

Before any AGM composite materials could be fabricated, first and foremost the difficult task of producing stable and homogenous suspensions in the hostile polymerization environment needed to be tackled.

2.1 Dispersion of clay minerals in the polymerization mixture

The conditions of the polymerization mixture prohibit the formation of stable clay particle suspensions and may lead to house of card and lamellar agglomeration. House of card agglomeration is caused by the different charge of clay edge and basal plane and hence the pH dependent charge of the clay edge plays a decisive role. Consequently, the pH dependency of the edge charge was investigated and a method to estimate the point of zero charge of the clay edge via streaming potential titration was developed. As the edge amounts only a small percentage of the total clay surface, it was addressed first for charge neutralization or charge reversion in order to avoid house of cards agglomeration as the amount of added modifier will be kept at low contents. Elimination of the positive edge charge was approached by charge neutralization via fluorination and charge reversion via phosphorylation. Lamellar agglomeration can be suppressed by electrostatic binding of sterically demanding modifiers to the negatively charged basal plane of the clay platelet. The charge of the basal plane is neutralized and thus house of card formation is avoided at once. A suitable modifier for the basal plane had to be identified and subsequently the minimum amount had to be quantified in order to stabilize the clay mineral suspensions while keeping non-absorbent content minimal.

2.2 Mechanical enhancement of bulk AGM

After succeeding in homogeneously and stably suspending the clay minerals in the monomer mixture the suspensions were polymerized and samples containing various types and amounts of clay minerals were prepared. As a comparison, reference samples without filler and varying amounts of organic crosslinker were prepared. Initially, all samples were investigated at fully swollen state and the swelling capacity in saline was calculated. In order to evaluate the gel strength of the AGM, the VLRH method was established and validated as an alternative to the more time-consuming rheological measurements of G-modulus. In order to identify possible dilution effects which might

occur with increasing swelling degree of the hydrogels the synthesized AGM samples were also investigated at intermediate swelling degrees.

2.3 Core – Shell concept: Enhancement of stress at break and strain at break

For the composition of the shell in a core – shell particle a clay mineral composite based on commercial AGM was chosen. In order to optimize strain at break and Young's - modulus in the above described way, the content of acrylic acid, organic crosslinker and clay mineral as well as the type of clay mineral and the degree of neutralization were varied and in each case compared to a reference sample without filler. The tensile properties of each sample were examined via stress – strain measurements. Therefore, the procedure of the measurement had to be optimized and adjusted to the features of the soft hydrogels. The exact position of the clamps during the measurements had to be considered to eliminate under- or overestimation of the results. Furthermore, slippage of the sample had to be avoided without damaging the sample prior to the measurement.

3 Materials and methods

3.1 Synthesis of AGM and AGM composites in the glass reactor

3.1.1 Synthesis of AGM

AGM is a copolymer from acrylic acid and sodium acrylate, crosslinked with an organic crosslinker. The ratio between acrylic acid and sodium acrylate is variable, as it is determined by the amount of sodium hydroxide added to the polymerization mixture to partially neutralize the acrylic acid. Consequently, for AGM any composition from a pure acrylic acid polymer to pure sodium acrylate polymer is possible. In this work, AGM polymers of acrylic acid and of acrylic acid neutralized to 75 % with sodium hydroxide were prepared.

For the synthesis of AGM the following educts were used:

- Acrylic acid
- Sodium hydroxide
- Methylene bis acrylamide (MBAA) as crosslinker
- Potassium persulfate (KPS) as initiator
- Tetra methyl ethylene diamine (TEMED) as catalyst
- Deionized water

The required amounts of educts for the synthesis of AGM used in this work were calculated according to following conditions:

Table 1. Calculation of the required amounts of educts for the synthesis of AGM

	Reference:	Chosen values:
• Acrylic acid	wt% referred to batch size	15 – 25 wt%
• Sodium hydroxide	mol% referred to acrylic acid	0 or 75 mol%
• MBAA		0.3 – 1.3 mol%
• KPS		0.1 mol%
• TEMED		0.05 mol%

The synthesis procedure consisted of the following steps, which had to be executed in the listed order. During all steps the polymerization mixture was stirred. The synthesis was accomplished via a subsequent step of initiation as soon as the reaction mixture appeared visually homogeneous.

- The crosslinker MBAA was dissolved in acrylic acid.
- The mixture was diluted with deionized water; about 10 ml of the deionized water was put aside
- The mixture was cooled with an ice bath
- The sodium hydroxide solution was added dropwise to the acrylic acid mixture
- Initiator and catalyst were dissolved in the remaining 10 ml of deionized water and added to the mixture

The monomer mixture was injected via a syringe into the reactor (described further in section 3.1.3) which was then purged with argon through the needle for approximately five minutes. The glass reactor containing the polymerization mixture was then placed in an ultrasonic bath for three minutes before it was kept in an oven at 60 °C over night to complete polymerization.

3.1.2 Synthesis of AGM composites

AGM composites in general incorporate inorganic fillers in the acrylic acid – sodium acrylate copolymer, either additionally to or instead of an organic crosslinker. In this work, clay minerals were chosen as inorganic filler. AGM composites including either the natural montmorillonite PGV® or the synthetic lithium hectorite were prepared. The clay mineral was incorporated into the polymer matrix additionally to an organic crosslinker.

For the synthesis of AGM composites the following educts were used:

- Clay mineral
- Modifier
- Acrylid acid
- Sodium hydroxide
- MBAA as crosslinker
- KPS as initiator

- TEMED as catalyst
- Deionized water

The calculation of the required amounts of educts for the synthesis of AGM composites containing clay minerals was done according to the following conditions:

Table 2. Calculation of the required amounts of educts for the synthesis of AGM composites

	Reference:	Chosen values:
• Clay	wt% of solids	0 – 10 wt%
• Modifier	wt% referred to clay content	0 – 45 wt%
• Acrylic acid	wt% referred to batch size	15 – 25 wt%
• Sodium hydroxide	mol% referred to acrylic acid	0 or 75 mol%
• MBAA		0.3 – 1.0 mol%
• KPS		0.1 mol%
• TEMED		0.05 mol%

For AGM composites, the order of the steps during synthesis had to be adjusted. Again it was of vital importance to stick accurately to the listed sequence in order to avoid agglomeration of clay platelets. The mixture was stirred during all steps of the synthesis. The synthesis was pursued with subsequent steps initiated as soon as the reaction mixture appeared visually homogeneous.

- The clay suspension was presented in a suitable vessel
- If possible the suspension was diluted with deionized water; about 10 ml of the deionized water was put aside
- The modifier was added to the clay suspension
- The crosslinker MBAA was dissolved in acrylic acid in a separate vessel
- The acrylic acid – MBAA mixture was added to the modified clay suspension
- The polymerization mixture was cooled with an ice bath
- The sodium hydroxide solution was added dropwise to the polymerization mixture
- Initiator and catalyst were dissolved in the remaining 10 ml of deionized water and added to the mixture

The monomer mixture was injected via a syringe into the reactor which was then purged with argon through the needle for approximately five minutes. Afterwards, the glass reactor containing the polymerization mixture was placed in an ultrasonic bath for three minutes before it was kept in an oven at 60 °C over night to complete polymerization.

3.1.3 Geometry of the glass reactor

For the analysis of the hydrogel samples via VLRH, rheometry, and stress – strain measurements, a plane surface of the sample was needed and the hydrogel samples had to have a certain thickness. Therefore, an appropriate disk geometry was chosen for the polymerization chamber. The most suitable material for the chamber was supposed to be glass. During the initiation of the polymerization oxygen was released by the initiator. It is important, that the generated gas bubbles are not trapped in the polymer gel to achieve a homogeneous sample for the subsequent measurements. The adhesion of oxygen on glass is low, so that the oxygen bubbles should not stick to the glass surface but easily detach.

The design of the glass chamber was developed by Procter & Gamble (Fig. 7).

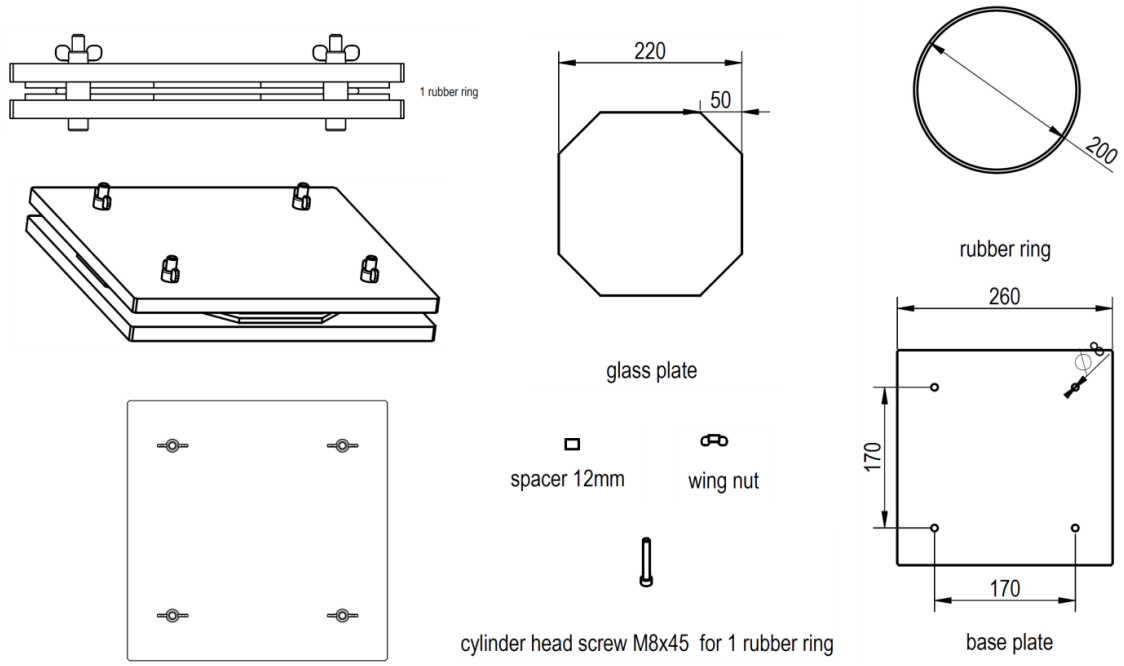

Fig. 7. Geometry of the glass reaction chamber used for the polymerization of hydrogel disks

The reactor consists of two Plexiglas® base plates, two glass plates, a rubber ring with a diameter of 20 cm, four spacers, four cylinder head screws and four wing nuts. Furthermore, two hollow needles were required.

The glass reactor had to be mounted according to the following procedure: One of the Plexiglas® base planes was equipped with the four cylindrical head screws. A glass plate was cleaned carefully with deionized water and acetone and was positioned on the Plexiglas® base plane. The rubber ring was put on the glass plate. In between the rubber ring and the glass plate the two needles were positioned. The second glass plate was put on the rubber ring after cleaning. The spacers were put over the screws to guarantee a specific distance between the two glass plates. Finally the second Plexiglas® plate was placed on top of the glass plate and the whole construction was fixed with the wing nuts. The dimensions of the spacers were chosen in a way that tightening of the screws lead to a slight squeezing of the rubber ring. In this way the whole reactor was sealed.

The thickness of the polymerized hydrogel disks is depending on the thickness of the rubber ring and the dimension of the spacer. In this work, two different thicknesses of the hydrogel disks were required for the analysis of the specific AGM composites.

Hydrogel disks with a thickness of 3.6 mm were used for samples analyzed via VLRH and via rheometry done by Procter & Gamble. To achieve a thickness of 3.6 mm for the as synthesized gel, the spacer had to have a thickness of 15.7 mm and the rubber ring had to have a diameter of 4 mm.

For the stress – strain measurements thinner hydrogel samples were required. The as-synthesized hydrogel disks had to have a thickness of 1.6 mm. Therefore, the spacers were chosen with a dimension of 13.7 mm and the diameter of the rubber ring was 2 mm.

For the synthesis of thick gel disks the size of the batch was 120 g, whereas for the synthesis of the thin gel disks the batch size was 70 g.

3.2 Estimation of the point of zero net proton charge of clay minerals

3.2.1 Problem statement

In order to gain full access to the benefitting contribution of the clay as filler in AGM a homogeneous distribution of the clay within the polymer matrix is mandatory.[59,60] Agglomeration of the clay platelets within the polymer matrix has to be avoided during the mixing of all educts as well as during the polymerization.

In order to prevent agglomeration of clay platelets within the polymer the chemistry of both basal planes and edges of the clay have to be considered. Many efforts have been made investigating and modifying the clay's basal planes.[65-67] The charge of the basal plane is permanently negative and results from isomorphic substitution of cations within the octahedral and/or tetrahedral sheets by cations with lower valence.[63] By electrostatic binding of suitable cationic modifiers to the basal plane the surface tension of the clay particle can be adjusted to the polarity of the polymer matrix. The influence of the edges on the agglomeration behavior of the clay has attracted less attention. The clay edge exhibits hydroxyl groups and its charge therefore is depending on the pH of the dispersion medium. In general, it is negative at high pH and positive at low pH. The exact charge of the clay edge is depending on the type of cations within the tetrahedral and octahedral sheets, more precisely on the mineral acid groups at the clay edge. Common tetrahedral and octahedral cations are Al^{3+}, Si^{4+}, Fe^{3+}, Fe^{2+}, Mg^{2+} and Li^{+}.[68] As a first approximation, the point of zero charge (PZC) of the oxides may be considered. Whereas for alumina the PZC is well documented at a pH of approximately 9, the values for silica are rather scattered. However the reported PZC values are always found at a pH lower than 3. Iron oxides generally show a PZC around pH 8 – 8.5. The PZC of magnesia is listed at about pH 12.[69] For lithium oxide no PZC value is reported because of rapid hydrolysis in water. In order to estimate the charge of the whole clay edge one would have to average the PZC of the oxides of the constituting structural cations of octahedral and tetrahedral sheets (Table 3).

Table 3. PZC of oxides of elements constituting typical clay minerals

Material	PZC
Al_2O_3	~ 9
SiO_2	< 3
Fe_2O_3	~ 8.5
Fe_3O_4	~ 8
MgO	~ 12

Especially if in-situ polymerizations comparable to those introduced by Haraguchi and Takehisa are carried out in aqueous media the pH of the reaction mixture has to be considered.[35] If the solutions of monomers show a pH below the PZC of the clay edge the then positively charged edge will be attracted to the negatively charged basal plane and so called house of cards structures are formed, which means the clay particles agglomerate.[70]

While comparison with PZC values of oxides already suggests that edge surfaces of hectorites will change sign and become positively charged at higher pH values as compared to montmorillonite, exact values for the clay edge under consideration were needed. In literature several approaches to determine the acidity of the clay edge theoretically by modeling are reported.[71,72] Especially for natural bentonite type of clays various attempts have been made to determine the acidity of the clay edge experimentally via potentiometric titration.[73-75] The results of these studies were picked up and several groups tried to determine the K_a value of the clay edges by fitting the experimental potentiometric titration data.[76-79] Due to different experimental setups and the presence of many fitting parameters, such as charge density on edge and basal surface, surface potential, edge surface area etc., these studies resulted in a variety of different models and therefore result in ambiguous and unclear interpretations. Bourg et al. gives an overview of various models used to describe montmorillonite edge surface chemistry and the results for the acidity of the surface groups of montmorillonite consequently are extremely variable.[80] Kaufhold et al. approached the pK_a of the clay edge by recalculating the titration data into proton affinity distributions.[81] An effect all these studies have in common is the dependency of the resulting point of zero edge charge on the electrolyte background. This means a point of zero salt effect (PZSE) does not exist. As the PZC is

defined as the common intersection point between PZSE and the point of zero net proton charge (PZNPC), its determination is not possible for 2:1 clays. Instead, the PZNPC, which is the intersection point between the raw titration curve for the blank and the suspension, is used to evaluate the acidity of clay edges.[73,82] A shift of the acid-base titration curve to lower pH values with increasing ionic strength occurs for all type of clays used by the different workgroups. This shift can be attributed to the effect of a "spillover" of the electrostatic potential from the basal plane onto the edge surface. This spillover is mentioned by Bourg et al. as a further reason for the diversity of models trying to describe the acidity of clay edges.[80] The spillover was described first in 1985 by Secor and Radke and later picked up by Chang and Sposito and is observed at low concentration of electrolytes and in case the thickness of the electric double layer of the basal plane is larger than the thickness of the lamella.[83,84] Confirmation for the spillover effect was later found in experimental data and is revealed by a shift of the acid-base titration curve of montmorillonites to lower pH values with increasing electrolyte concentration as mentioned above.[74,80,84,85]

Wanting to determine the point of zero charge of clay edges experimentally, another severe challenge emerges. Looking at the morphology of a clay platelet, it is clear that the edge charge accounts only for a minor part of the total charge of the clay. The relative quantity of the edge charge compared to the overall clay charge is depending on the actual particle diameter. Typical clay diameters stretch from about 10 nm for synthetic Laponite® clays over 300 nm for natural montmorillonites up to 10 μm for synthetic hectorites. In Fig. 8, the number of Si – atoms residing at the clay edge are referred to the total number of Si – atoms within a clay platelet in dependency of the particle diameter.

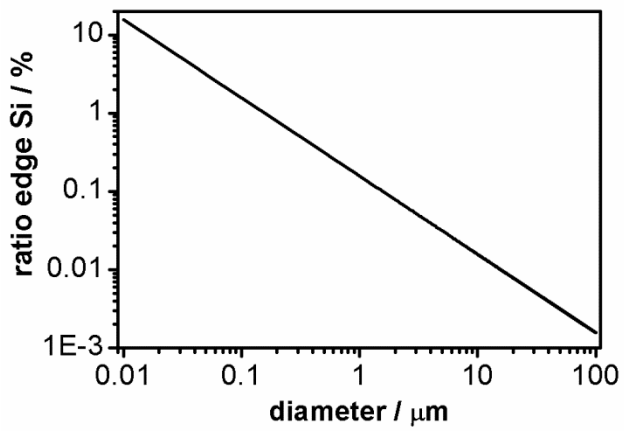

Fig. 8. Ratio of Si – atoms residing at the clay edge as referred to the total number of Si – atoms in dependency of the particle diameter

It is clear that the edge charge is always superimposed by the much larger permanently negative basal charge. Whereas for clays with large diameter the silicon atoms at the clay edge amount to less than 0.1 % of the total silicon content, for Laponite® clays with a low diameter of circa 10 nm the silicon atoms at the clay edges amount more than 15 %. Especially for these clay materials with low diameter the pH dependency of the clay edge's charge has to be considered.

Potentiometric titrations of clays are additionally hampered by partial cation exchange. It is often impossible to distinguish between cation exchange of protons into the interlayers or on the external basal planes and the pH dependent adsorption of anions and cations on the clay edge.[86] The competitive adsorption of hydronium ions on the basal plane and in the interlayer was also mentioned in connection with the determination of the cation exchange capacity (CEC). The CEC often is underestimated due to competitive H^+ adsorption during the measurement, especially if it is done at low pH.[87] Duc et al. examine the contribution of the cation exchange on the proton consumption and state it can be neglected only under moderate pH and high electrolyte concentrations. The latter however causes coagulation of the clay suspension which reduces the accessibility of the surface sites.[82] Tournassat et al. suggest a discontinuous backtitration technique combined with CEC measurements in order to differentiate between protons adsorbed to the basal plane and protons adsorbed to the clay edge.[75]

The method applied in this thesis allows overcoming the above mentioned challenges by irreversibly binding a polycation to the basal plane. Thereby the dominating negative charge of the basal plane is neutralized. By irreversibly binding polycations to the clay's

basal plane its electrostatic potential and a possible spillover effect are eliminated and hence the detection of the edge charge is possible independently of any electrolyte effect. At the same time cation exchange at the basal plane is avoided as the polycations show much higher affinity to the basal plane than protons. Delhorme et al. theoretically investigated the titratable charge of clay minerals using a Monte Carlo method.[76] They demonstrate that the PZC of clay edges is independent of the electrolyte concentration in case the clay exhibits no structural basal charge or in case the structural basal charge is neutralized by counterions. Pecini and Avena picked up this idea and neutralized the charge of their montmorillonite samples prior to the determination of the isoelecric point of the edge surface by using electrophoretic mobility measurements.[88]

3.2.2 Streaming potential titration

Streaming potential measurement allows examining the charge of solid particles even if they are not stable towards sedimentation and therefore it is perfectly suitable to investigate clay suspensions. Streaming potential titrations were executed on a Stabisizer®, a charge titration system of the company Particlemetrix.

The investigated suspension is filled in a cylindrical Teflon chamber with an oscillating Teflon piston. Both chamber and piston carry only very little charge. A fraction of the particles contained in the suspension is immobilized at the surface of the chamber's wall. The oscillation of the piston causes a flow of the liquid within the gap between chamber and piston, which results in mechanical sheering of the particles' diffuse double layer. An alternating voltage, the streaming potential, is detectable. Depending on the characteristics of the particle suspension diverse pistons with different notches are available influencing the degree of sheering. For the investigations described in this work the piston with notches of 200 μm was chosen.

During the first step the clay suspension is titrated with a solution of cations. Suitable cations are e.g. alkyl ammonium cations, mono- or multivalent complex-cations or polymeric polycations. In this work, the polycation Poly (diallyl dimethyl ammonium chloride) (PDADMAC) was chosen. The particular cations electro-statically bind to the negative basal planes of the clay and neutralize the basal charge. By neutralization of the basal charge the direct detection of the edge charge becomes possible. During the second step, the pH titration, the PZNPC of the clay edge is revealed.

Determination of the PZNPC via streaming potential titration was carried out with montmorillonite PGV® and Laponite® RD suspensions. Therefore, 10 ml of a 0.1 wt% suspension of montmorillonite PGV® in deionized water were titrated with a 0.001N solution of PDADMAC. Subsequently, pH titration was carried out with 0.01M hydrochloric acid. Investigations on Laponite® RD were executed with a 1 wt% suspension of the clay mineral in deionized water. 10 ml of the Laponite® RD suspension were titrated with 0.01 N PDADMAC for neutralization of the negative charge of the basal plane. Following pH titrations were carried out with 0.01M hydrochloric acid.

3.3 Investigation of the sedimentation stability of clay suspensions

Due to the characteristics of the polymerization mixture, clay suspensions were not stable without the addition of a stabilizing agent. The formed agglomerates either settle or float. In order to investigate the stabilizing effect of an added modifier on the suspensions of the clay minerals, different approaches have been applied. First of all, a fast and easy method for screening a huge amount of samples was required to identify suitable stabilizing agents qualitatively. In the next step, the identified modifiers were further investigated to confirm the findings of the qualitative screening and finally a quantitative analysis was done.

3.3.1 Preparation of the samples

The sedimentation stability of clay suspensions were tested under polymerization conditions in acrylic acid/acrylate. To prevent polymerization during the analysis, however, neither crosslinker nor initiator and catalyst were added. The educts had to be added in the order described in the following. After the addition of each reactant the vial was shaken manually to guarantee thorough mixing. The next ingredient was added as soon as the reaction mixture appeared visually homogeneous.

- The clay suspension was presented in a vial
- If possible the suspension was diluted with deionized water
- The modifier was added to the clay suspension
- The acrylic acid was added to the modified clay suspension
- The polymerization mixture was cooled with an ice bath

- The sodium hydroxide solution was added slowly to the polymerization mixture
- The remaining volume of deioinzed water was added

Analysis of the suspension of clay minerals in the polymerization mixture had to be carried out directly after the sample preparation. The polymerization mixture had a final pH of about 5. The acidic pH causes degradation of clay minerals, known as acid activation. Additionally, other aging effects of the polymerization mixture were possible, like beginning polymerization of monomers. Consequently, the composition of the sample changes with time not allowing comparison of samples.

3.3.2 Fast qualitative screening of sedimentation stability via visual testing

Visual sedimentation tests are the easiest method to get a qualitative impression of the stability of dispersion with little effort. Especially if a huge amount of samples has to be screened visual sedimentation test can be very useful. In this work, visual investigations were used to monitor both edge and basal modifications.

Visual examination – edge modification

For the modification of the clay edge, either sodium fluoride or sodium pyrophosphate decahydrate were applied. The number of hydroxyl groups at the clay edge and thus the amount of modification reagent required was estimated by considering the density of the clay material of 2.5 g/cm^3, the Si – Si distance (0.303 nm) and the diameter of a single clay platelet. Furthermore, a hexagonal shape of the clay platelets was assumed.

The concentration of the clay mineral in the investigated monomer mixtures was 5 wt% of solids, which equals to 2.66 wt% of the total mass. A content of acrylic acid of 20 wt% of the total mass was chosen and it was neutralized with sodium hydroxide to 75 %.

The proportion of edge surface and hence the number of exchangeable hydroxyl groups of the different types of clays applied vary significantly due to the very pronounced difference in lateral extension. Efficiency of edge modification was tested on montmorillonite PGV® suspensions. For montmorillonite PGV® a typical side length of 150 nm was assumed in the calculation. Consequently, a necessary amount of modifier of about 0.16 mmol was assumed.

Visual investigation of the edge modified clay suspensions suggested a significant reduction of agglomeration with increasing amounts of edge modifiers. Agglomerates were no longer visible only for the samples treated with large amounts of modifiers (17 mg/g and 178 mg/g of sodium fluoride and sodium pyrophosphate decahydrate, respectively).

To corroborate and verify the subjective visual impressions, the montmorillonite PGV® suspensions were additionally checked for house of card agglomerates by determining the particle size distributions applying static light scattering. Note that the investigated montmorillonite PGV® clay platelets have a medium diameter of about 260 nm. Therefore, this clay is well suited for particle size measurements via static light scattering with the device LA-950 of the company Retsch.

Visual examination – basal plane modification

27 different modifiers for the basal plane were initially screened regarding their stabilizing effect on the suspension of clay minerals in the AGM polymerization mixture.

The clay mineral montmorillonite PGV® was used for the sedimentation tests after modification of the basal plane. Visual testing of the sedimentation stability is not applicable for lithium hectorite due to its large particle size. However the basic mechanism of stabilizing the clay suspension is the same for both clays as it is achieved through electrostatical binding of polycations to the negatively charged basal plane of comparable layer charge. The results regarding the suitability of a modifier should therefore be transferable from montmorillonite PGV® to lithium hectorite.

Sedimentation tests were carried out in 40 ml snap cap vials. The chosen concentration of montmorillonite PGV® was 1 wt% of solids. The amount of modifier was varied from 0 to 100 wt% referred to clay weight. An acrylic acid content of 20 wt% referred to the total mass of the sample was chosen and neutralized to 75 % with sodium hydroxide. After preparation, the samples were left to sediment over night. The next day, the samples were investigated visually to judge the sedimentation stability in a qualitative way and pictures were taken.

Visual evaluation of the sedimentation stability is of course highly subjective and only qualitative picture is obtained that moreover relates to a long period of time as compared

to the relevant time scale which requires only stability in the much shorter timeframe of polymerization.

Therefore, for the most suitable modifiers the sedimentation behavior was further examined in a semi-quantitative way by applying forced sedimentation measurements using a LUMiFuge®.

3.3.3 Quantitative study of sedimentation stability via LUMiFuge® measurements

The screening of 27 modifiers by visual sedimentation tests revealed two modifiers (OD and ODD) to be particularly suitable to stabilize the clay mineral suspension in the monomer mixture. Forced sedimentation test were restricted to these two modifiers. The semi-quantitative LUMiFuge® measurements were used to optimize sedimentation stability within a more appropriate shorter timeframe (Fig. 9) as a function of the amount of modifier applied. Both clays of interest, montmorillonite PGV® and lithium hectorite, were studied.

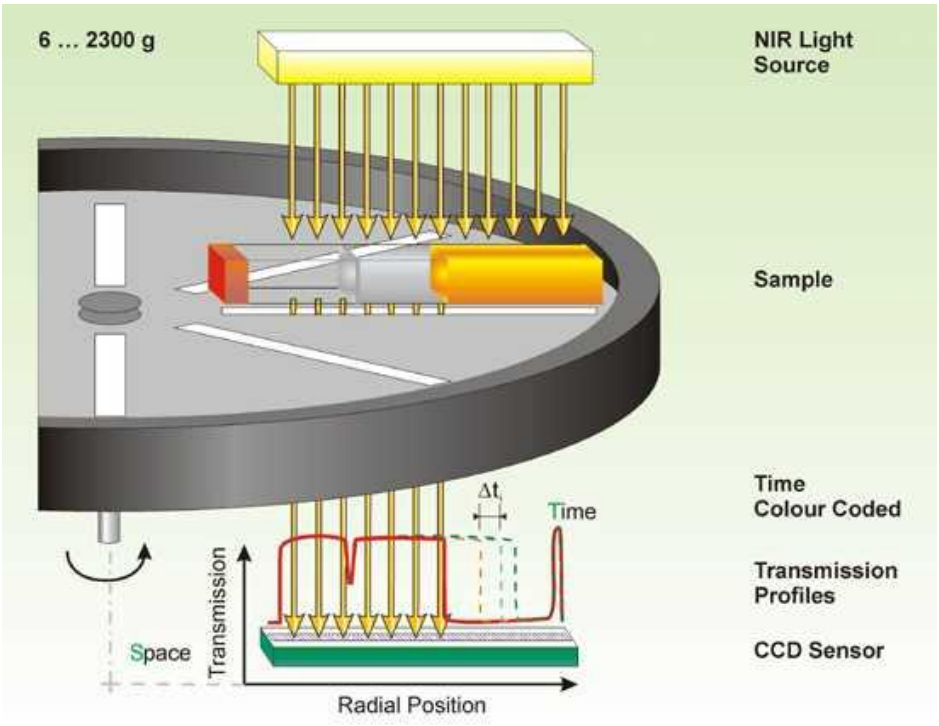

Fig. 9. Scheme of the working principle of LUMiFuge®[89]

For LUMiFuge® measurements the particle suspension is filled into a cuvette which is fixed horizontally on a disk. The disk is rotated during the measurement with a speed in the range of 300 rpm – 3000 rpm which causes forced sedimentation of the particles. The

concentration of the particles remaining in suspension is detected by measuring the transmission through the suspension as a function of time and position. The cuvette is irradiated with parallel light with a wavelength of 880 nm. The light is scattered or adsorbed by the particles while it can pass unhindered through the clear solvent. The intensity of the transmitted light is detected by an optoelectronic charge coupled device sensor. As result of the measurement, the transmission of light in dependency of the radial position is displayed. Transmission profiles can be recorded in intervals between ten seconds and 600 seconds. The transmission is comparatively low for every radial position as long as the suspension is homogenous. With ongoing centrifugation, the particles settle and the suspension clarifies. Hence, the transmission rises. The chronological evolution of the transmission profiles during the centrifugation allows the quantification of dispersion stability.

The parameters for the measurement have to be adjusted to the characteristics of the particle suspension. The concentration of the investigated suspension is depending on the index of refraction of the particles and on their size. It has to be adjusted experimentally to reach a reasonable value for the transmission at the beginning of the measurement to allow the registration of any change thereof during the measurement. An initial transmission of about 50 – 60 % was found to be suitable for the investigation of clay suspensions. Additionally, suitable centrifugation speeds and recording intervals have to be chosen. Both parameters are of course highly correlated as faster centrifugation leads to faster sedimentation of the particles and hence the recording interval needs to be shorter. The most appropriate centrifugation speed is mostly determined by the size of the particles and hence must differ significantly for montmorillonite PGV® and lithium hectorite (Table 4). If centrifugation speed is chosen too high, the particles settle to fast even if the smallest recording interval of 10 seconds is selected. Changes in the sedimentation behavior related to the particular modification will then be harder to be detected and to be quantified.

Table 4: Parameters of the LUMiFuge® measurements

	Montmorillonite PGV®:	Lithium hectorite:
• Concentration	1 wt%	1 wt%
• Centrifugation speed	2000 rpm	300 rpm
• Recording interval	10 s	10 s

The clay suspensions were filled into disposable poly carbonate cuvettes with an optical path length of 2 mm. The duration of the LUMiFuge® measurement was 25 minutes.

3.4 Judging the gel strength of hydrogels: VRLH measurement

One of the major goals of this work was mechanical enhancement of the hydrogel without suffering a loss of swelling capacity. For an efficient approach to this topic a fast an easy method for evaluating the gel strength of the hydrogel was essential. In general, the mechanical strength of AGM is determined by measuring the storage modulus G'. However, the whole procedure of sample preparation and the execution of the rheometry measurement itself requires several weeks of work. For this reason, the measurement of "very low rubber hardness" (VLRH) was chosen for screening purposes. Testing of the mechanical strength via the VLRH method reduced the time for a measurement to few minutes per sample and hence the duration of the measurement procedure is determined by the duration of the sample preparation. Furthermore, the method is easy to handle. VLRH measurement is a method introduced by the company Bareiss and is certified according DIN ISO 27588. The setup for this method includes the VLRH measuring device which is used in combination with the digi test II testing device (Fig. 10).[90]

Fig. 10. left: digi test II testing device and control unit;
right: VLRH measurement device with exchangeable indenter

The hardness of a sample is determined by measuring the indentation depth (μm) of an indenter into the test specimen with an applied force of 100 mN. Different shapes and

sizes of indenters are available. The indenter can be exchanged easily and adapted to the conditions of the sample. The resulting VRLH value is found in the range between 0 and 100 and is generated through the following equation:

$$VLRH = 100 - 0.1 * D \quad (5)$$

where D stands for the depth of indentation in μm.

For the investigation of AGM and AGM composites synthesized in this work, two different indenters were chosen. Both were round plates, one with a diameter of 16.2 mm and the other one with a diameter of 10 mm.

3.4.1 Sample preparation – Swelling of the AGM hydrogels

VLRH measurements were used to quickly characterize the mechanical properties of AGM and AGM composites. The hydrogels were synthesized as described in section 3.1. For VLRH measurements, gel disks with a thickness of 3.6 mm were required. AGM and AGM composites were examined in both fully swollen and in partially swollen state. For this purpose, the as-synthesized gel disks were cut into quadratic pieces of 2.5 cm * 2.5 cm size.

These samples were swollen individually in saline with a salinity of 0.9 wt% and a conductivity of 16.05 mS/cm ± 0.20.

The sample preparation for fully swollen and partially swollen state differed from one another.

Fully swollen AGM hydrogels

The samples were put into a closed container and covered completely with the saline. The AGM hydrogels were left to swell completely to equilibrium. To ensure equilibration, the samples were allowed to equilibrate for at least 10 days at ambient temperature. During this period, the closed container was swung several times to avoid sticking of the hydrogel sample to the walls of the container which might lead to non-uniform swelling. During the swelling process, the hydrogel increased dramatically in size. Therefore, the amount of saline in the vessel was controlled in order to ensure that the sample was fully covered at any time.

Partially swollen AGM hydrogels

The exact degree of swelling of the as-synthesized samples was not known precisely. In order to be able to adjust a defined swelling degree, the hydrogel pieces first had to be dried completely and then swollen to the desired degree. For a complete dehydration the gel pieces were dried in an oven at 60 °C for three days. The weight before and after drying was measured and the solid content was calculated for at least three different gel pieces of one sample. When the relative deviation of the solid content of the individual samples was less than 1.5 % the samples were considered as dry. The dry gel pieces were weighed and put into zip-lock bags. A specific amount of saline was added to achieve the desired degree of swelling, given in gram saline per gram solid AGM. In this work, swelling degrees of 3 g/g, 6 g/g and 12 g/g were chosen and three samples of each swelling degree were prepared. The dry gel pieces were arranged lying flat on a plain surface in the zip lock bags in order to allow homogeneous swelling. Furthermore, long equilibration times (> 10 days) were chosen to ensure equilibration and thus uniform swelling. During this period the position of the gel piece in the saline was regularly controlled. To minimize alterations of the degree of swelling by evaporation of water, handling times were kept as short as possible. The gel pieces were removed from the zip lock bag, weighed to determine the exact swelling degree, and VLRH was immediately measured.

3.4.2 Method validation

In order to ensure that the VLRH method is reproducible independently of the location and the person executing it, a method validation was done by measuring the same fully swollen hydrogels at Procter & Gamble and Bayreuth. Data analysis by Procter & Gamble revealed the following trends:

- The variability of VLRH values was higher for soft hydrogel samples, meaning at low VLRH values.
- Nevertheless, for low VLRH values the sensitivity of the method was higher, meaning that the difference between samples was more pronounced as compared to values measured for stiffer samples.
- It is advantageous to use a smaller indenter for stiffer samples.
- In order to reduce errors at least six measurements should be done per sample.

- The data gained with VLRH measurement correlated well to the storage modulus G'.
- The sample preparation was found to be crucial. In particular, friction caused by lubrication with saline remaining at the surface was detrimental and had to be strictly avoided.

Summarizing, VLRH measurement is a suitable method to estimate the mechanical strength of hydrogel samples. The indenter with a diameter of 16.2 mm is restricted to samples that deliver a VLRH value smaller then 85. For samples of higher stiffness, it is recommended to exchange the indenter for another one with smaller diameter, which leads to higher sensitivity for stiffer samples. The VLRH data showed a good correlation to storage moduli G' determined for identical samples by rheometry which is most frequently used to judge the mechanical strength of hydrogels.

3.5 Stress – Strain measurement

The diameter of the sample is the most crucial parameter for the evaluation of the stress – strain data. Therefore, a dog bone shaped knife, conform to DIN 53504 S3a, was used to cut the hydrogels (Fig. 11).

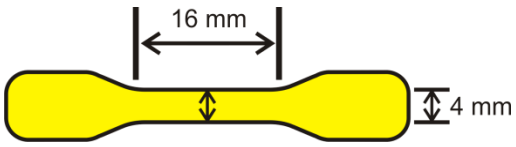

Fig. 11. Diameters of dog bone shaped sample, cut with knife conform to DIN 53504 S3a

The decisive diameters of the dog bone shaped sample are width and length of the thin zone and the thickness of the sample. The width and the length of the thin zone are determined by the choice of the cutting knife. For the chosen knife (DIN 53504 S3a), the width was 4 mm and the length is 16 mm. The thickness of the sample was depending on the composition and swelling degree of each sample, which are in turn determined by sample preparation. The thickness varied slightly for each hydrogel prepared and had to be measured individually for each sample prior to the stress – strain measurement for accurate determination of cross-section area and tensile modulus.

Stress – strain measurements were carried out with a universal tester, model 5565 (Instron). The universal tester was equipped with a 10 N load cell. The stress – strain measurements were carried out with a velocity of 100 mm per minute of straining. The pressure of the hydraulic clamps was chosen between 0.5 and 1 bar.

Tensile testing via stress – strain measurements allows the determination of Young's -modulus, tensile stress and tensile strain of a material up to failure. Characteristic points of a typical stress – strain curve are tensile stress at break and tensile strain at break. The Young's -modulus quantifies the stiffness of a material undergoing tension (or compression). The Young's -modulus can be calculated by dividing tensile stress by tensile strain in the linear elastic region of the stress – strain curve at low elongation.

Note, that ASTM standards use the terms "tensile elongation" and "tensile strength" while ISO standards use the terms "tensile strain" and "tensile stress" for identical parameters. In this work, the ISO terminology is used.

3.5.1 Preparation of the samples

All samples investigated via stress – strain measurements were intermediately swollen samples with a known swelling degree. Consequently, the preparation of the samples was comparable to the preparation of intermediately swollen samples for VLRH measurements. The hydrogels were synthesized as described in section 3.1. For stress – strain measurements, the thinner gel disks with a thickness of 1.6 mm were required.

The gel disks were cut in 6 cm * 6 cm big pieces. As stated before, the exact swelling degree of the as-synthesized samples was not known. Therefore, identical and homogeneous swelling degrees for all samples that allow comparison of the data could only be assured by drying and controlled rehydration as described in the VLRH section. For stress – strain measurements, swelling degrees of 3 g/g and 6 g/g were chosen. During the swelling period the position of the gel piece in the saline was regularly controlled. To minimize dehydration effects, again handling times were kept as short as possible. The average handling time for one sample including several measurements was about 20 minutes.

3.5.2 Method development

As the investigated hydrogel is highly elastomeric and rather soft, clamping of the samples was not trivial. First of all, the hydraulic pressure of the clamps fixing the sample had to be individually adjusted to each sample according to its softness. On one hand, clamping has to be tight enough to avoid sample slippage. On the other hand, too severe squeezing baring the risk of damaging the clamped ends of the dog bone prior to the measurement had to be avoided. Furthermore, the sharp edges of the clamps tended to cut into the sample inducing fracture at the rim. Any failure outside the thin zone gives erroneous values as it underestimates stress and strain at break. Therefore, special attention was paid to sample preparation and the following modifications were made to the standard procedure.

3.5.2.1 Positioning of the dog bone sample

Ideally, for the evaluation of the data only the elongation of the thin zone of the dog bone should be considered. Therefore, it is important to pay attention to the exact position of the clamp. The thin zones concentrate most of the stress due to their minimal cross-section area compared to the cross-section at the broader ends. The ideal place for the clamp is in the area where the width of the dog bone is just starting to narrow down towards the thin zone. Hydrogel samples are, however, flexible and slippery and therefore hard to position. As a consequence, there was always some variation in the clamping position. Variability in the clamp position introduces error in the overall stress dissipated by the sample and for precise measurements of elastic properties it is advisory to keep track of clamp position by means of sample marking and calculating a corrected elongation from the measured value. The typical clamping of the sample at the beginning of the measurement is shown in Fig. 12 on the left. When applying stress in addition to a_0 also b_0 zones are stretched. At any given stress, however, the broader regions of b_0 do not stretch as much as the thin zone a_0. Consequently, the maximum strain measured would be underestimated. Therefore, the measured strain for each sample had to be corrected.

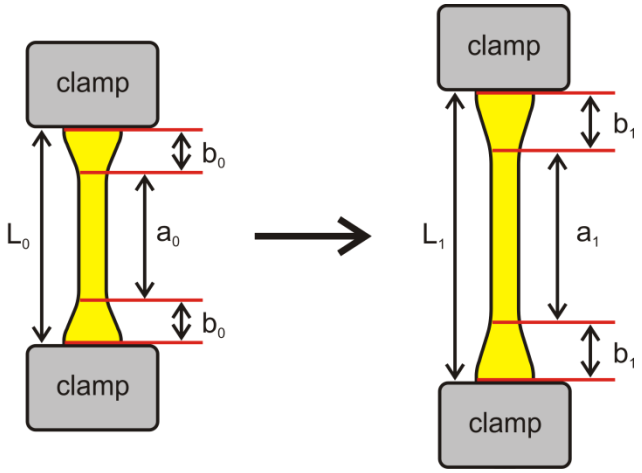

Fig. 12. Clamping of the dog bone;
left: before starting the measurement right: during the stress-strain measurement;
red lines: ink marks

3.5.2.2 Calculation of the correction factor for the measured strain

In order to calculate a correction factor for the measured strain, the thin zone and the position of the clamps were marked on the sample (Fig. 12) after the clamping but prior to measurement. The length of the zone b_0 was determined. The stress – strain measurement was started and then stopped at a known degree of strain before the sample fractured. Again the distance in between the ink marks was determined (b_1). The experimentally measured strain ($strain_{exp}$) can then be corrected ($strain_{corr}$) by applying the following equations:

$$strain_{exp} = \frac{L_1 - L_0}{L_0} \quad (6)$$

$$strain_{corr} = \frac{a_1 - a_0}{a_0} \quad (7)$$

$$strain_{corr} = \frac{(strain_{exp} + 1)L_0 - 2b_1 - a_0}{a_0} \quad (8)$$

The above mentioned procedure of marking the dog bones and determining $strain_{exp}$, a_0, b_0 and b_1 was done for 20 samples of different composition. Evaluation of the data revealed that the correlation between the experimental strain and the corrected strain was expectedly a constant value of 1.256 (adjusted $R^2 = 0.998$) regardless of the composition

of the hydrogel, the type and amount of filler, and the degree of swelling (Fig. 13). The constant represents the bias that emerges from the dog bone geometry.

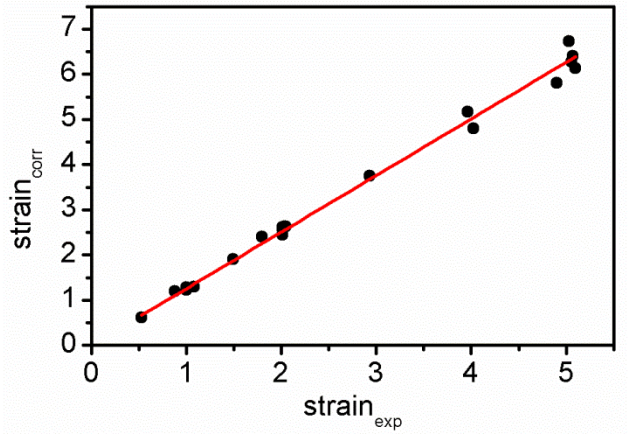

Fig. 13. Linear correlation of experimental strain and corrected strain

Consequently, a much simpler empirical correction (9) was applied to correct the experimental strain for all remaining samples:

$$strain_{corr} = strain_{exp} * 1.256 \quad (9)$$

3.5.2.3 Taping of the dog bone sample to avoid slippage and damaging

The hydrogel samples were fixed between the clamps with a hydraulic system. The pressure applied had to be adjusted manually to the individual softness and brittleness of the samples, as these parameters are determined by the composition and the swelling degree of the AGM. It was noticed that, at a pressure sufficient to avoid slippage of the samples, the hard edges of the clamps frequently damaged the AGM dog bone, especially for the samples with higher swelling degree or higher crosslinking level. Protecting the hydrogel sample with a tape in the clamping area turned out to be an easy and reliable solution to the problem. The tape of choice was “Tesa® Gewebeband”.

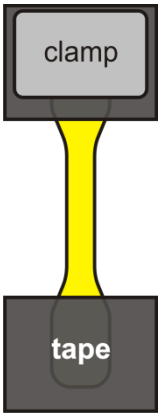

Fig. 14. Mounting of the tape to the hydrogel dog bone

The tape was mounted at the broad area of the dog bone from both sides, as shown in Fig. 14. Taping of the hydrogel samples made them less sensitive to the normal pressure applied by the clamping and made it easier to adjust the pressure in order to avoid slippage of the sample. Moreover, the dog bone was less prone to damage by the rims of the clamps.

3.6 Lithium hectorite

Lithium hectorite with a nominal layer charge of - 0.8 was synthesized according to a melt synthesis method developed by Kalo et al. in our laboratory.[91] The synthesis consists of three steps: 1. Synthesis of a glass precursor with the composition Li_2O-$2SiO_2$ 2. Synthesis of MgO-SiO_2 as sources for MgO and SiO_2 3. Combination of glass precursor Li_2O-$2SiO_2$ and the MgO-SiO_2 mixtures with MgF_2. The nominal composition of the lithium hectorite was $Li_{0.8}[Mg_{2.2}Li_{0.8}][Si_4]O_{10}F_2$.

According to Kalo et al. the synthesized lithium hectorite showed the following characteristics:

Powder X-ray diffraction (PXRD) traces were dominated by the hectorite peaks, while only traces of crystalline impurities could be detected.

Colorometric determination of the cation exchange capacity by $[Co(en)_3]^{3+}$ [92] gave a value of 130 meq / 100 g. This was significantly lower than expected considering the nominal formula, which suggested that some amorphous impurities were present.

As judged by a well defined hydration behavior, the material exhibited a uniform intra-crystalline reactivity corroborating a homogeneous charge density. In deionized water the sample showed osmotic swelling eventually leading to a complete delamination as confirmed by AFM images.

As synthesized lithium hectorite was purified and delaminated by suspending it in deionized water followed by dialyses until the conductivity of the surrounding water decreased to a value less than 50 μS and its pH stayed at a constant value (≈ 8). Subsequently to dialysis, the lithium hectorite suspension was concentrated to about 4.5 wt% by evaporating water. The concentrated lithium hectorite suspension was then milled in a stirred media mill in order to sheer remaining stacks and complete delamination.[93] For milling zirconium oxide particles coated with yttrium oxide with a size if 0.6 – 0.8 mm were used. The chamber of the mill was filled with the beads to 80 % of its volume. The pump speed was 100 rpm and the agitator speed was kept at 1000 rpm. Only one cycle of milling was applied. The particle size of the lithium hectorite was finally determined by focused beam reflectance measurement. The average particle size of lithium hectorite used for hydrogel composites was determined to be 14 μm. Assuming complete delamination, the average aspect ratio consequently was found to be more than 10000.

As described in section 3.2, the PZNPC of lithium hectorite with Mg and Li in the octahedral sheet is expected to be slightly above pH = 7.

3.7 Montmorillonite PGV®

3.7.1 Montmorillonite PGV® – Characteristics of the raw material

Montmorillonite PGV® was provided by Nanocor and is described as high purity aluminosilicate. As it is a natural product only a generic formula is given: $M^{+}_{y}(Al_{2-y}\ Mg_{y})(Si_4)O_{10}(OH)_2 * nH_2O$. It is pointed out, that due to variations in the degree of isomorphous substitution of cations the layer charge of the material is inhomogeneous and consequently the exact formula varies. Despite variations in the composition, Nanocor attributes the natural clay material high phase purity of more than

98% montmorillonite. The aspect ratio of the montmorillonite PGV® is stated to be 150 – 200. The cation exchange capacity of the material is given at 145 meq / 100 g ± 10 %.

3.7.2 Purification of montmorillonite PGV®

Montmorillonite PGV is a natural material and thus contains different types and amounts of impurities. Nanocor applies different physical purification steps but accessory minerals tightly intergrown with the clay platelets can only be removed by a selective chemical dissolution. Since such impurities may influence the polymerization process, they were removed. In particular, quenching of initiated radicals by amorphous iron oxyhydroxides binders could influence the polymerization. Furthermore, these impurities can act like a "glue" and hamper disaggregation of clay platelets. The purification process for clay minerals implies several selective dissolution steps,[94] which are described in the following section.

3.7.2.1 Decomposition of Carbonates

During the first purification step carbonates are decomposed by adjusting the pH of the clay suspension to a slightly acidic level. Furthermore, released cations, like calcium, were removed from equilibrium by ethylene diamine tetra acetate (EDTA). Montmorillonite PGV® powder was suspended in deionized water (≈ 5 wt%) and stirred until no clumps are left and a visually homogeneous suspension was obtained. Na_4EDTA was added in portions to a final concentration of 0.1 M. The clay suspension was then stirred at about 55 °C for two hours. In order to remove the metal complexes formed and excessive EDTA salt the suspension was dialyzed against deionized water. Progress of the dialysis was controlled by measuring the conductivity of the deionized water. The dialysis was ended when the conductivity decreased to a value less than 50 µS.

The stability of EDTA complexes increases with pH. For complete removal of magnesium carbonate a higher pH of around 8 is recommended. Therefore, in the next step fresh Na_4EDTA (0.1 M) was added and the pH was adjusted to 8. The clay dispersion was stirred at about 55 °C for two hours. The dispersion was again dialysed against deionized water in order to remove the EDTA complex and excessive EDTA salt. Progress of the dialysis was controlled by measuring the conductivity of the deionized water. The dialysis was ended when the conductivity decreased to a value less than 50 µS.

3.7.2.2 Dissolution of iron oxyhydroxides

Amorphous iron oxyhydroxide can be selectively removed by the dithionite/citrate/ bicarbonate method, suggested by Mehra and Jackson.[94] Fe(III) is reduced to Fe(II) by sodium dithionite which increases the solubility of iron. Moreover, citrate can form a stable and water soluble complex with Fe(II). Sodium carbonate serves as buffer to provide a pH of approximately 7.3 in order to prevent disproportionation of the dithionite. Some structural iron of montmorillonite is also reduced in this process but is quickly re-oxidized without any precautions.[95]

Sodium citrate was added to the PGV® suspension (0.3 M in citrate). The suspension was buffered with 5 ml 1M sodium bicarbonate per 40 ml 0.3 M citrate solution. The suspension was heated to 80 °C. 1 g sodium dithionite per g clay was added and the suspension was stirred at 80 °C for one hour. The color of the suspended clay changed from beige to green. After cooling the suspension to room temperature, just enough sodium chloride was added to provoke flocculation of the clay. This allows centrifugation of the clay. Proper sedimentation of the clay particles during the centrifugation is crucial to not lose a fraction of small particles. Therefore centrifugation was carried out at 3700 rpm for ten minutes with the device Multifuge 1L of the company Heraeus. The clay dispersion was washed once via centrifugation to remove most part of the unreacted dithionate as it can damage the dialysis tube. After centrifugation the dispersion was dialysed in deionized water in order to remove the citrate complex and excessive citrate and dithionite. Progress of the dialysis was controlled by measuring the conductivity of the deionized water. The dialysis was ended when the conductivity decreased to a value less than 50 μS.

3.7.2.3 Oxidation of organic compounds

During the final purification step, organic compounds like humic substances are removed from the dispersion by oxidation.

The PGV® suspension was purged with ozone produced by an ozonizer during three days.

3.7.2.4 Mechanical disaggregation

Subsequently to the purification process the clay suspension was sheered in a stirred media mill adopting a method described in literature in order to break up remaining aggregates and narrow the particle size distribution.[93]

For the milling zirconium oxide particles coated with yttrium oxide with a size if 0.6 – 0.8 mm were used. The chamber of the mill was filled with the beads to 80 % of its volume. The pump speed was 100 rpm. The agitator speed was kept at 1000 rpm for 30 minutes, followed by another 15 minutes at 2000 rpm.

3.7.3 Montmorillonite PGV® – Characteristics of the purified material

As the specifications of the montmorillonite PGV® changed during the purification procedure and the milling, its characteristics were determined afterwards.

Particle size distribution was determined via static light scattering. The mean value of the particle size of purified montmorillonite PGV® could be reduced and the particle size distribution diminished by milling in the stirred media mill. The mean value for the particle size changed from 2 ± 6 μm to 0.26 ± 0.07 μm (Fig. 15).

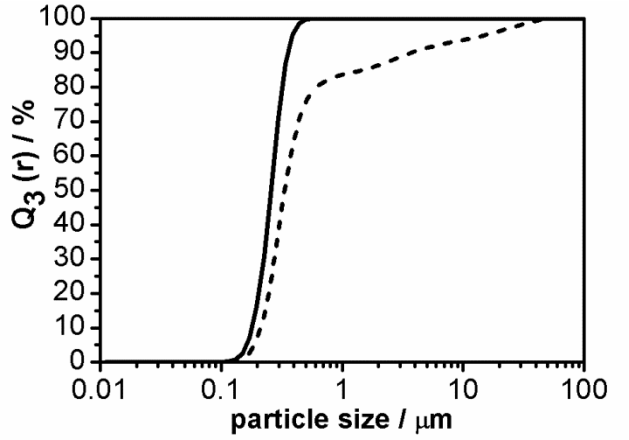

Fig. 15. Particle size distribution of montmorillonite PGV® - - - before milling and ─ after milling

The typical thickness of sodium montmorillonite tactoids in deionized water is 1 – 3 nm, which means they consist of 1 – 3 lamellas.[96-98] However, even with highly swelling interlayer cations like sodium, high ionic strength will hamper exfoliation.[98] As the ionic strength in the AGM polymerization mixture is high, thicker tactoids of 7 – 10 lamellas would have to be expected. Given an average lateral extension of 260 nm, the aspect ratio

for montmorillonite suspended in the polymerization mixture was assumed to be in the range 25 – 35.

Cation exchange capacity (CEC) was analyzed applying both the copper complex method described by Ammann et al.[92] and the barium chloride method (DIN ISO 11260). Both methods delivered almost identical results. The cation exchange capacity of purified montmorillonite PGV® determined by the copper complex method was 123 meq / 100 g. The method according to DIN ISO 11260 delivered a CEC of 122 meq / 100g.

Furthermore, the PZNPC of the clay edge was estimated with the method described in section 3.2.

4 Results and Discussion

4.1 Dispersion of clay minerals in the polymerization mixture

AGM is a polymer based on acrylic acid with a degree of neutralization (DN) that can be chosen from pure acid to fully neutralized. Consequently, any composition from pure poly (acrylic acid) to pure poly acrylate is possible. Most frequently for applications in hygiene products a DN of 75 % is chosen. Neutralization of the acrylic acid is accomplished by the addition of sodium hydroxide. For the synthesis of AGM the content of acrylic acid in the polymerization mixture has to be at least 15 wt%. Furthermore, the polymerization mixture contains organic crosslinker, initiator and catalyst. For AGM composites, inorganic fillers and necessary modifiers are additionally added.

In this work, AGM with degrees of neutralization for the acrylic acid of 0 % and 75 % were investigated. Consequently, the pH of the monomer mixture was acidic. The content of acrylic acid in the polymerization mixture was chosen between 15 wt% and 25 wt%. The pH of the monomer mixture was determined with colorimetric pH test paper. The non-neutralized monomer mixture showed a pH of about 2. If the acrylic acid was neutralized to 75 %, the pH of the monomer mixture was found to be pH 5.

The scope of this work was to incorporate different clay minerals into the AGM polymer and synthesize a new type of AGM composite. As stated in the introductory section, the incorporation of clay minerals into the described AGM was not straight forward due to immanent surface properties of clay minerals. House of cards agglomeration is expected to be provoked due to the acidic dispersion medium. Furthermore, the high ionic strength of the monomer mixture could cause lamellar agglomeration.

4.1.1 Modification of the clay edge – Prevention of house of cards structure

Lithium hectorite has an aspect ratio higher than 10000. Consequently, the clay edge amounts to only a small percentage of the whole clay surface, namely 0.1 %. Therefore, a Laponite® clay was chosen to model for lithium hectorite to determine the PZC of the edges. Like the lithium hectorite, Laponite® clays are also synthetic clays. The

composition of both materials at the clay edge is similar. However, Laponite® has an aspect ratio of 10. This means, the ratio of Si – atoms at the clay edge compared to the total Si - content is much higher in Laponite® clays (≈ 15 %) as compared to lithium hectorite which improves detectability for any chemistry selective for edges a great deal.

PZNPC of clay edges

The PZNPC of the clay edge determines the pH below which the clay edge exhibits a positive charge and therefore is decisive for the onset of formation of house of cards agglomeration. Montmorillonite PGV® and lithium hectorite differ in composition of octahedral sheets and therefore in the acidity of hydroxyl groups located at edges. While for both montmorillonites and lithium hectorites the tetrahedral sheets contain essentially only Si, the octahedral sheets are composed of Al/Mg and Mg/Li, respectively. Consequently, the PZNPC is expected to be found at lower pH for montmorillonite as compared to hectorite.

PZNPC of montmorillonite PGV®

First the polycation PDADMAC was irreversibly bound to the basal plane of the clay suspension at pH 8. Hence the charge of the clay, which is dominated by the surface charge of the basal planes, is monitored by the streaming potential. PDADMAC was added to the point where the streaming potential approached a value of - 40 mV. Then the PDADMAC – modified montmorillonite PGV® suspension was titrated with hydrochloric acid. The pH region with a streaming potential of ≈ 0 corresponds to the PZNPC (Fig. 16). The PZNPC for montmorillonite PGV® clay edges is found at pH 5.

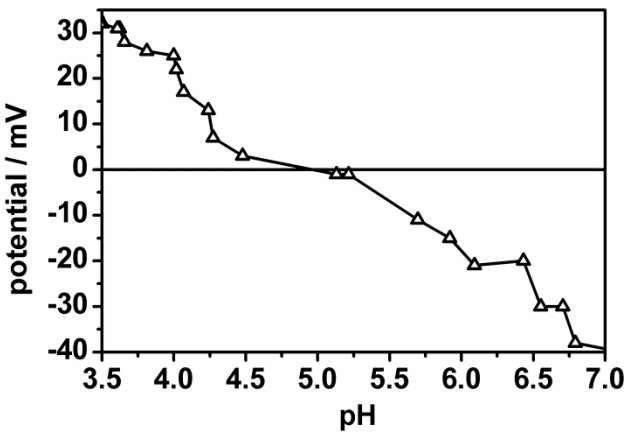

Fig. 16. pH titration of purified PGV® after neutralizing the negative charge of the basal planes with PDADMAC.

In literature, PZC values for different types of montmorillonite were reported to be in the range from pH 5 to pH 8.5. This broad scatter is attributed to the absence of a PZSE and side reactions during the potentiometric titrations, such as cation exchange.[82,86] Benna et al. studied the PZC of the clay edge via rheological and electrokinetic measurements at low electrolyte concentration and suggested a PZC at pH 7.5 – 8 (glass electrode) or pH 6 (colorimetric test paper).[70] Rozalén et al. investigated the PZNPC via surface titration and confirm its dependence on the ionic strength of the suspension medium.[85] They found the PZNPC in a range between pH 7.6 and pH 8.1. Wanner et al. determined the PZNPC at pH 6.1 via alkalimetric and acidimetric titrations at different ionic strengths.[86] Duc et al. investigate the PZNPC via continuous titration and regard the dependence of the PZNPC on the ionic strength.[73] They conclude that by extrapolating the ionic strength to infinity the PZC of sodium montmorillonite could be estimated even lower than pH 5.2. This is in good agreement with our findings, assuming an infinite ionic strength eliminates a possible spillover effect. However, cation exchange can still occur, which would explain the remaining discrepancy. Pecini and Avena neutralized the structural basal charge by binding either methylene blue or tetraethylenepentamine copper(II) and determined the isoelectric point of the edge surface of their montmorillonite sample within an upper limit of 5.3 ± 0.2 and a lower limit of 4.0 ± 0.2.[88]

PZNPC of Laponite® RD

The dominating negative charge of the basal plane was neutralized by irreversibly binding the polycation PDADMAC in order to allow detection of the edge charge of Laponite® RD. PDADMAC was added until the streaming potential approached a value of approximately - 15 mV. Subsequently, the pH of the surface modified Laponite® RD suspension was titrated with hydrochloric acid. For Laponite RD, the PZNPC of the clay edge was found around pH 8 (Fig. 17). A polynominal fit was applied to get a clearer image of the progression of the curve, which confirmed a pH of 8 as PZNPC of Laponite® RD and hence hectorite clay edges.

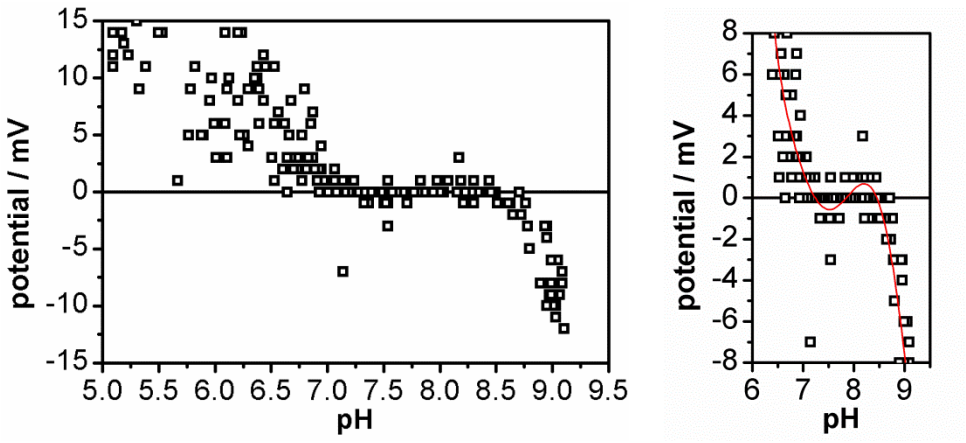

Fig. 17. pH titration of Laponite® RD after coverage of the basal plane with PDADMAC

As expected, the PZNPC of the Laponite® clay edge is less acidic compared to the montmorillonite. To the best of our knowledge an experimentally determined PZNPC for Laponite® clays was never reported in literature before. Tournassat et al. proposed a PZC at an alkaline pH of approximately 10 for hectorites referring to the structure that mainly contains magnesia.[79]

As mentioned previously, the pH of the monomer mixture for the polymerization of AGM, which is based on acrylic acid, was 2 in case of a non-neutralized polymer and 5 in case of the 75 % neutralized polymer. Hence, dispersing hectorites in the polymerization mixture will definitely charge the edges positively for both degrees of neutralization and house of cards agglomeration is likely. Consequently, modification of lithium hectorite is mandatory to achieve a stable and homogeneous dispersion of the filler in the AGM composite.

For montmorillonite PGV® a PZNPC at pH 5 was estimated. Dispersing the clay in the non-neutralized acrylic acid mixture for the polymerization will still lead to positively charged clay edges and house of cards agglomeration might occur. The pH of the 75 % neutralized acrylic acid polymerization mixture of 5 is similar to the PZNPC of montmorillonite PGV®. Therefore, it is unclear whether PGV® might suffer from house of cards agglomeration in partially neutralized monomer mixtures.

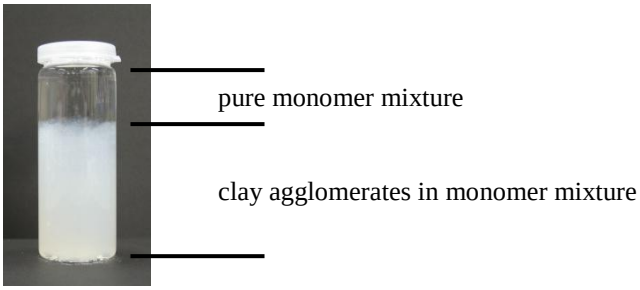

Fig. 18. Sedimentation test: montmorillonite PGV® in monomer mixture, DN 75 %

In any case visual sedimentation test (Fig. 18) revealed that the dispersion of montmorillonite PGV® in the monomer mixture with DN 75 % was not stable. After leaving the vial to rest over night, the upper 30 % of the volume of the vial contained clear monomer solution. The clay particles agglomerated and settled, visible as voluminous agglomerates in the lower turbid part of the vial. Additionally, the particle size distribution of the formed agglomerates in DN 75 % monomer mixtures was determined by means of static light scattering measurements and compared with montmorillonite PGV® homogeneously dispersed in deioized water (Fig. 19).

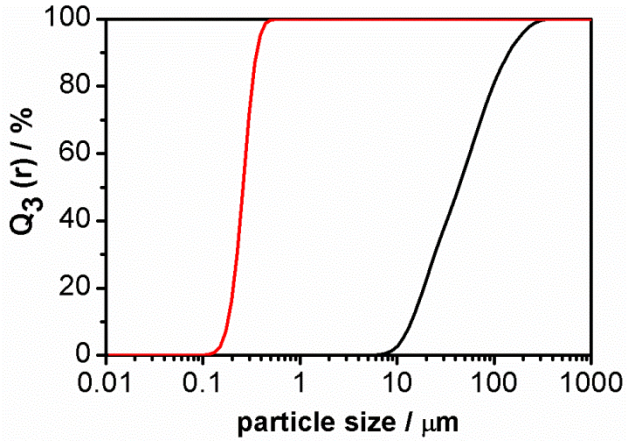

Fig. 19. Particle size distribution of montmorillonite PGV®:
— in deionized water; — in monomer mixture DN 75 %

The measurement of the particle size distribution of montmorillonite PGV® in deionized water showed a mean value of the particle size of 0.26 ± 0.07 μm. In the monomer mixture with DN 75 % the mean value of the particle size was 62 ± 57 μm suggesting severe agglomeration in the 75 % neutralized polymerization mixture.

At this point it remains, however, unclear whether the observed agglomerates are formed by attractive edge – basal plane interactions or by basal plane – basal plane interactions caused by the high ionic strength.

4.1.1.1 Modification of clay edges

Two different approaches were pursued to achieve a modification of clay edges that would remove the pH-dependency of the edge charge:

- Conversion of Si – OH groups to Si – F groups by ion exchange via fluorination
- Charge reversion by strongly binding multivalent anions to octahedral cations via phosphorylation

As described in some detail in section 3.3.2, the number of hydroxyl groups at the clay edge was estimated assuming a density of the clay material of 2.5 g/cm^3, a Si – Si distance of 0.303 nm, a hexagonal shape of clay platelet, and a typical size which differs for the two types of clays applied.

Fluorination of the clay minerals was carried out with sodium fluoride. The phosphorylation was done with sodium pyrophosphate. The efficiency of these two edge modifiers to prevent or reduce agglomeration in a polymerization environment was mainly judged by particles size distributions as measured by static light scattering.

Montmorillonite PGV® is particularly well suited to monitor any agglomeration since its primary particles (tactoids) are in the range of 260 nm which can safely be spotted in static light scattering and this size of primarily particles is well separated from much larger aggregates or agglomerates. Laponite® diameters are way too small to be detected with static light scattering and hectorite is so large that its primary particles might fall within the range of aggregates or agglomerates.

Edge modification of montmorillonite PGV®

The number of hydroxyl groups at the edges of montmorillonite PGV® was estimated to be 0.16 mmol assuming a typical side length of 150 nm for the hexagonal platelets.

Fluorination of montmorillonite PGV®

Fluorination of the clay edge converts the Si – OH groups into Si – F groups and consequently the clay edge will no longer vary with pH. To evaluate the efficiency of edge fluorination on the agglomeration behavior of montmorillonite PGV® in the monomer mixture with DN 75 %, the amounts of sodium fluoride applied was varied systematically and the stability of the following suspensions were compared:

- Unmodified montmorillonite PGV®
- Modification with 1.0 fold of the estimated amount of sodium fluoride
- Modification with 1.5 fold of the estimated amount of sodium fluoride
- Modification with 2.5 fold of the estimated amount of sodium fluoride

With increasing amounts of edge modifier applied, the extent of agglomeration as judged visually was decreasing. Agglomeration seemed to be completely gone in case a 2.5 fold amount of sodium fluoride was applied. The results of the visual sedimentation tests were quantified by analyzing the suspensions via static light scattering (Fig. 20).

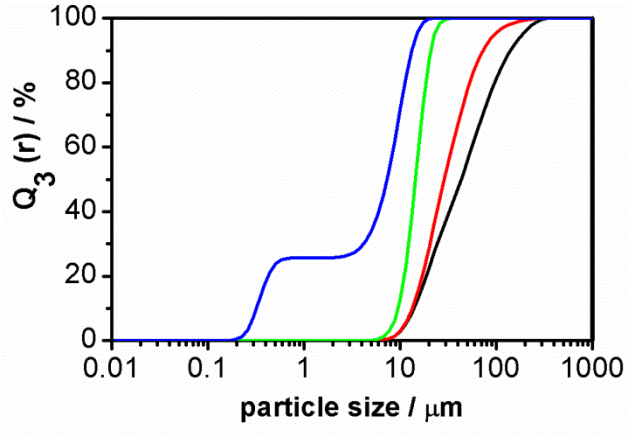

Fig. 20. Particle size distribution of montmorillonite PGV® in monomer mixture DN 75 %
─ unmodified, ─ 1 fold sodium fluoride, ─ 1.5 fold sodium fluoride, ─ 2.5 fold sodium fluoride

The mean particle size for montmorillonite PGV® in the monomer mixture DN 75 % decreased considerably with increasing fluoride amounts. The unmodified montmorillonite PGV® showed a mean value for the particle size of 62 ± 57 μm. This particle size could be diminished by modification of the clay edge with increasing amounts of sodium fluoride (Fig. 20). For modification with a 2.5 fold amount of modifier, a mean value for the particle size of 7 ± 5 μm was achieved. When comparing the best suspension (blue line) with montmorillonite PGV® in water (Fig. 19) it can be estimated, that only 25 vol% of the clay tactoids do not show agglomeration. The majority of the clay tactoids still agglomerate, suggesting that edge modification with fluorine is unable to assure a stable suspension in the polymerization environment.

Phosphorylation of montmorillonite PGV®

Pyrophosphate is capable to form chelate complexes at the clay edge with Al-cations of the octahedral sheet which was hoped to charge the edges permanently negative

independently of the pH. To evaluate the efficiency of edge phosphorylation, again the agglomeration behavior of montmorillonite PGV® in the monomer mixture with DN 75 % with increasing amounts of modifier applied were compared:

- Unmodified montmorillonite PGV®
- Modification with 1.0 fold of the estimated amount of sodium pyrophosphate
- Modification with 1.5 fold of the estimated amount of sodium pyrophosphate
- Modification with 2.5 fold of the estimated amount of sodium pyrophosphate

Similar to fluorination, with increasing amounts of sodium pyrophosphate, the extent of agglomeration decreases as judged visually. For the suspension of montmorillonite PGV® modified with the 2.5 fold estimated amount of sodium pyrophosphate no obvious agglomeration remained. Again the results of the visual sedimentation tests were quantified by analyzing the particle size distribution of the clay mineral in the suspensions (Fig. 21).

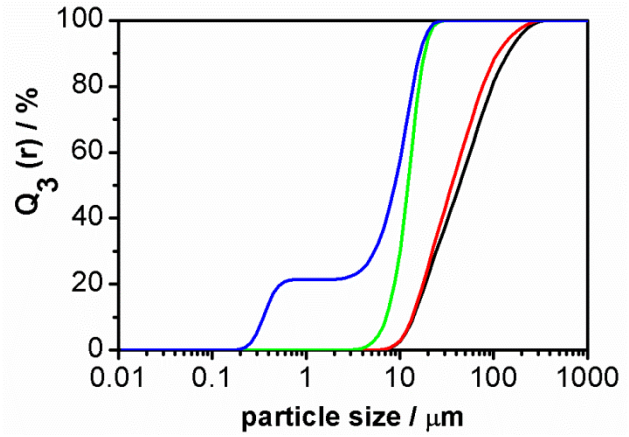

Fig. 21. Particle size distribution of montmorillonite PGV® in monomer mixture DN 75 % ─ unmodified, ─ 1 fold sodium pyrophosphate, ─ 1.5 fold sodium pyrophosphate, ─ 2.5 fold sodium pyrophosphate

The mean particle size of montmorillonite PGV® in the monomer mixture DN 75 % decreased with increasing amounts of sodium pyrophosphate. The mean particle size was reduced from 62 ± 57 µm for unmodified montmorillonite PGV® to 9 ± 6 µm for montmorillonite PGV® modified with 2.5 fold of the estimated amount of pyrophosphate. Again a plateau is observed the particle size distribution between 300 nm and 3 µm allowing to state that, comparable with the results of the fluorine modification, some 75 % of the primary particles are still agglomerated even at the highest concentrations of modifier applied. Both edge modifiers tested show a significant

reduction in agglomeration tendency. However, they both fail to assure a well dispersed and stable suspension in the rather harsh polymerization environment of AGM.

Summarizing, one can say, that edge modification of the clay clearly helped to reduce the extent of agglomeration of clay particles in the acidic monomer mixture. However, flocculation could not be completely avoided. Consequently, edge modification alone is not sufficient to establish a homogeneous distribution of clay minerals in AGM. Therefore, next the possibility of basal plane modification was probed in order to reduce band-like agglomerate structures fostered by the high ionic strength.

4.1.2 Modification of basal planes – Prevention of lamellar agglomeration

As explained in the introduction, high ionic strength of the suspension medium reduces the electrostatic repulsion between the permanently negatively charged basal planes and therefore leads to lamellar agglomeration of clay platelets. The effect will be even more severe in solvents of lower dielectric constant, e.g. monomer mixtures. Consequently, the basal planes of the clay mineral had to be modified to achieve an (elctro-)steric stabilization in the polymerization environment. As the basal planes of clay minerals are permanently negatively charged, they can easily be modified by electrostatic binding of polycations. Possible charge reversion of the basal plane additionally helps avoiding the formation of house of cards structures at low pH values where the edges are also positively charged.

4.1.2.1 Identification of suitable basal modifiers

27 different modifiers of various composition and molecular weight were screened by visual sedimentation tests (Table 5).

Table 5. Modifiers screened by visual sedimentation tests; charge at pH 5

Cationic	OD	poly (ethylene imine), ethoxylated (1 unit)
	ODD	poly (ethylene imine), ethoxylated (chain length: 20 units)
	POD	poly (ethylene imine), ethoxylated (chain length: 10 units) and propoxylated (chain length: 7 units)
	HOD	poly (ethylene imine), ethoxylated (chain length: 24 units) and propoxylated (chain length: 16 units)
	PAM	poly (acrylamide)

	PB hexamethylene diamine, ethoxylated (chain length: 24 units), quaternized with methyl chloride Sokalan HP56K poly (vinylpyrrolidone – co – vinylimidazol) Dimethyl aminoethyl methacrylate (monomer) Tris(hydroxymethyl) amino methane Poly (ethylene imine), 80% ethoxylated (Sigma Aldrich) PAMAM dendrimer
Anionic	Sokalan CP 5 poly (maleic acid – co – acrylic acid) Sokalan CP 10S modified poly (acrylic acid) Carboxymethylcellulose
Non-ionic	RV grafted poly (ethyleneglycol) Sokalan HP 53 poly (vinylpyrrolidone)
Zwitterionic	ZPB zwitterionic poly amine
Various confidential material of P&G	RD#164877; RD#169525; RD#169527; RD#170766; RD#170768; RD#171741; RD#171744; RD#173387; RD#173490; RD#1694276

Suspensions of montmorillonite PGV® in the monomer mixture with DN 75 % were prepared with varying amounts of each tested modifier. Due to the large particle sizes of lithium hectorite, suspensions tend to sediment in any medium. The tests were therefore restricted to montmorillonite PGV® and it is assumed that the results can be transferred to lithium hectorite.

After sedimentation over night, all samples were investigated visually to judge the sedimentation stability qualitatively and pictures were taken (Fig. 22). Note that voluminous flocculation was easily detectable by eye. However, on the pictures flocculation is harder to identify and might be mistaken for stable dispersion.

a) cationic modifiers

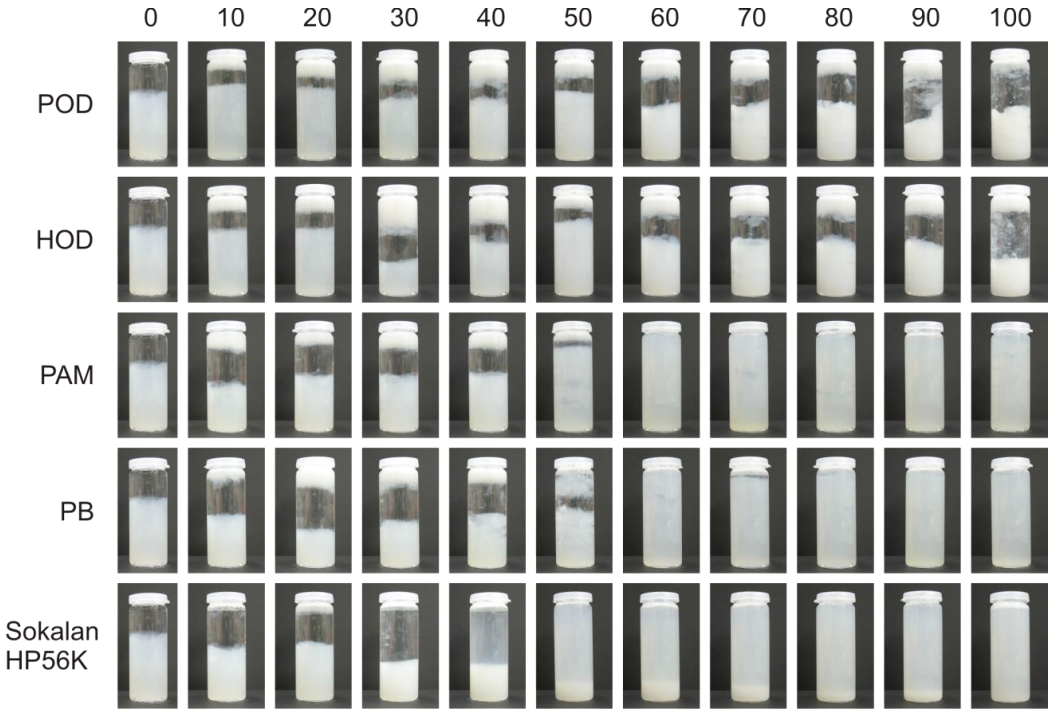

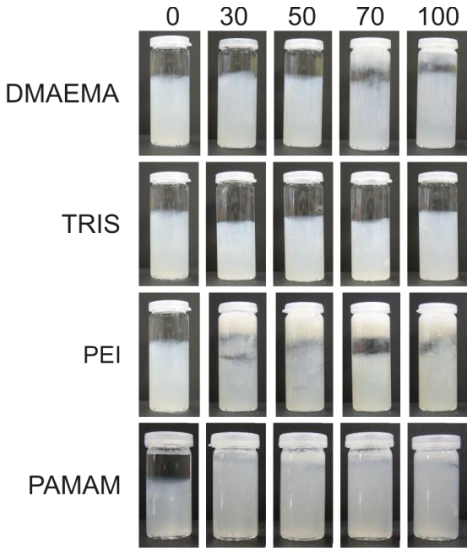

b) anionic modifiers

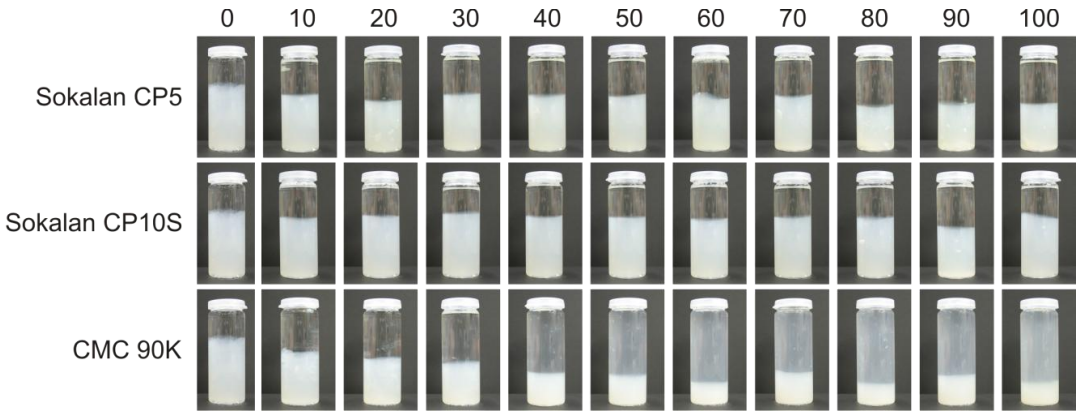

c) non-ionic modifiers

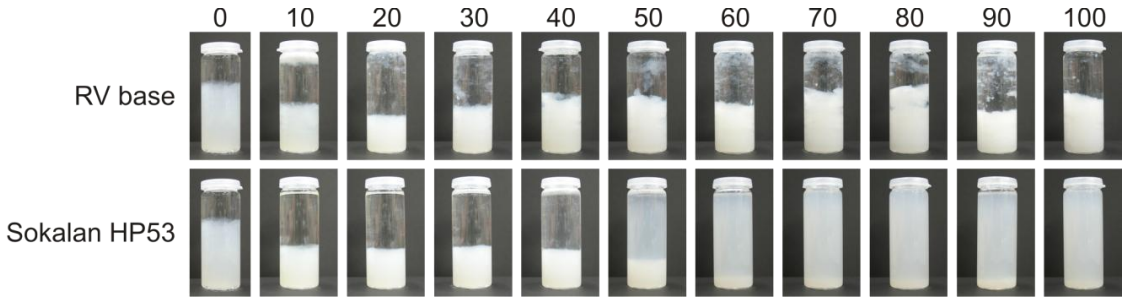

d) zwitterionic modifiers

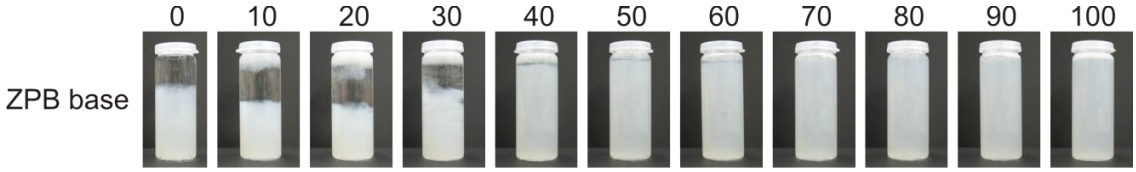

e) confidential material of P&G

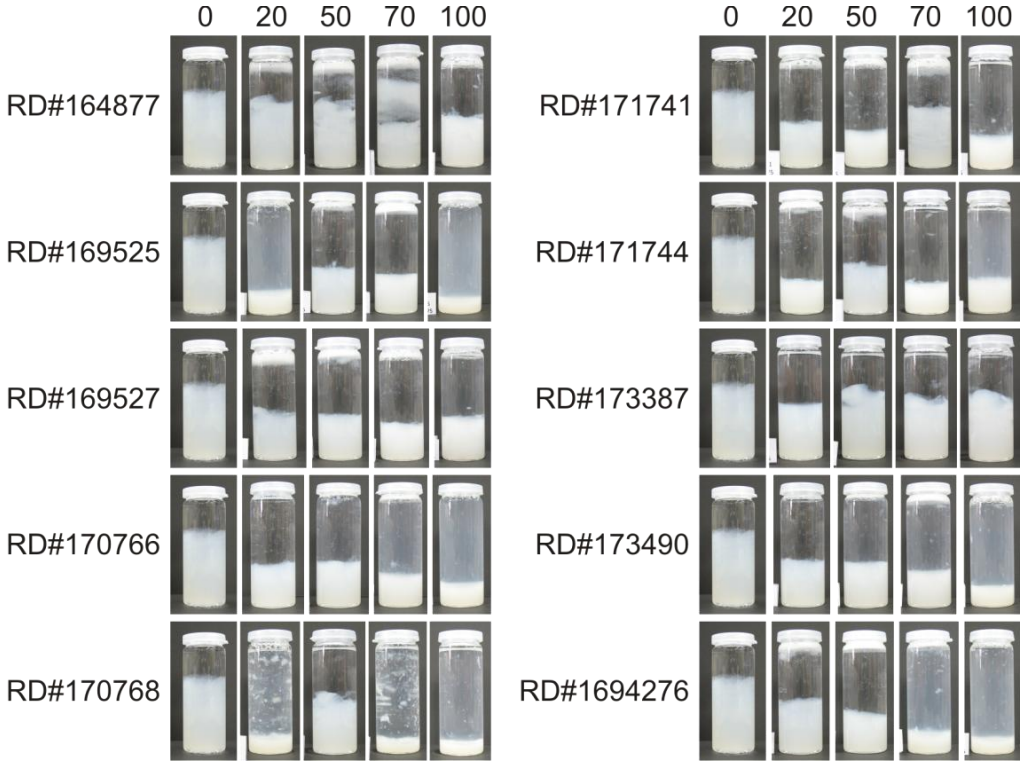

Fig. 22. Visual sedimentation test of montmorillonite PGV® suspended in monomer mixture DN 75 % stabilized with different amounts of modifier (wt% referred to clay)

None of the above shown modifiers was able to sufficiently stabilize the dispersion of montmorillonite PGV in the monomer mixture with DN 75%.

In the visual screening two suitable modifiers could be identified, OD and ODD, which will be shown in the following seperatly.

The sedimentation behavior overnight of montmorillonite PGV® suspensions stabilized with various amounts of OD is displayed in Fig. 23.

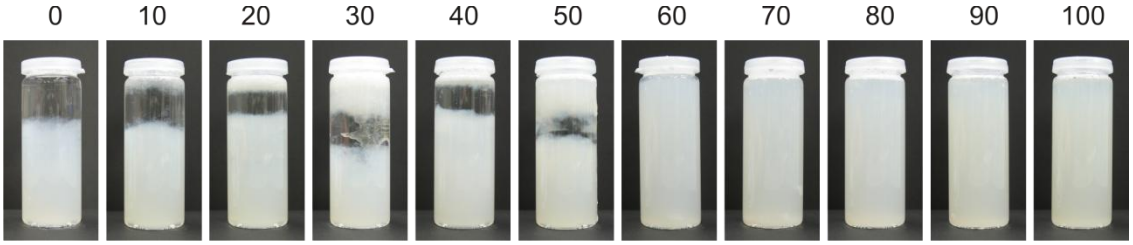

Fig. 23. Visual sedimentation test of montmorillonite PGV® suspended in monomer mixture DN 75 % stabilized with different amounts (wt% referred to clay) of OD

The results of the sedimentation tests for ODD base are shown in Fig. 24.

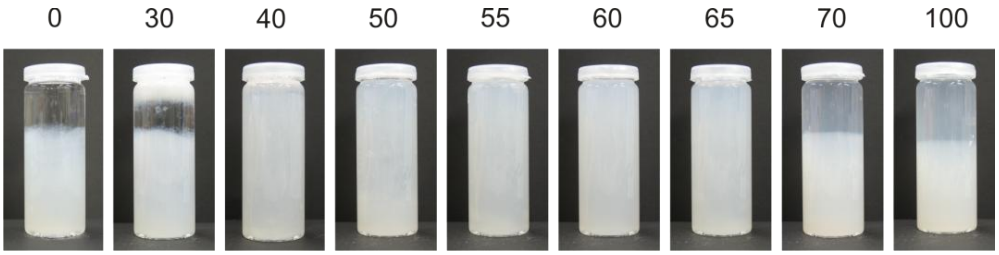

Fig. 24. Visual sedimentation test of montmorillonite PGV® suspended in monomer mixture DN 75 % stabilized with different amounts (wt% referred to clay) of ODD

Sedimentation tests suggested that both modifiers OD and ODD were clearly capable to stabilize the suspension of montmorillonite PGV® in the monomer mixture with DN 75 %. However the required amount of modifier for optimal stabilization of the clay suspension was different. This is due to the composition and structure of the modifiers.

Composition and structure of OD and ODD

OD and ODD were both provided by Procter & Gamble. OD consists of a poly (ethylene imine) network as a core with a single ethylene oxide group at the end of each exterior ethylene imine unit. ODD consists of a poly (ethylene imine) network as a core with an ethylene glycol chain of an approximate chain length of 20 ethylene oxide units attached to each ethylene imine unit (Fig. 25).

a) b)

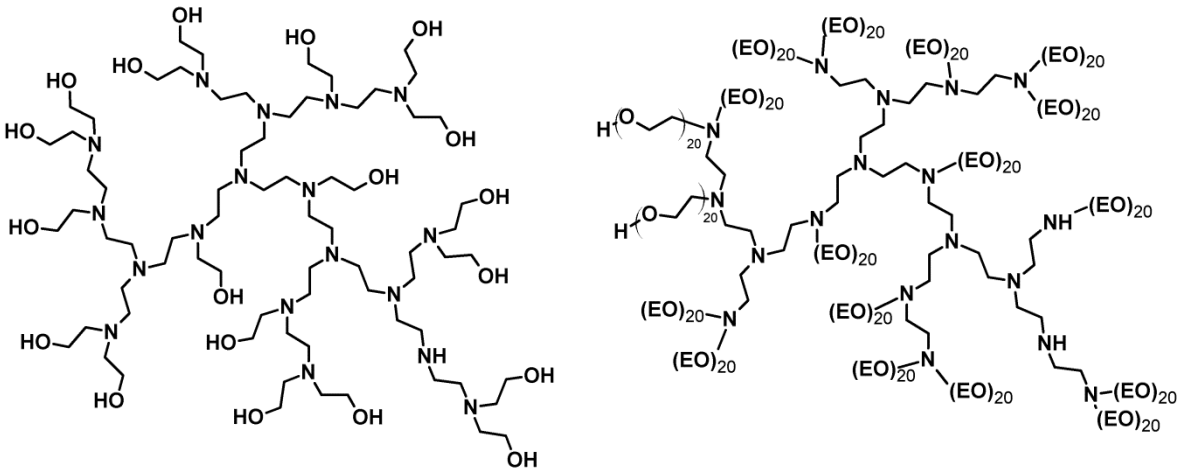

Fig. 25. Structure of a) OD; b) ODD

The poly (ethylene imine) core of both modifiers is readily protonated in acidic media. Hence in the polymerization mixture for the AGM composites, which possesses a pH of 5 or lower, both OD and ODD are polycationic.

After OD and ODD were identified as useful modifiers for the stabilization of montmorillonite PGV® in the monomer mixture with DN 75 %, next the required optimal amount had to be determined.

High affinity of poly (ethylene imine) towards adsorption on clay particles due to the electrostatic attraction of the polycation and the negative basal plane was demonstrated by Öztekin et al.[99] Applying an excess of modifier is therefore expected to induce charge reversal. The visual tests for ODD suggest that excess adsorption might act destabilizing. Streaming potential titrations were carried out to analyze the sign of the charge of the clay surface as a function of modifier applied. Furthermore the stability of the clay dispersions with different amounts of modifier was analyzed via LUMiFuge® measurements.

4.1.2.2 OD as basal modifier for montmorillonite PGV® – quantitative analysis

Aqueous suspensions of montmorillonite PGV® were acidified with acrylic acid to achieve protonation of OD. Therefore, 445 µl of a 11.24 wt% suspension of montmorillonite PGV® were diluted with 8 ml of deionized water and acidified with 2 ml of acrylic acid and subsequently titrated with a 0.5 g / 100 ml solution of OD in deionized water. The streaming potential was recorded as a function of the amount of OD added (Fig. 26).

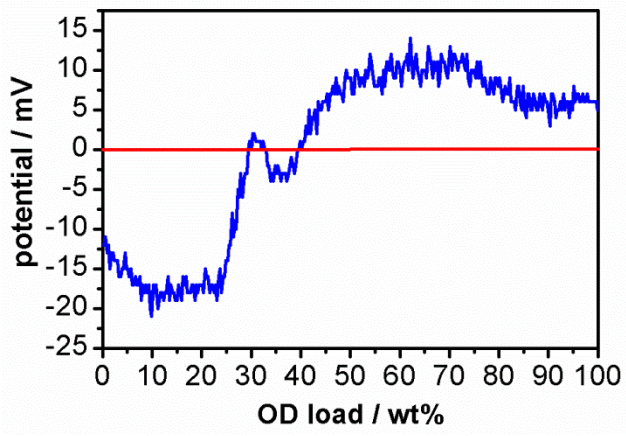

Fig. 26. Streaming potential of montmorillonite PGV® in acidic medium in dependency of the OD load in wt% referred to clay

In acidic aqueous medium, the streaming potential of the clay was negative. With increasing amount of OD, the negative charge of the basal plane was more and more neutralized due to the binding of the polycation OD to the clay surface. At an OD load of approximately 45 wt% OD referred to the clay content, the negative charge was completely covered and a streaming potential of zero was achieved. If the OD amount was further increased, charge reversal of the clay platelets occurs.

The result of the streaming potential titration suggested that for OD a minimum amount of about 45 wt% referred to clay content had to be used to avoid the formation of agglomerates. However the visual sedimentation tests (Fig. 23) suggested that this amount was not sufficient to stabilize the suspension of montmorillonite PGV® when it was dispersed in the monomer mixture with DN 75 %. Consequently, a mere neutralization of the basal charge of the clay was not sufficient to generate a stable clay suspension. The surface of montmorillonite PGV® had to be charge reversed.

Next, LUMiFuge® measurements were carried out to determine the minimum OD amount necessary to guarantee the most stable suspension of montmorillonite PGV® in the monomer mixture with DN 75 %. Transmission profiles were recorded every ten seconds. The transmission profiles at chosen times of centrifugation for different contents of OD in wt% referred to clay were compared (Fig. 27).

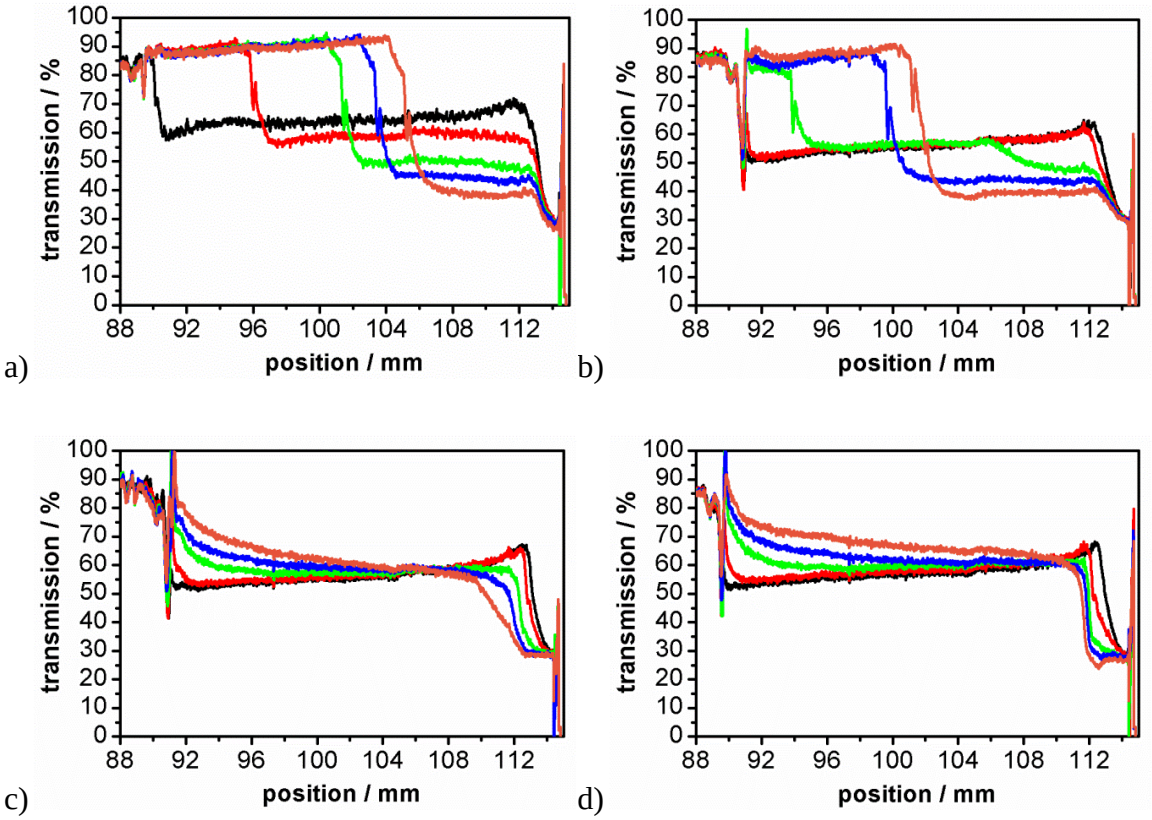

Fig. 27. LUMiFuge® measurements of montmorillonite PGV® suspended in monomer mixture DN 75 %, recorded after: ─ 10 s, ─ 1 min, ─ 5 min, ─ 10 min, ─ 20 min
a) without modifier; b) with 72 wt% OD; c) with 75 wt% OD; d) with 77 wt% OD

Unmodified montmorillonite PGV® (Fig. 27 a)) was still homogeneously dispersed after ten seconds of centrifugation in the LUMiFuge®. After a minute the clay already started settling. With ongoing centrifugation the sedimentation process quickly proceeded. Significantly different results are obtained when OD is added to the clay suspension. The optimum amount of OD was, however, found at much higher concentrations as needed for charge neutrality. With 72 wt% of OD (Fig. 27 b)) sedimentation is clearly slowed down as compared to the unmodified sample but pronounced sedimentation still sets in after 10 min. With 75 wt% (Fig. 27 c)) of OD an optimal sedimentation stability is reached than could not be improved further with 77 wt% OD (Fig. 27 d)).

In summary, OD was found suitable to stabilize the dispersion of montmorillonite PGV® in monomer mixture with DN 75 %. The optimum amount of OD was 75 wt% referred to clay, which was already roughly indicated by the visual sedimentation tests. A modification of montmorillonite PGV® with 75 wt% of OD has already been shown by streaming potential experiments (Fig. 26) to cause charge reversal of the clay platelet. A mere charge neutralization of the negative basal charge was not sufficient to stabilize the

clay suspension. Studies of Fuente et al. concerning flocculation mechanisms and properties induced by high molecular weight poly (ethylene imine) added to calcium carbonate dispersions indicated the same trend.[100] Öztekin et al. also found that increasing poly (ethylene imine) adsorption on a natural Ca-bentonite clay and on Na-bentonite obtained from the Ca-bentonite finally causes charge reversion of the basal plane and prevents coagulation.[99] Charge reversion of bentonite clays by poly (ethylene imine) adsorption was later confirmed via zeta potential measurements.[101]

The high amount of OD required led to the conclusion that due to the high ionic strength of the monomer mixture with DN 75 % charge reversal alone was not the optimal solution for stabilizing suspended clay minerals. An additional steric stabilization could be benefitting and assist the stabilization of the dispersion. The visual sedimentation tests supported this hypothesis, as they suggested that lower amounts of the sterically more demanding ODD modifier are required to stabilize the clay dispersion compared to OD. Quantitative analysis of ODD was next carried out analogously to investigations concerning OD.

4.1.2.3 ODD as basal modifier for montmorillonite PGV® – quantitative analysis

Aqueous dispersions of montmorillonite PGV® were acidified with acrylic acid to achieve protonation of ODD. Therefore, 250 µl of a 9 wt% suspension of montmorillonite PGV® were diluted with 8 ml of deionized water and acidified with 2 ml of acrylic acid and subsequently titrated with a 0.5 g / 100 ml solution of ODD in deionized water. Streaming potential was recorded as a function of the amount of ODD added (Fig. 28).

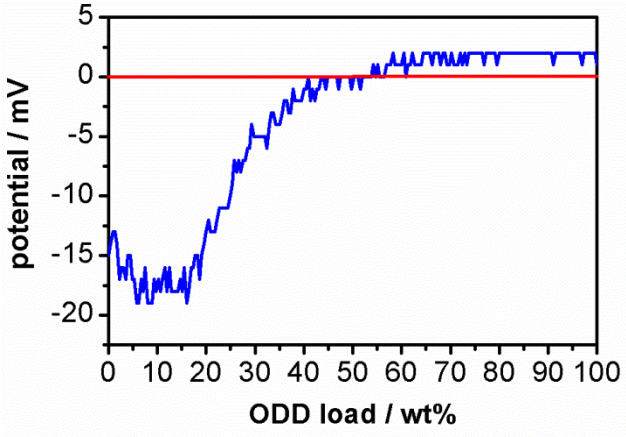

Fig. 28. Streaming potential of montmorillonite PGV® in acidic medium in dependency of the ODD load in wt% referred to clay

With ODD, the negative surface potential of the clay was neutralized when 45 wt% referred to the content of clay were added. However, with further increase of ODD amount, a much lower positive streaming potential was observed as compared to OD. This might suggest that with the better solubility in water and the higher steric demand provided by the PEG side chains, charge reversal of the clay platelets was less pronounced and might even be within the precision of the measurement.

Visual sedimentation tests (Fig. 24) indicate that contrary to OD, with ODD the amount of approximately 45 – 50 wt% needed to neutralize the basal charge could in fact also represent the optimum in respect to stabilization of the clay in the monomer mixture with DN 75 %.

The results of the visual sedimentation tests were quantified by analyzing the suspensions via static light scattering. The particle size distributions were determined at three modifier levels – below, above and an intermediate one of 50 % that later turned out to be very close to the optimal amount of 45% for stabilizing montmorillonite PGV® suspensions (Fig. 29).

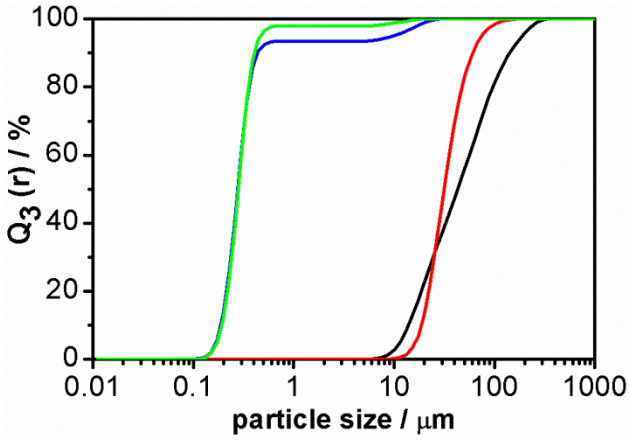

Fig. 29. Particle size distribution of montmorillonite PGV® in monomer mixture DN 75 %
─ unmodified, ─ 20 wt% ODD, ─ 50 wt% ODD, ─ 100 wt% ODD

The particle size distributions for samples prepared with either 20 wt%, 50 wt%, or 100 wt% of ODD referred to montmorillonite PGV® showed that the optimum level of modifier should lie between 20 wt% and 50 wt% to prevent aggregation of particles. At a modifier amount of 50 wt%, already more than 90 vol% of the clay tactoids do not show aggregation.

Quantitative analysis and precise determination of the optimum amount of ODD required for stabilizing montmorillonite PGV® in the monomer mixture with DN 75 % was carried out via LUMiFuge® measurements. Suspensions with different amounts of ODD modifier were prepared and investigated. Transmission profiles of the different samples were recorded every ten seconds. Transmission profiles at chosen times of centrifugation were compared (Fig. 30).

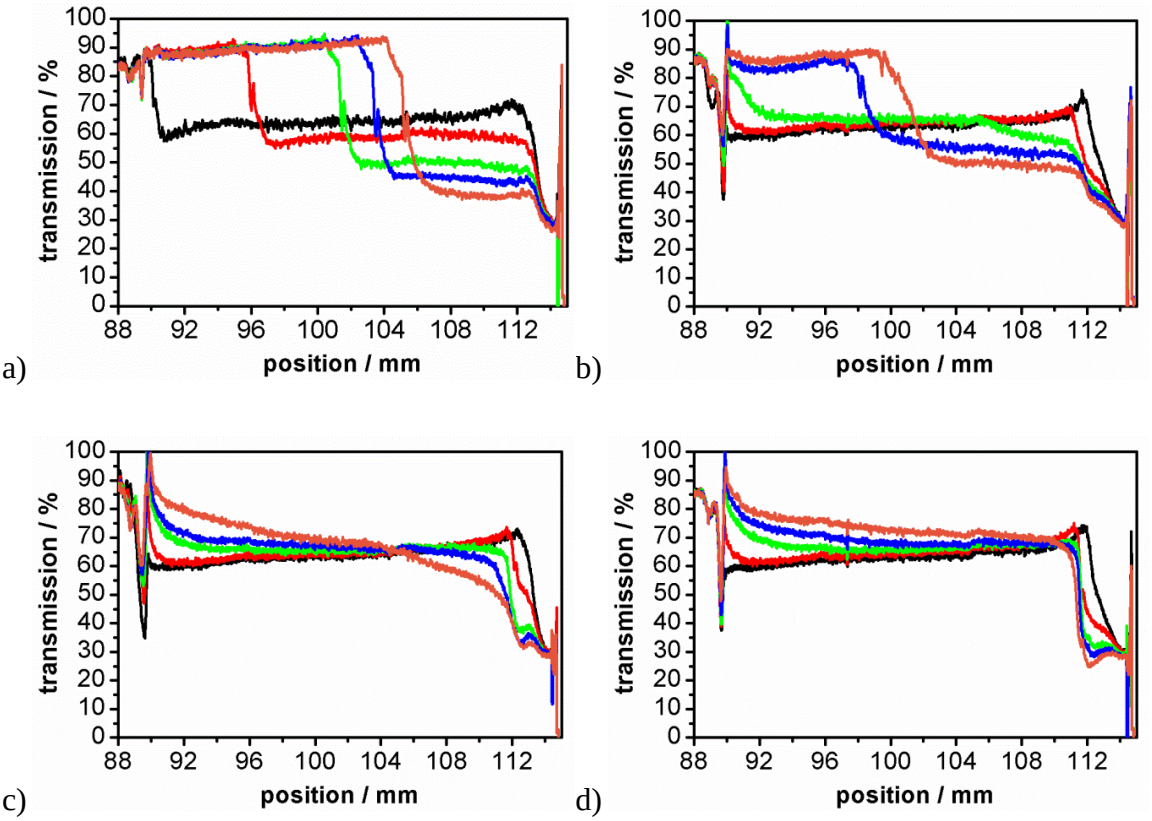

Fig. 30. LUMiFuge® measurements of montmorillonite PGV® suspended in monomer mixture DN 75 %, recorded after: ─ 10 s, ─ 1 min, ─ 5 min, ─ 10 min, ─ 20 min
a) without modifier; b) with 42 wt% ODD; c) with 45 wt% ODD; d) with 47 wt% ODD

The transmission profiles for unmodified montmorillonite PGV® were already discussed but are repeated in Fig. 30 a) to make comparison easier. With ODD lower amounts were needed to approach the optimum stabilization. For 42 wt% ODD referred to clay (Fig. 30 b)) the suspension was already stable during centrifugation for five minutes. Stable dispersions over the whole period of centrifugation were achieved with an ODD amount of 45 wt% or more (Fig. 30 c), d)). The montmorillonite PGV® suspension only slightly clarified during the centrifugation, but sedimentation of particles as it was seen for samples with lower amounts of ODD was not detected.

Summarizing, ODD was identified to be the most suitable modifier for montmorillonite PGV® in respect to maximum stabilization of suspensions in the monomer mixture with DN 75 %. In order to stabilize the clay suspension a minimum ODD amount of 45 wt% referred to montmorillonite PGV® was estimated with the help of LUMiFuge® measurements. This quantity was already indicated by the visual sedimentation tests. At this level of modification the negative clay charge is neutralized as it was demonstrated by streaming potential measurements. In contrast to the modifier OD, with ODD neutralization of the negative clay charge was sufficient to stabilize the clay suspension. Most likely, the (electro-) steric stabilization introduced by the PEG-side chains allowed a significant reduction of the amount of modifier required for optimum stabilization of clay suspension in an environment with high ionic strength as it is present in the monomer mixture.

While it may be safely assumed that ODD will display a similar stabilization efficiency for lithium hectorite, the optimal amount still needs to be determined since the charge density of this clay differs from montmorillonite PGV®.

4.1.2.4 ODD as basal modifier for lithium hectorite – quantitative analysis

First again the variation of the streaming potential of lithium hectorite was studied in dependency of the amount of ODD added to the suspension. Lithium hectorite was presented in acidic suspension that contained acrylic acid to ensure a polycationic nature of ODD. Therefore, 1 ml of a 5 wt% suspension of lithium hectorite were diluted with 8 ml of deionized water and acidified with 2 ml of acrylic acid and subsequently titrated with a 0.5 g / 100 ml solution of ODD in deionized water. Streaming potential was detected while ODD was titrated to the suspension (Fig. 31).

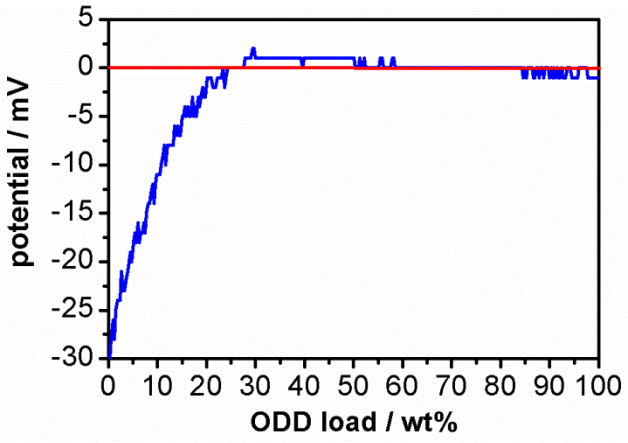

Fig. 31. Streaming potential of lithium hectorite in acidic medium in dependency of the ODD load in wt% referred to clay

The negative streaming potential of pristine lithium hectorite was reduced with increasing ODD content and neutralized at an ODD load of approximately 30 wt% referred to clay. With further addition of ODD, the streaming potential of the clay stayed constant at around 0 mV. This suggests that as with montmorillonite PGV® no significant charge reversal of lithium hectorite was possible with ODD. Since the cation exchange capacity of lithium hectorite is slightly higher than for montmorillonite PGV® (130 meq / 100g and 123 meq /100g, respectively) it is counterintuitive that less ODD was required for lithium hectorite to achieve neutralization of the basal surface as compared to montmorillonite PGV®.

For quantitative analysis of the optimum amount required for stabilization, LUMiFuge® measurements were carried out for samples with different ODD amounts added. Transmission profiles were recorded every 10 seconds. The results at chosen times of centrifugation were compared (Fig. 32).

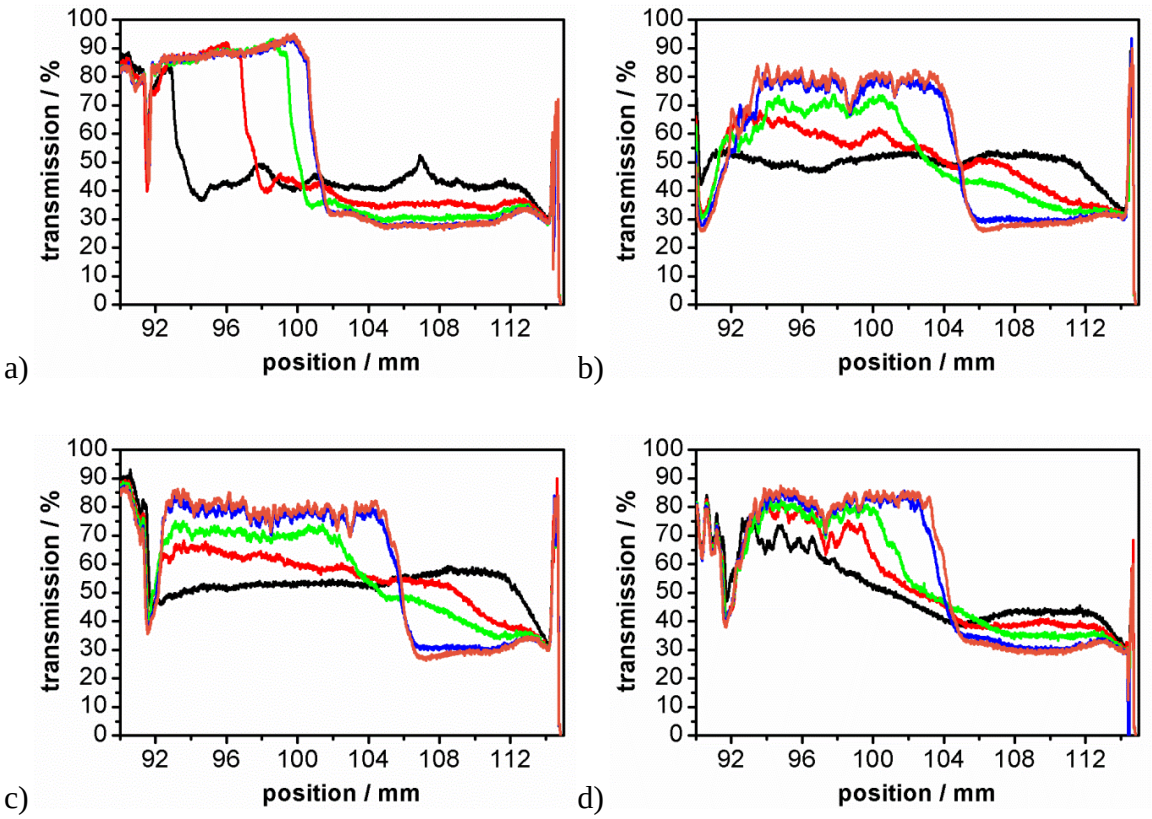

Fig. 32. LUMiFuge® measurements of lithium hectorite suspended in monomer mixture DN 75 %, recorded after: ─ 10 s, ─ 30 s, ─ 1 min, ─ 3 min, ─ 5 min
a) without modifier; b) with 30 wt% ODD; c) with 40 wt% ODD; d) with 50 wt% ODD

The transmission profile of unmodified lithium hectorite is shown in Fig. 32 a). Sedimentation of particles in the monomer mixture with DN 75 % was detected already after 30 seconds and was almost completed after only a minute of centrifugation. With the addition of ODD the sedimentation of lithium hectorite was significantly slowed down. However, as expected for such large particles, sedimentation is never suppressed completely as for montmorillonite PGV®. Although a clear stabilization effect was established for lithium hectorite ODD amounts exceeding 30 wt% referred to clay (Fig. 32 b),c),d)), no clear difference among the particular samples was detected. Due to the large diameter of primary particles, the scattering power of agglomerates is not significantly higher and therefore the differences might be masked. It is, nevertheless, still likely that agglomeration was also greatly suppressed by ODD modification. In any case it seems that even for this coarse grained clay, sedimentation is sufficiently retarded to suppress sedimentation of the filler during polymerization periods and will thus allow obtaining AGM with homogenously distributed fillers.

Since anyhow no differences were noted, the amount of ODD applied to modify lithium hectorite was chosen to be at the same level of 45 wt% as proven optimal for montmorillonite PGV®. This way, samples with identical compositions but different clay mineral could be directly compared and the mere effect of higher or lower aspect ratios could be studied.

In conclusion, for both clays, montmorillonite PGV® and lithium hectorite, modification of the clay was essential to provide stable dispersions in the monomer mixture. For both clays edge modification showed a positive effect on the agglomeration behavior. However, agglomeration could not be completely avoided. Due to the high ionic strength of the monomer mixture, lamellar agglomeration of the clay particles occurred. Hence a suitable modifier for basal modification was identified and the minimum necessary amount for stabilization of the clay minerals in the monomer mixture was determined. The sterically demanding modifier ODD delivered stable and homogeneous dispersions of the clay minerals at a level of 45 wt% referred to clay content. Since sufficient stabilization could be obtained solely with basal modification, we abstained from additional edge modification to minimize addition of non-absorbing / capacity-hampering mass to the gel formulations.

4.2 Enhancement of the gel strength of bulk AGM

Incorporation clay minerals as filler into the bulk AGM should cause enhancement of the gel strength of AGM in two ways:

(1) Homogenization of the distribution of crosslinking points
(2) Enhancement of Young's -modulus by incorporation of filler materials

Homogeneous distribution of crosslinking points

As already stated in the introduction, a key factor for designing an AGM with high swelling capacity and high gel strength is crosslinking. One aspect thereof is the crosslinking density. Higher crosslinking density leads to less swelling capacity and higher gel strength. The crosslinking density is easily adjustable by the varying the amount of added crosslinker to the polymerization mixture. A second and trickier aspect is the homogeneity of crosslinking. Maximum swelling capacity and gel strength would be found in an ideal polymer network. No irregularities like loops, loose chain ends, or entanglements would occur in this network and the crosslinking points are uniformly distributed. Consequently, the AGM will swell equally in every dimension until each single polymer chain between crosslinking points is equally stressed and fully extended.

For AGM composites with clay minerals as filler, crosslinking density is regulated by the content of organic crosslinker and the clay mineral. In order to provide a uniform crosslinking, the clay mineral has to be homogeneously distributed in the AGM composite polymer. Dispersion of the clay mineral and maximization of the sedimentation stability was extensively discussed in section 4.1.

Enhancement of Young's -modulus by incorporation of filler materials

Enhancement of the Young's -modulus of polymers by incorporation of filler materials of different kinds and shape, e.g. like spheres, fibers, hollow fibers or platelets is reported numerous times in literature for diverse polymer matrices, from elastic hydrogels to bulk metallic glass materials with high toughness. Theories have been developed to predict potential reinforcing effects of filler materials, e.g. the Halpin-Tsai equations. The Halpin-Tsai equations enable calculating the reinforcement that might be realized as a function of the volume fraction of the filler, the relative Young's -moduli of the components, and the geometry of the filler. The latter is a crucial parameter and hence the

aspect ratio of the filler is the most important property of the filler.[49] As mentioned before, lithium hectorite or Montmorillonite PGV® differ most significantly in respect to their aspect ratio and therefore comparison of the two types of fillers will allow judging the importance of filler reinforcement on AGM performance.

After establishing basal surface modifications that yield stable and homogeneous suspensions of the clay minerals in AGM polymerization mixtures, AGM composites were synthesized containing lithium hectorite or montmorillonite PGV®. Additionally, reference samples without filler were prepared for comparison. By variation of the crosslinker content of the reference samples a tradeoff line was established. The effect of incorporation of clay minerals on swelling capacity and gel strength of AGM hydrogels was then investigated and evaluated in respect to the tradeoff given by the reference samples.

4.2.1 Analysis of the mechanical properties of fully swollen hydrogels

The quality of AGM is defined by its swelling ability and the corresponding gel strength at capacity or as a function of intermediate saline load. Both variables are inversely related, as gels with higher swelling degree are softer and hence their gel strength is low.

Calculation of the maximum swelling capacity

The maximum swelling capacity is defined as the amount of saline (0.9 wt%) in gram that can be absorbed per gram of dry AGM. The maximum capacity was calculated with following formula:

$$capacity = \left(\frac{m_{swollen}}{m_{as\ prep} * \ \sigma}\right) - \ 1 \qquad (10)$$

$$\sigma = \frac{m_{dry}}{m_{as\ prep}} \qquad (11)$$

A piece of the as-synthesized gel was weighed to get $m_{as\ prep}$. The same gel piece then was swollen to equilibrium as described in section 3.4.1 and weighed again to get $m_{swollen.}$ σ is

the solid content of the material and calculated by weighing a piece of gel directly after the synthesis to get $m_{as\ prep}$ and the same gel piece after complete drying to get m_{dry}.

Evaluation of the gel strength

For initial evaluation of the gel strength of the AGM samples, the method of measuring "very low rubber hardness" (VLRH) was chosen. The fully swollen hydrogels were investigated after determining $m_{swollen}$ with the indenter with a diameter of 16.2 mm.

4.2.1.1 Success criterion – trade off curve

Reference samples without filler and varying amounts of organic crosslinker were synthesized according to the procedure described in section 3.1.1. The following compositions were chosen for AGM reference gels:

- Acrylic acid 20 wt% referred to batch size
- Sodium hydroxide 75 mol% referred to acrylic acid
- KPS 0.1 mol% referred to acrylic acid
- TEMED 0.05 mol% referred to acrylic acid
- MBAA 0.3 – 1.3 mol% referred to acrylic acid

By analyzing the maximum swelling capacity and the VLRH value of the resulting samples a trade off curve is developed that serves as threshold for the AGM composites (Fig. 33).

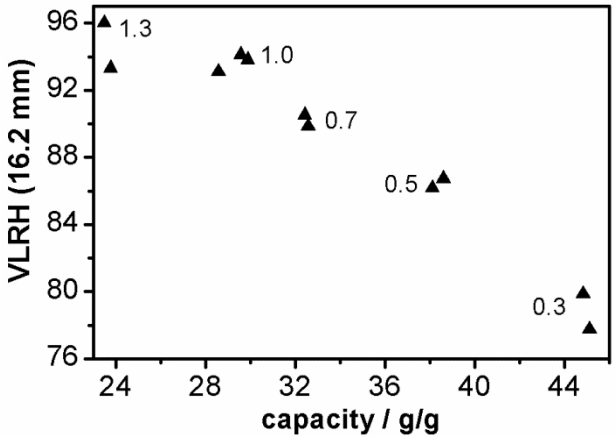

Fig. 33. VLRH vs. capacity for bulk AGM with various content of crosslinker in mol% referred to acrylic acid

Crosslinking density, which was controlled by the amount of crosslinker added to the reaction mixture, affected swelling capacity and gel strength in the expected way. High

crosslinking level resulted in a stiff hydrogel with high VLRH value but low maximum swelling capacity. The polymer chain length in between two crosslinking points was short. Hence the flexibility of the hydrogel was low which led to a stiff hydrogel with restricted swelling ability. With decreasing crosslinking density, the bulk AGM got softer and the VLRH value decreased. The chain length in between two crosslinking point increased more and more, which causes higher flexibility of the polymer network. Consequently the VLRH value for the AGM reference samples decreased while at the same time the maximum swelling capacity increased.

By incorporation clay minerals the stiffness of the AGM should be enhanced and the trade off line should be surpassed if the loss in capacity is disproportionately smaller. The synthesized AGM composites with either montmorillonite PGV® or lithium hectorite as filler were compared to mentioned reference samples.

4.2.1.2 Analysis of AGM composites containing montmorillonite PGV®

AGM composites were synthesized applying the modifier amount defined in section 4.1. The following parameters were chosen for the AGM composites:

- Montmorillonite PGV® 5 wt% vs. solids
- Modifier amount 45 wt% referred to clay content
- Acrylic acid 20 wt% referred to batch size
- Sodium hydroxide 75 mol% referred to acrylic acid
- KPS 0.1 mol% referred to acrylic acid
- TEMED 0.05 mol% referred to acrylic acid
- MBAA 0.3 mol% referred to acrylic acid

The maximum swelling capacity was calculated for each sample and the VLRH values were determined. The results were examined in comparison to the trade off line (Fig. 34).

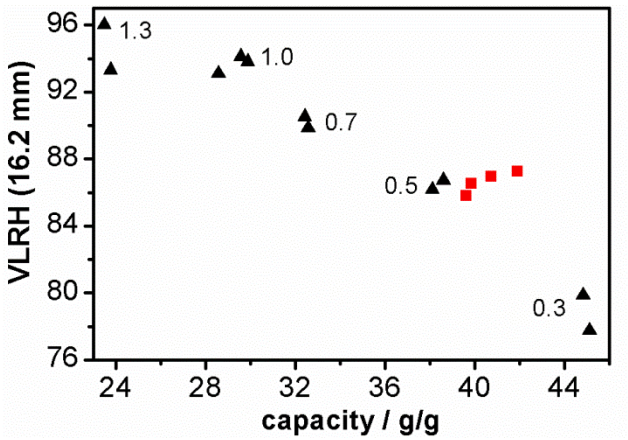

Fig. 34. VLRH vs. capacity for the ■ AGM montmorillonite PGV® composite samples in comparison to ▲ bulk AGM with various content of crosslinker in mol% referred to acrylic acid

Regarding the maximum swelling capacity, the AGM composite showed a decrease compared to the reference AGM with the same crosslinking density of 0.3 mol% referred to acrylic acid. As the capacity is defined as the uptake of saline in gram per solid AGM in gram, an approximate 7 – 8 % decrease of the maximum swelling capacity was actually expected as the incorporated filler and filler modifier replace 7 – 8 % of the superabsorbent AGM. This is because the clay mineral amounted to 5 wt% of the solid content and the content of modifier was 2.25 %. Clay minerals exhibit some swelling ability, which is caused by hydration of the cations in the interlayer space of the tactoids.[102,103] However, compared to the extraordinary swelling ability of bulk AGM the clays' swelling ability is negligibly small. However, the swelling capacity decreased more than what would have been expected from the inert mass of filler added. The maximum swelling capacity decreased from an average of 45 g/g for the reference sample to an average of 40.5 g/g for the montmorillonite PGV® AGM composite, which corresponds to a loss of capacity of 10 %. This means, swelling capacity is not only lost by replacing parts of the superabsorbent polymer by non-swellable material. Swelling appears to be also restricted by addition of the clay mineral montmorillonite PGV®.

Comparing the VLRH value of bulk AGM and the AGM composite, in agreement with expectations a clear mechanical reinforcement of the hydrogel was observed. The VLRH value was increased from an average of 79 for the reference sample with a crosslinking amount of 0.3 mol% referred to acrylic acid to an average of 87 for the montmorillonite PGV® AGM composite. The VLRH value of the montmorillonite PGV® composite hence was approximately 10 % higher than the VLRH value of the bulk AGM. The intended increase of the gel strength by incorporating the clay mineral was achieved.

Regarding the trade off curve which is defined by the data of the reference samples, an improvement of the material's mechanical properties could be detected. Compared to the reference at equal VLRH value corresponding to a crosslink amount of 0.5 mol%, an enhancement of the maximum swelling capacity from 38.4 g/g to 40 - 42 g/g is achieved, which is an improvement of about 5 – 10 %. This means, the loss of maximum swelling capacity of the nanocomposite was compensated by a disproportionate increase of the gel strength.

4.2.1.3 Analysis of AGM composites containing lithium hectorite

AGM composites incorporating lithium hectorite were synthesized with the modifier amount defined before. The following parameters for the AGM composite were chosen:

- Lithium hectorite 5 wt% vs. solids
- Modifier amount 45 wt% referred to clay content
- Acrylic acid 20 wt% referred to batch size
- Sodium hydroxide 75 mol% referred to acrylic acid
- KPS 0.1 mol% referred to acrylic acid
- TEMED 0.05 mol% referred to acrylic acid
- MBAA 0.3 mol% referred to acrylic acid

The maximum swelling capacity was calculated for each sample and the VLRH values were determined. The results were examined in comparison to the trade off line (Fig. 35).

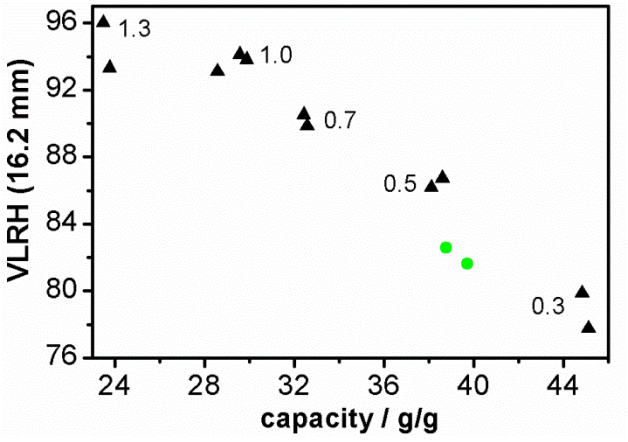

Fig. 35. VLRH vs. capacity for the ● AGM lithium hectorite composite samples in comparison to ▲ bulk AGM with various content of crosslinker in mol% referred to acrylic acid

The AGM lithium hectorite nanocomposite also showed lower swelling ability than the corresponding AGM with the crosslinking level of 0.3 mol%. The swelling ability was reduced from an average of 45 g/g for the reference sample to 39.7 g/g for the lithium hectorite AGM composite, which was a loss of swelling capacity of 12 %. Analogous to the montmorillonite PGV® composite, part of the swelling ability was lost due to the replacement of highly swellable AGM by clay mineral and modifier. Furthermore, beyond this dilution effect an additional swelling restriction was observed by incorporation of lithium hectorite. Lithium hectorite restricted the maximum swelling capacity even more than montmorillonite PGV® which might be ascribed to the higher aspect ratio.

The VLRH value of the lithium hectorite AGM nanocomposite was found at an average of 82. Hence again an enhancement of the gel strength was observed when comparing the lithium hectorite AGM composite with the reference sample of the same crosslinking density which exhibited a VLRH of 79. However the increase in VLRH amounted to less than 5 %. Contrary to expectations based on Halpin-Tsai equations, the mechanical reinforcement achieved by incorporating lithium hectorite was lower than for incorporating montmorillonite PGV® into the AGM polymer.

The capacity and VLRH properties of the lithium hectorite AGM composite are found below the trade off curve determined by the reference samples.

AGM composites made with both types of clay showed a reduction of the maximum swelling capacity. Swelling capacity is not only lost by replacing part of the superabsorbent polymer by less-swellable material. Swelling is restricted beyond this dilution effect by addition of clay minerals and this is more pronounced for higher aspect ratio fillers. Regarding the montmorillonite PGV® AGM composite, this loss in the maximum swelling capacity was compensated by an increase in the gel strength of the hydrogel. By combining both effects it was possible to beat the trade off curve. While the lithium hectorite AGM composite also showed some mechanical reinforcement as compared to the sample with the same amount of organic crosslinker, surprisingly the gain in gel strength was, despite the much larger aspect ratio, less pronounced for the lithium hectorite AGM composite as for the montmorillonite PGV® AGM composite. Consequently, in combination of gel strengthening and swelling reduction, the lithium hectorite AGM composite even ended up below the trade off curve.

4.2.2 Analysis of the mechanical properties of partially swollen hydrogels

AGM are hardly ever really swollen to full capacity when applied in hygiene products. It is therefore necessary to check whether the trend that was established for the mechanical reinforcement of fully swollen hydrogels would also be confirmed for the intermediate swollen state. It was decided to explore the capacity – gel strength tradeoff behavior of the samples at equal intermediate swelling degrees. Consequently, both AGM composites with either montmorillonite PGV® or lithium hectorite as filler were swollen to different degrees of swelling (x-load) and compared to the corresponding reference sample.

Calculation of the swelling capacity

Swelling of the samples with intermediate x-load was carried out as described in section 3.4.1. After equilibration for 10 – 14 days in the zip lock bags at room temperature the swollen samples were weighed and the exact degree of swelling was calculated.

Evaluation of the gel strength

The VLRH method could also be applied for judging the gel strength of the AGM samples with intermediate swelling state. The method validation executed in cooperation with Procter & Gamble showed, that the measurements done with the indenter with a diameter of 16.2 mm were restricted to samples that delivered a VLRH value smaller then 85. For samples of higher stiffness the use of an indenter with a smaller diameter was recommended to achieve higher sensitivity in this measurement range. For samples with low x-load, high VLRH values were expected. Therefore, the indenter of the VLRH device was exchanged and an indenter with a diameter of 10 mm was used for the analysis of intermediate swollen samples. Additionally to the intermediate swollen samples also the fully swollen hydrogel was measured with the smaller indenter.

4.2.2.1 Analysis of AGM composites containing montmorillonite PGV®

Analysis of AGM composites at intermediate swelling state was carried out with montmorillonite PGV® AGM composites of identical composition as the samples studied in fully swollen state. The composition of the montmorillonite PGV® AGM composite is described in section 4.2.1.2.

The VLRH values for the different x-loads of montmorillonite PGV® AGM composite were compared to the corresponding reference AGM with a crosslinking amount of 0.3 mol% referred to acrylic acid (Fig. 36).

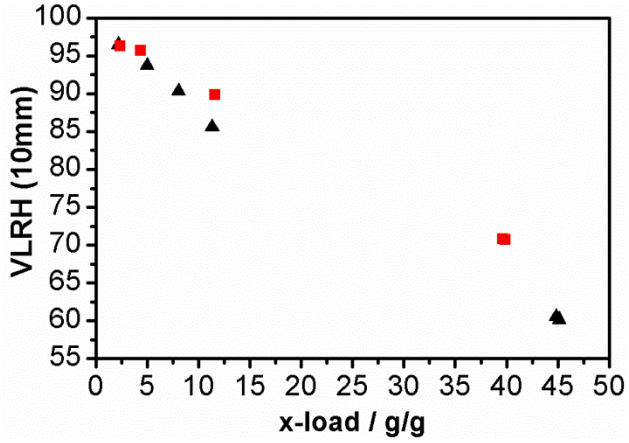

Fig. 36. VLRH vs. x-load for the ■ montmorillonite PGV® AGM composite in comparison to ▲ bulk AGM with the same crosslinking content

As the smaller indenter (10.0 mm) is more sensitive, the differences in the gel strength of the AGM composite and the reference sample appear more pronounced. For instance, the VLRH value of the montmorillonite PGV® AGM composite at fully swollen state was 20 % higher than the VLRH value of the reference sample as compared to 10 % found with the larger indenter.

The sample with an x-load of approximately 2.5 g/g exhibited no significant difference in the VLRH value. All montmorillonite PGV® nanocomposites at higher x-load were, however, found above the corresponding non-filled AGM. With increasing saline uptake, the reinforcing effect of the montmorillonite PGV® became increasingly obvious. Apart from the higher accuracy of the VLRH method values between 90 and 60, this is in line with expectations from Halpin-Tsai equations. With increasing swelling the gel becomes softer and the correspondingly increasing ratio of the moduli of filler and matrix predicts increasingly better relative reinforcements.

4.2.2.2 Analysis of AGM composites containing lithium hectorite

Analysis of AGM composites at intermediate swelling state was carried out with lithium hectorite AGM composites of identical composition as the samples studied in fully swollen state. The sample composition is described in section 4.2.1.3.

The exact x-load after swelling in the zip lock bag for ten days was calculated and the VLRH values for each sample were determined and compared to the specified value for the corresponding reference AGM with a crosslinking amount of 0.3 mol% referred to acrylic acid (Fig. 37).

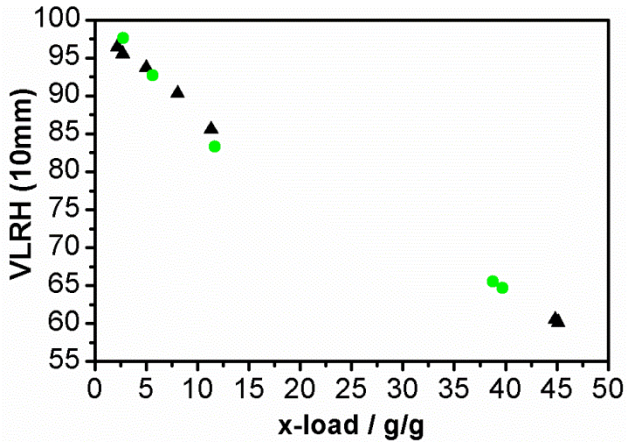

Fig. 37. VLRH vs. x-load for the ● AGM lithium hectorite composite in comparison to ▲ bulk AGM with the same crosslinking content

Again, the enhancement of the gel strength of the hydrogel as measured with the 10.0 mm indenter appeared stronger due to increased sensitivity. The VLRH value of the nanocomposite at fully swollen state showed an increase of about 10 % in comparison to the reference sample as compared to approximately 5 % found with the larger indenter. Regardless of the indenter, the performance of the fully swollen lithium hectorite AGM composite was found below the trade off curve, as already demonstrated in section 4.2.1.3.

At low swelling degrees analysis of the intermediately swollen hydrogels revealed slightly higher modulus of the AGM lithium hectorite composite compared to the reference sample. The AGM composite with an x-load of approximately 2.5 g/g exhibited a higher VLRH value than the reference AGM. With increasing swelling degree a crossover was observed at a swelling degree calculated at approximately 5.5 g/g. AGM composites swollen to x-loads higher than 5.5 g/g showed lower Young's -moduli than the reference AGM with identical amount of organic crosslinker.

4.2.3 Discussion of possible failure mechanisms of the AGM – composite system

Contrary to montmorillonite PGV®, at higher swelling degrees lithium hectorite filled AGM underperforms the trade off curve. This deviation from expectations for the larger aspect ratio lithium hectorite suggests that the stress transfer from the matrix to the nanofiller might be failing at some point. It is known, that incompatible fillers decrease the Young's -modulus and gel strength of nanocomposites compared to the unfilled reference. Since the quality of compatibilization is the same for both clays and does change in the same way with swelling, it is still a riddle why stress transfer works better with montmorillonite PGV®. The two materials differ in respect to three parameters: 1. While both materials show in plane moduli > 150 GPa [104], lithium hectorite is more sensitive to the acidic environment and might be weakened by acid activation. 2. The lateral extension of lithium hectorite is an order of magnitude higher than for montmorillonite PGV®. Consequently, only lithium hectorite might be large enough to negatively influence the crosslinking network during polymerization. 3. Since the weight content of the filler was kept at comparable values, for montmorillonite PGV® the number of independent particles is several orders of magnitude higher than for lithium hectorite. This in turn will influence the stress developed at a single filler platelet during the swelling process. During the swelling process, the volume of the hydrogel samples increased by ~ 1.5 orders of magnitude. In case a cavity is included in the hydrogel, it would increase its size proportionally together with the hydrogel matrix upon swelling to satisfy geometrical requirements for uniform swelling (Fig. 38 a)).

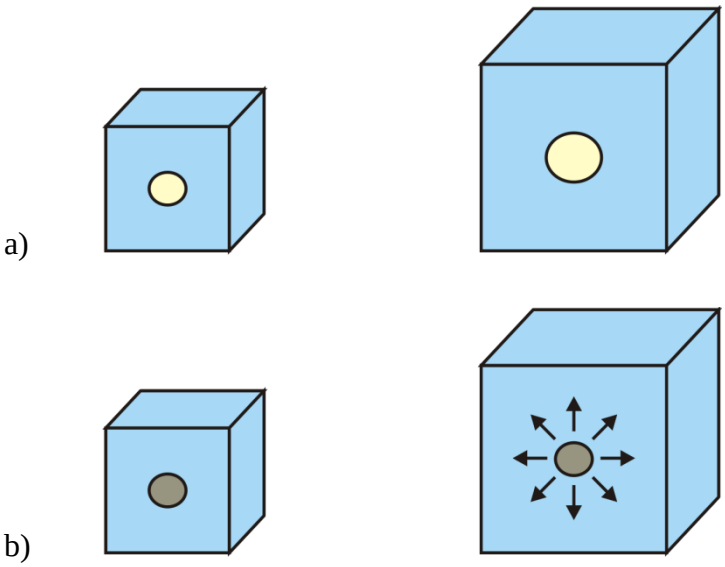

Fig. 38. Swelling of hydrogels a) including an air bubble; b) including a filler

If a hard and indeformable filler particle is included into the hydrogel, expansion upon swelling causes stress at the interface of polymer matrix and filler (Fig. 38 b)). The stress induced during swelling can cause failure of the composite material. Several mechanisms of failure are possible and are discussed in more detail as follows.

In respect to the location of failure, three different types of failure may be identified:

- Failure of the filler
- Failure of the matrix
- Failure of the interface due to insufficient stress transfer

Failure of the filler

A first potential location for failure of the AGM composite is the filler itself. In case of the clay minerals, either breakage or (partial) dissolution of the clay platelets may occur.

Due to the comparatively high strength of the clay tactoids, breakage of the tactoids appeared very unlikely as the implemented forces during the swelling process and the VLRH measurement were too small to cause rupture of the clay tactoids.

Clay minerals are sensitive towards acidic and basic media and dissolve if the environment gets too harsh.[105-108] The progress of the dissolution is depending on the pH of the suspension medium and the composition of the particular clay. Hectorites show a much higher PZC and therefore are considerably more sensitive to acid attack compared to montmorillonite. At a pH = 5 of the polymerization mixture, slightly elevated temperature and typical synthesis and polymerization times of 45 min., dissolution of the lithium hectorite may not be negligible anymore while montmorillonite PGV® is expected to be much more robust. It is, however, very unlikely even for lithium hectorite that the strength of the clay platelet would be so much deteriorated that the clay platelet would rupture.

The mechanical strength of agglomerates would, however, be much lower as compared to clay platelets themselves. Agglomerates formed by insufficient stabilization by the chosen surface modifier would serve as possible points of failure. Due to the largely differing sizes of lithium hectorite and montmorillonite PGV®, it was difficult to judge whether the same degree of stability towards agglomeration could be achieved for both fillers since force sedimentation tests applied to judge agglomeration stability are always

overlapped by sedimentation stability which is of course largely dependent on the size of the clay platelets. Not surprisingly, montmorillonite PGV® with a diameter of 260 nm showed much higher stability towards sedimentation in the monomer mixture with DN 75% compared to the lithium hectorite with a diameter of 12 μm when both clays were modified with the same stabilizing agent ODD. This fact was also reflected by the conditions chosen for the LUMiFuge® measurements. While for the lithium hectorite the slowest speed of centrifugation of 300 rpm was selected, montmorillonite PGV® required a speed of 2000 rpm in order to observe sedimentation in a decent period of time. Even for short periods of centrifugation the sedimentation stability of the modified lithium hectorite appeared inferior as apparent from the transmission profiles.

Failure of the matrix

A second potential location for failure of the AGM composite system is the matrix: the polymer network. Failure of the polymer network means cleavage of C – C bonds of the polymer. As discussed in some detail in the introduction, the gel strength of the polymer network is mostly determined by the distribution of the crosslinking points. The very large lithium hectorite platelets might indeed suppress crosslinking over large areas excluded by the clay, resulting in a less homogenous crosslinking network and locally reduced gel strength. At the same time the capacity of the AGM would be reduced in the volumes with increased crosslinking density. The detrimental effect would not show up at low degrees of swelling as long as no chains are fully stretched. While this reasoning would be capable to explain both the differences with the two clays and the crossing of the trade off curve with lithium hectorite it is difficult if not impossible to be verified experimentally.

Failure of the interface due to insufficient stress transfer

Finally, failure at the interface of filler and matrix can occur in different ways:

- Failure of the modifier itself
- Failure at the interface of modifier and filler
- Failure at the interface of modifier and polymer network

Since the total stress generated by swelling can always be dissipated more efficiently by a much higher number of particles due to the larger specific interface area for AGM

composites of montmorillonite PGV® as compared to lithium hectorite while the type and strength of interaction at the various potential failures is comparable, the latter material will always be affected more severely.

Failure of the modifier itself

Failure of the modifier is comparable with the failure of the polymer network. The strength of chemical bonds in the modifier is comparable with the ones in the matrix and therefore chances of failure are comparable to pristine AGM. Insufficient chemical stability of the modifier can also be ruled out as failure mechanism as all types of bonds found within the modifier are stable in the polymerization environment.

Failure at the interface of modifier and filler

The probability of failure at this interface is depending on the interaction of the modifier to the filler. The modifier ODD interacts with the clay minerals via electrostatic interactions. The adsorption of ions on charged surfaces is a reversible process. Competing interactions in this context would have been cation exchange of the ODD against cations present in the monomer mixture, sodium and protons, which both are monovalent. At the pH of the monomer mixture with DN 75 %, the modifier was polycationic. Hence the interacting forces of the ODD with the negatively charged basal plane of the clay were much stronger than the interactions of sodium or protons with the clay surface. Partial exchange for sodium or proton and partial “debonding” of ODD is therefore very unlikely. Failure at this interface appears rather unlikely. Moreover, the charge densities of montmorillonite PGV® and lithium hectorite are too similar to explain the different behavior of composites of these two fillers.

Failure at the interface of modifier and polymer network

The most likely location for failure is the interface of the modifier with the polymer network. This interface lacks covalent bonding and relies on van der Waals and hydrogen bonding to transfer stress. In case of the modifier ODD and the poly (acrylate co acrylic acid) polymer, the dominant interaction is hydrogen bonding between the hydroxyl groups of the ODD and the acrylate groups of the polymer. The interaction across this interface nevertheless is the weakest of all possible failure planes discussed, possibly with the exception of agglomerate disruption.

Strengthening the interaction between modifier and matrix therefore appears the most promising measure to improve stress transfer. In this line, the hydroxyl groups of the modifier were functionalized to allow covalent linkage of the filler with the polymer network. Since for reasons mentioned before, analytics in respect to dispersion quality are more meaningful for montmorillonite PGV®, attempts to improve stress transfer by covalent linkage was restricted to this filler.

4.2.4 Covalent linking of the modifier to AGM polymer

The modifier, which is electrostatically bound to the clay surface, was functionalized with a double bond in order to prevent a possible mechanical failure between AGM matrix and filler. The introduction of a double bond (Fig. 39) enables covalent incorporation of the modifier into the polymer backbone. Ideally, in this way the capacity of AGM should not be diminished while the covalent linkage of the modifier (and indirectly the clay mineral) to the polymer backbone should lead to higher gel strength of the hydrogel. Since the clay platelets carry modifiers on both sides, however, additional crosslinking points are introduced that are mediated via the clay by electrostatic forces.

The modifier was functionalized by adding allylglycidyl ether to the alcohol groups at the end of the ethoxy chains surrounding the poly (ethylene imine) core (Fig. 39).

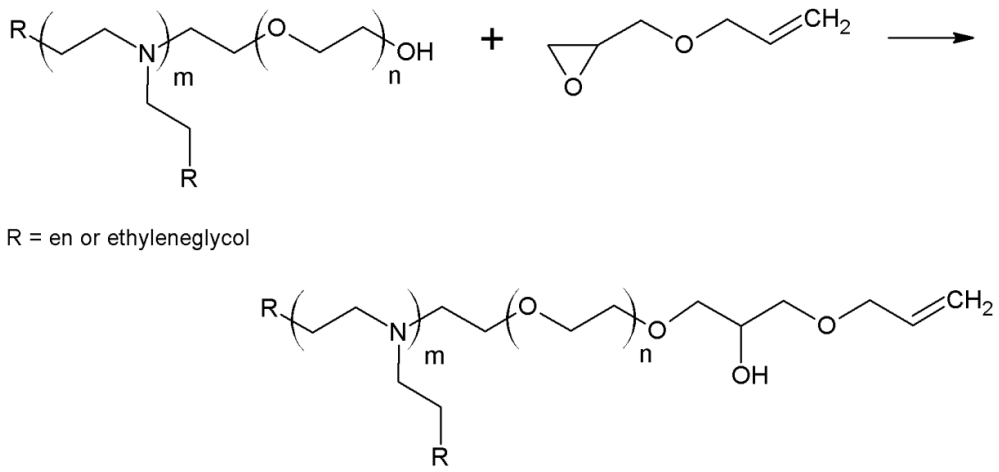

Fig. 39. Functionalization of ODD with Allylclycidyl ether

The functionalized ODD was named Allyl-ODD. The synthesis was carried out at the chair for Organic Chemistry at the University of Bayreuth by Bernhard Biersack. Since the pristine ODD represents a commercial product that is not well defined in respect to

molar mass and the particular length of the ethoxy chains, the analytics for Allyl-ODD were restricted to ^{1}H NMR and ^{13}C NMR spectroscopy and C,H,N elementary analysis. The degree of functionalization of ethoxy chains achieved was estimated to be approximately 30 %. As the chemical structure of ODD and Allyl-ODD were quite different, it was expected that the surface properties of the modifier would have been significantly altered by the functionalization as well. Consequently, the stability of clay dispersions modified with Allyl-ODD had to be reevaluated.

As for ODD, as a first step, visual sedimentation tests were carried out. Montmorillonite PGV® was modified with different amounts of Allyl-ODD and dispersed in the monomer mixture with DN 75 % (Fig. 40).

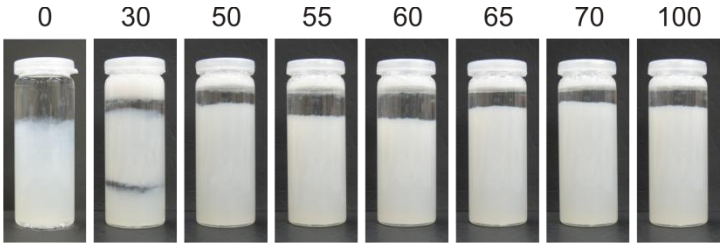

Fig. 40. Visual sedimentation test of montmorillonite PGV® suspended in monomer mixture DN 75 % stabilized with different amounts of modifier Allyl-ODD in wt% referred to clay

Visual evaluation of sedimentation suggested that Allyl-ODD fails to stabilize the dispersion of montmorillonite PGV® in the monomer mixture with DN 75 %.

Since for visual sedimentation tests the samples were left for sedimentation overnight, it remains unclear if some stabilization of the clay mineral is achieved at shorter periods of time. Therefore, LUMiFuge® measurements were executed to quantify the effect of Allyl-ODD on the montmorillonite PGV® suspensions.

Several suspensions of montmorillonite PGV® modified with different amounts of Allyl-ODD in monomer mixture with DN 75 % were prepared. The concentration of montmorillonite PGV® was 1 wt%. Transmission profiles were recorded every ten seconds. As discussed before, the unmodified montmorillonite PGV® started settling after short time of centrifugation and already after one minute the clay has been completely removed from some 30 % of the suspension by sedimentation (Fig. 41 a)). With addition of increasing amounts of Allyl-ODD as modifier, the stability of the suspension improved. A uniform distribution of montmorillonite PGV® could be achieved over longer periods of time. The most stable suspensions were obtained with an

Allyl-ODD content between 40 wt% and 50 wt% referred to clay content. In this case, the suspension appeared homogeneous for more than five minutes of centrifugation. However, stability of suspension over the whole period of the measurement of 20 minutes, like it was observed for neat ODD modification, could not be reproduced for Allyl-ODD.

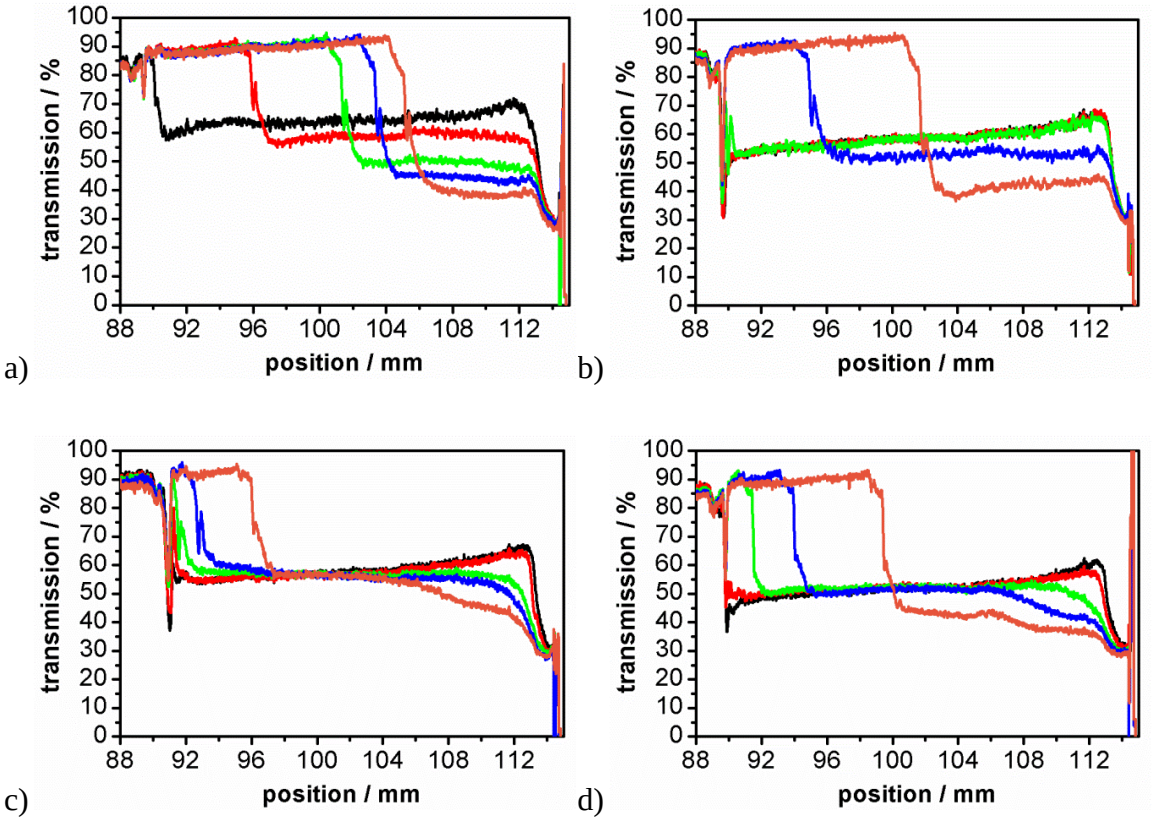

Fig. 41. LUMiFuge® measurements of montmorillonite PGV® suspended in monomer mixture DN 75 %, recorded after: ─ 10 s, ─ 1 min, ─ 5 min, ─ 10 min, ─ 20 min
a) without modifier; b) with 40 wt% Allyl-ODD;
c) with 50 wt% Allyl-ODD; d) with 55 wt% Allyl-ODD

Summarizing, Allyl-ODD showed an improvement of the sedimentation stability of the unmodified montmorillonite PGV® suspensions in the monomer mixture with DN 75 %. However, the sedimentation stability was in any case inferior compared to suspensions of montmorillonite PGV® modified with neat ODD.

Analysis of AGM composites containing Montmorillonite PGV®, stabilized with Allyl-ODD

The influence of covalent linkage of modifier and polymer network was investigated on montmorillonite PGV® AGM composites in fully swollen state. Calculation of the swelling capacity and the evaluation of the gel strength were carried out as described in section 4.2.1. The fully swollen hydrogels were investigated after determining $m_{swollen}$ with the indenter with a diameter of 16.2 mm.

Several AGM composites with montmorillonite PGV® as filler were synthesized with various amounts of modifier Allyl-ODD.

The following parameters for the AGM composite were chosen:

- Montmorillonite PGV® 5 wt% vs. solids
- Modifier amount 30 / 40 / 45 / 60 wt% referred to clay
- Acrylic acid 20 wt% referred to batch size
- Sodium hydroxide 75 mol% referred to acrylic acid
- KPS 0.1 mol% referred to acrylic acid
- TEMED 0.05 mol% referred to acrylic acid
- MBAA 0.3 mol% referred to acrylic acid

The maximum swelling capacity was calculated for each sample and VLRH values were determined. The results for the montmorillonite PGV® AGM composites stabilized with varying amounts of Allyl-ODD were compared to the reference AGM samples (Fig. 42).

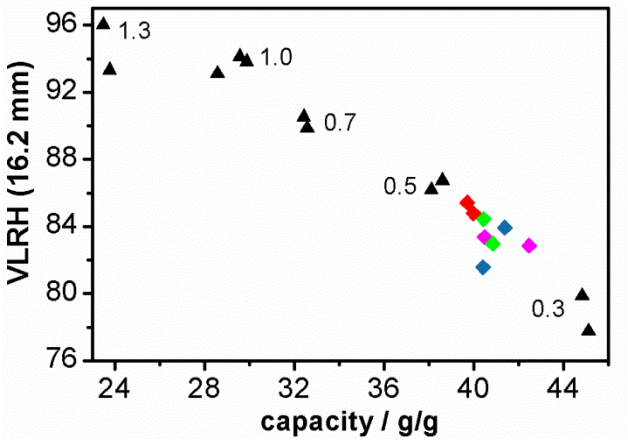

Fig. 42. VLRH vs. capacity for montmorillonite PGV® AGM composites stabilized with various amounts of Allyl-ODD: ♦ 30 wt%, ♦ 40 wt%, ♦ 45 wt%, ♦ 60 wt% referred to clay in comparison to ▲ bulk AGM with various content of crosslinker in mol% referred to acrylic acid

The maximum swelling capacity of the montmorillonite PGV® AGM composites decreased with increasing amounts of modifier Allyl-ODD added. This trend was expected, as the modifier does not contribute to the swelling capacity. With increasing modifier content, the non-swellable mass per gram solid increases. The maximum swelling capacity decreased from an average of 45 g/g for the reference sample with the identical crosslinking amount of 0.3 mol% to an average of 40.9 g/g for the AGM composite with a modifier amount of 45 wt% referred to clay. This is comparable to the result found for non-functionalized ODD, which was 40.5 g/g for the montmorillonite PGV® AGM composite.

The VLRH values increased with increasing amounts of Allyl-ODD added for modification. This means, the addition of Allyl-ODD to the hydrogel causes stiffening of the sample. However the increase of the VLRH value was less for all Allyl-ODD stabilized samples as compared to corresponding AGM composites stabilized with non-functionalized ODD. This can be attributed to the lower stability of the clay suspension indicating some agglomeration.

In respect to the combination of maximum swelling capacity and gel strength, it was striking that within experimental error, all AGM composites were found on the trade off curve. With increasing Allyl-ODD amount, the data points shifted along the trade off curve from the values found for the reference sample with the organic crosslinker amount of 0.3 mol% towards the values of the reference sample with the organic crosslinker amount of 0.5 mol%. This suggests that indeed covalent linking to the modifier is equivalent to increasing the amount of organic crosslinker. This implies that the targeted transgression of the trade off curve could not be achieved by the application of Allyl-ODD.

In order to confirm this hypothesis several AGM composites with a fixed amount of Allyl- ODD but a varying amounts of organic crosslinker were prepared.

The following parameters for the AGM composite were chosen:

- Montmorillonite PGV® 5 wt% vs. solids
- Modifier amount 45 wt% referred to clay
- Acrylic acid 20 wt% referred to batch size
- Sodium hydroxide 75 mol% referred to acrylic acid

- KPS 0.1 mol% referred to acrylic acid
- TEMED 0.05 mol% referred to acrylic acid
- MBAA 0.1 / 0.2 / 0.3 mol% referred to acrylic acid

The maximum swelling capacity for each AGM composite was calculated and VLRH values determined. The results for the montmorillonite PGV® AGM composites were compared with the reference AGM samples (Fig. 43).

Varying the amount of organic crosslinker with constant Allyl-ODD amount delivered VLRH – capacity values which were found on the trade off curve. This corroborates that increasing of the Allyl-ODD amount is equivalent to increasing the amount of organic crosslinker. Consequently, it will indeed be impossible to overcome the trade off line by varying and combining different amounts of Allyl-ODD and organic crosslinker.

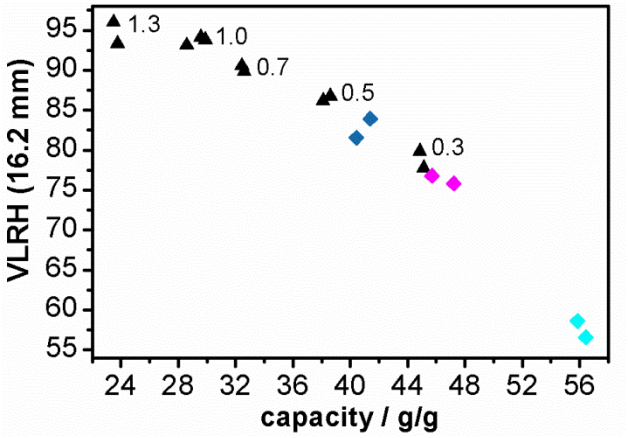

Fig. 43. VLRH vs. capacity for AGM Montmorillonite PGV® composites, stabilized with Allyl ODD and various content of organic crosslinker: ♦ 0.1 mol%, ♦ 0.2 mol%, ♦ 0.3 mol% referred to acrylic acid in comparison to ▲ bulk AGM with various content of crosslinker in mol% referred to acrylic acid

4.2.5 Summary of attempts to enhance the gel strength of bulk AGM

Analysis of the fully swollen AGM composites containing either montmorillonite PGV® or lithium hectorite revealed a loss of maximum swelling, which was related to the replacement of superabsorbent polymer by non-swellable clay and modifier needed to achieve stable suspensions. Moreover, at least the larger lithium hectorite might somehow restrict swelling. The montmorillonite PGV® AGM composites nevertheless showed an enhancement of the gel strength of the composite as indicated by VLRH values, which was disproportionate enough to overcompensate the loss in maximum swelling capacity.

Therefore, the montmorillonite PGV® AGM composites were found above the trade off curve defined by clay-free reference samples with various amounts of organic crosslinker. For lithium hectorite, the enhancement of the gel strength found for AGM composites, however, was too low to compensate the loss of swelling capacity and consequently lithium hectorite AGM composites were found below the trade off curve.

At intermediate swelling montmorillonite PGV® AGM composites were found above the trade off curve over the whole range of swelling degrees. For lithium hectorite AGM composites, however, a crossover was found and this composite outperformed the un-filled AGM only up to swelling degrees of 5.5 g/g. It is unclear whether this may be attributed to changes in the crosslinking network expected for this clay or to higher stress developed at a single clay platelet.

Concerning possible failure mechanisms responsible for the disappointing enhancement of bulk AGM's gel strength achieved by reinforcement with clay minerals the following conclusions were made:

Failure of the filler material was judged as improbable, as the forces arising during the swelling process were not high enough to break clay platelets with in plane moduli >150 GPa. At the given pH and duration of synthesis of AGM composites dissolution of clay minerals may be regarded irrelevant. The larger lithium hectorites might hamper formation of a homogeneous crosslinking network and this way introduce defects, restrict swelling or foster failure of the matrix at higher degrees of swelling. Experimental validation of this hypothesis would be, however, very difficult. Most probable failure of the composite likely occurs at the interface between modifier and polymer network, where stress is insufficiently transferred by rather weak hydrogen bonds. In line with this, the problem is more pronounced for the much larger lithium hectorite, where at the same weight content of filler much fewer platelets are incorporated at which the same total stress has to be dissipated.

When attempting to eliminate this failure mode by covalently linking the modifier and the polymer network the gel strength decreased. Apparently for this setup, the covalently linked filler acts simply like an additional crosslinking and hence the trade off curve could not be surpassed.

The best result for enhancing the bulk AGM's properties was accomplished by incorporating montmorillonite PGV® into the polymer network. The filler was stabilized in the monomer suspension applying the modifier ODD in amounts of 45 wt% referred to the content of the clay mineral. The achieved improvement was 5 – 10 % capacity at same gel stiffness measured as VLRH.

4.3 Core – shell concept: Enhancement of stress at break and strain at break

The optimum superabsorbent material for application in hygiene products exhibits high maximum swelling ability combined with high pressure resistance of shape in order to avoid gel blocking. Chapter 4.2 presented an approach to optimize these parameters for the bulk AGM by incorporation of clay minerals as fillers into the polymer network.

Another approach to improve the interplay of the maximum swelling capacity and the pressure resistance of shape of the material is presented by the core – shell concept. The main advantage of the core – shell concept is that the requirements of high swelling ability and high gel strength do not have to be fulfilled by one single material at the same time. Instead, the requirements are spatially separated to core and shell: While the core should provide a high swelling capacity, the shell should provide the mechanical stability required to reduce gel blocking.

Requirements on the core

The core material is optimized to provide high swelling capacity. The mechanical stability is of minor importance as long as a minimum stability is provided that allows handling the core polymer before the shell is attached, e.g. via spray coating. For the core, bulk non-surface treated AGM can be selected, as the chemistry of this hydrogel and its handling is well-known.

Requirements on the shell

The shell ideally must provide the required mechanical strength of the AGM particle to avoid breakage and deformation upon swelling under pressure. During the swelling process, the AGM in the core of the structure increases its volume by ~ 1.5 orders of

magnitude. Consequently, the shell has to be highly expandable and at the same time resistant to the stress developed during its extension. The minimum elongation to break is needed at 300 – 400 % in order to secure sufficient capacity of the swollen particle and not break upon swelling. Own swelling capacity is not required for the shell, but certainly a benefit as it would offset potential capacity loss. The shell furthermore has to be chemically compatible with the core and permeable to water.

These requirements on the shell were addressed by using bulk AGM as matrix that was reinforced with clay minerals as fillers. Since the chemistry of core and shell materials is the same, compatibility was obviously ensured. The clay mineral should accomplish enhancement of Young's -modulus, strain at break, and maximum stress that is applicable before the polymer ruptures.

Enhancement of the strain at break:

Incorporation of clay minerals into the elastomeric AGM polymer and other hydrogels increases its strain at break.[109] The cause for the increase of strain at break by incorporation of clay minerals into a polymer matrix is widely discussed in literature. Several authors compare hydrogels "crosslinked" by clay minerals with hydrogels crosslinked by an organic crosslinker. Laponite® clay was used as filler in these nanocomposites and the clay was claimed to operate as inorganic crosslinker for the polymer network although no specific bonding of the clay to the matrix was realized as it was described in section 4.2.4. Nevertheless, the authors claimed that the Laponite® clay platelets were tied to each other by polymer chains, which means that the polymer provides bridging between clay platelets. It should be stressed that in all these nanocomposites, the chemical interaction between matrix and Laponite® could only be based on hydrogen bonding. Since Laponite® platelets have, however, a very small diameter (< 20 nm), the platelets, additionally might be "entangled" by polymer chains. The "intercrosslinking" distance between the clay platelets is much longer than the intercrosslinking distance in organically crosslinked polymer networks. Consequently, the length of the polymer chains in between two crosslinking points was claimed to be higher in the Laponite® crosslinked polymer. In other words, the effective network chain density is lower in the inorganically crosslinked polymer. Hence strain at break of the Laponite® hydrogel nanocomposite is higher than strain at break of hydrogels crosslinked with an organic crosslinker.[110-113] Upon swelling, the clay platelets align in respect to the force

applied. Interestingly, for low and high (> 10 mol%) clay contents the clay platelets were found to align differently: perpendicular[110,111] and parallel to the stretch direction,[110] respectively.

Less research was done on systems combining organic crosslinking with inorganic crosslinking by clay minerals. Haraguchi and Song combined MBAA and a Laponite® clay as crosslinker in a poly (*N*-isopropyl acrylamide) network. They describe the formation of microstructures with a high chemical crosslinking density near the periphery of the clay particles and a low chemical crosslinking density in the polymer network far from the clay. Haraguchi and Song consequently attribute the high strain at break of their composites with low degrees of organic crosslinking in both tensile and compression measurements to diluted chemical crosslinking between polymer chains, as the organic crosslinker segregates into areas close to the clay.[114]

The structure of the hydrogel nanocomposite discussed in this work differs from the systems discussed in literature. Both clay mineral and organic crosslinker were combined. However, both clay minerals applied here had much larger diameters. Moreover, for the AGM matrix they had to be stabilized in the monomer mixture by means of a modifier adding to the total volume of the filler platelets. “Entanglement” of these fillers by polymer chains therefore seems very unlikely. Hence, the matrix will only interact by hydrogen bonding to the modifier on the basal surface of the clay platelets.

Only little information was published dealing with fracture toughness, crack formation and propagation in hydrogels. Lin et al. reported, that incorporation of silica into poly (dimethyl acylamide) slows down crack velocity.[115] A similar effect can also be supposed for clay minerals incorporated into hydrogels. Furthermore extrinsic toughening by crack bridging like it was described for bulk metallic glass materials is possible [116], provided that the filler dimension is larger than the crack opening displacement. Recently[93], a number of toughening mechanisms including crack deflection, crack debonding and platelets pull-out were described for such high aspect ratio nanoplatelets in PMMA matrix.

Enhancement of tensile stress at break

Incorporation of clay minerals into hydrogels of different kinds enhances the materials’ Young’s -modulus and tensile stress at break.[109,110,113,114,117] Okay and Oppermann

observed an increase of the Young's -moduli for their poly (acryl amide) gels containing Laponite®. Their rheological investigations further revealed large energy dissipation in clay containing gels. They ascribe it to a dynamic adsorption-desorption equilibrium between the polymer chains and the clay mineral or alternatively to a friction of the clay – polymer interface resulting from sliding of the adsorbed chains along the clay surface.[118] Abdurrahmanoglu et al. picked up the idea that these rearrangements are a reason for the excellent mechanical performance of Laponite® composite gels. They studied the elastic properties of Laponite® composites based on poly acrylamide, poly (N,N-dimethylacylamide) and poly (N-isopropylacrylamide) and observe a dependency of the higher Young's -moduli of the Laponite® composites on the strength of attractive interactions between polymer and clay.[119] Incorporation of clay minerals into soft polymers furthermore causes strain hardening. Strain hardening means, the material is strengthened when it is expanded. Hence, the more the material is expanded, the higher the force needed to expand it further. Wang et al. observed strain hardening for a poly (*N*-isopropyl acrylamide) – Laponite® nanocomposite. This strain hardening effect was enhanced with increasing Laponite® content in the nanocomposite gel. Wang et al. attribute the strain hardening effect to the orientation of the Laponite® platelets which is induced upon stretching, as described above.[120] This effect should support the form stability of the AGM particles during the swelling process and consequently gel blocking should be avoided.

Earlier investigations at Procter & Gamble on core – shell particles identified several key attributes of the shell. As mentioned earlier, the strain at break of the shell has to be higher than 300 – 400 % of elongation to secure sufficient final capacity. Other requirements depend on the diameters of core and shell. The lower the Young's -modulus of the shell, the higher its thickness has to be. As the intention is to keep the diameter of the shell low, high Young's -modulus for the shell and high average elastic modulus (secant modulus) in the 0 – 400 % strain region are desirable, which due to strain hardening also implies a high stress at break of the material. As an example, earlier investigations at Procter & Gamble revealed that for AGM particles with a size of 500 µm the Young's -modulus of the shell needs to be higher than 100 kPa in order to make a shell thickness of less than 20 µm sufficient to produce core - shell materials with superior tradeoff vs. reference.

4.3.1 Stepwise optimization of the synthesis parameters for the shell

Since, as already mentioned, the swelling capacity is of minor importance for the shell, the composition of the shell AGM nanocomposite may be varied in several ways in order to optimize elongation and stress at break. For example, the clay content could be raised to high levels, which restricts the swelling abilities of the hydrogel, however according to literature extraordinary mechanical properties can be expected.[110,112,114,117,121]

The synthesized AGM composites consisted of following educts:

- Clay mineral
- Modifier ODD
- Acrylic acid
- Sodium hydroxide
- KPS
- TEMED
- MBAA

While keeping the composition of the nanocomposite materials simple by fixing the amounts of initiator KPS (0.1 mol% referred to acrylic acid), catalyst TEMED (0.05 mol% referred to acrylic acid), and modifier ODD (45 wt% referred to the content of clay), elongation and stress at break were sought to be optimized by systematically varying the following parameters:

- Type of clay mineral
- Acrylic acid content
- Sodium hydroxide content – degree of neutralization
- Amount of organic crosslinker
- Clay mineral content

For each AGM composite, a reference sample with identical composition, however without clay and modifier, was synthesized. Like for enforcement of bulk AGM, montmorillonite PGV® and lithium hectorite were applied for shell AGM nanocomposites to probe the effect of the different aspect ratio of the filler.

All samples were investigated at two different degrees of swelling. X-loads of 3g/g and 6 g/g were chosen. These intermediate swollen samples were prepared like described in section 3.5.1.

All prepared samples were characterized with stress – strain measurements and the derived Young's -modulus, stress at break, and strain at break were compared.

4.3.1.1 Influence of the amount of organic crosslinker

The influence of the amount of organic crosslinker was studied by preparing identical samples with three different crosslinking amounts. The chosen amounts were 0.3 mol%, 0.7 mol% and 1.0 mol% of organic crosslinker MBAA in reference to the amount of acrylic acid.

In this series of hydrogels the amount of acrylic acid was fixed at 25 wt% referred to the mass of the polymerization mixture. The degree of neutralization was 75 mol% referred to acrylic acid. The content of the clay mineral was 5 wt% referred to the content of solids.

The amount of organic crosslinker was indicated by labeling the samples with "0.3", "0.7" or "1.0" in respect of the corresponding crosslinker content. Furthermore, reference samples were denoted with "Ref", the lithium hectorite composite with "LiHec", and the montmorillonite PGV® composite with "PGV". As an example, the "PGV 0.3" represented the composite with montmorillonite PGV® as filler and the crosslinker amount of 0.3 mol% referred to acrylic acid.

At a swelling degree of 3 g/g, a clear enhancement of Young's -modulus, stress at break and strain at break was only observed for the samples with low crosslinking content of 0.3 mol% (Table 6). At a crosslinking level of 0.7 mol% no significant effects on Young's -modulus and stress at break were observed for the two types of clay minerals while the strain at break was improved with both fillers. At a crosslinking level of 1.0 mol% measurement of the reference sample was not possible as the sample was too brittle. However, measurements at this high crosslinking content were possible for both composite materials indicating improved hydrogel properties by incorporating clay minerals although reference values are lacking.

Table 6. Young's -modulus, stress at break and strain at break for hydrogels with varying crosslinker amount at a swelling degree of 3 g/g

		Young's -modulus / kPa	Stress at break / kPa	Strain at break
Ref	0.3	32 ± 2	57 ± 7	3.1 ± 0.6
Ref	0.7	84 ± 2	62 ± 11	1.3 ± 0.3
Ref	1.0	-	-	-
LiHec	0.3	41 ± 8	149 ± 41	8 ± 1
LiHec	0.7	82 ± 17	56 ± 7	2.1 ± 0.3
LiHec	1.0	88 ± 12	48 ± 2	1.2 ± 0.1
PGV	0.3	52 ± 1	137 ± 16	5.2 ± 0.7
PGV	0.7	83 ± 4	92 ± 15	2.1 ± 0.2
PGV	1.0	141 ± 12	157 ± 46	2.2 ± 0.6

As expected, the Young's -modulus was increasing with increasing crosslinking content within each type of hydrogel. For the stress at break no clear trend could be observed. For the LiHec series stress at break continuously decreased with increasing crosslinker content while for the PGV series the maximum was observed at 1.0 mol%. The strain at break was found to decrease dramatically with increasing amount of crosslinker for all three series of hydrogels. Consequently, at low swelling degree a small amount of organic crosslinker seems most advantageous.

At a higher swelling degree of 6 g/g the trends observed for the less swollen hydrogels were mostly confirmed (Table 7). Enhancement of Young's -modulus, stress at break and strain at break was again found for the samples with 0.3 mol% of organic crosslinker. At a crosslinking level of 0.7 mol% converse effects on the Young's -modulus were observed for the two types of clay minerals while stress and strain at break were improved with both fillers. The favorable influence of incorporating clay minerals into the hydrogel with a crosslinker content of 1.0 mol% was again evident as the reference sample was too fragile to be measured while the composite materials were stable enough. However the exact amplification could not be evaluated.

Aside the expected increase of Young's -modulus with increasing crosslinking level, at the x-load of 6 g/g a decrease of stress at break with increasing organic crosslinker amount was observed for the lithium hectorite composites. Furthermore, a decrease of

strain at break with increasing organic crosslinker amount for the reference and both composites became evident.

Table 7. Young's -modulus, stress at break and strain at break for hydrogels with varying crosslinker amount at a swelling degree of 6 g/g

		Young's -modulus / kPa	Stress at break / kPa	Strain at break
Ref	0.3	19 ± 1	18 ± 5	1.0 ± 0.3
Ref	0.7	52 ± 2	29 ± 2	0.87 ± 0.05
Ref	1.0	-	-	-
LiHec	0.3	30 ± 3	52 ± 15	3.3 ± 1.0
LiHec	0.7	43 ± 3	39 ± 2	1.8 ± 0.2
LiHec	1.0	57 ± 7	34 ± 9	1.1 ± 0.2
PGV	0.3	26 ± 2	48 ± 6	2.9 ± 0.4
PGV	0.7	58 ± 3	46 ± 9	1.3 ± 0.3
PGV	1.0	79 ± 2	36 ± 14	0.7 ± 0.3

Xiong et al. incorporated Laponite® clays into a copolymer consisting of acrylamide and sodium acrylate with various amounts of organic crosslinker MBAA. They observed the same trend of decreasing stress at break and strain at break with increasing MBAA content above an amount of 0.25 mol% referred to monomers as the network chain mobility is more and more restricted.[113] Haraguchi and Song found similar effects when increasing the MBAA amount in their poly (*N*-isopropyl acryliamide) Laponite® composites.[114]

The hydrogels got more brittle with increasing crosslinking amount and were harder to handle and prepare for the measurement without damaging them in advance. Hence, although the Young's -modulus was higher for higher organic crosslinker content, the significant reduction of strain at break suggests that for the shell composition a low amount of organic crosslinker is favorable.

4.3.1.2 Influence of the acrylic acid content and the degree of neutralization

Samples with 15 wt% and 25 wt% of acrylic acid referred to the total mass of the polymerization mixture were prepared. The influence of the acrylic acid content was

investigated for both non-neutralized polymer and the 75 mol% neutralized polymer in order to check for possible cooperative effects.

The amount of organic crosslinker was chosen with 0.3 mol% referred to acrylic acid. The content of the clay mineral was 5 wt% referred to the content of solids.

Samples were labeled with respect to the investigated variable. Here, samples were marked with AA *n*, where *n* was the amount of acrylic acid in wt% referred to the amount of monomer mixture. Furthermore, the degree of neutralization was denoted by DN *m*. "Ref" was used for the reference, "LiHec" for the lithium hectorite composite and "PGV" for the montmorillonite PGV® composite. For example, "LiHec AA15 DN 75" would be the AGM composite with lithium hectorite as filler and 15 wt% of acrylic acid with 75 % neutralization.

At a swelling degree of 3 g/g, all clay containing samples of the non-neutralized polymer exhibited higher Young's -modulus, stress at break and strain at break (Table 8) as compared to reference samples. Increasing the acrylic acid content resulted in higher Young's -moduli for the reference samples and both nanocomposite and in case of the reference samples also in higher stress at break. No significant change of strain at break was found for the reference samples with increasing acrylic acid content. Both AGM composites, however, become less elastic with higher acrylic acid amount. Consequently a clear decision whether high or low acrylic acid content should be favored could not be drawn at this point.

Table 8. Young's -modulus, stress at break and strain at break for non-neutralized hydrogels with varying acrylic acid content at a swelling degree of 3 g/g

		Young's -modulus / kPa	Stress at break / kPa	Strain at break
Ref	AA 15 DN 0	29 ± 1	39 ± 5	2.4 ± 0.6
Ref	AA 25 DN 0	48 ± 4	86 ± 19	3.6 ± 1.0
LiHec	AA 15 DN 0	38 ± 1	176 ± 10	9.6 ± 0.8
LiHec	AA 25 DN 0	59 ± 2	186 ± 2	6.2 ± 0.1
PGV	AA 15 DN 0	45 ± 5	140 ± 15	7.3 ± 0.7
PGV	AA 25 DN 0	67 ± 6	179 ± 33	4.6 ± 0.8

At a swelling degree of 6 g/g, still all clay containing samples exhibit higher Young's -modulus, stress at break and strain at break (Table 9) as compared to reference samples. The AGM hydrogels containing 25 wt% of acrylic acid were, however, found to be too soft and brittle to allow stress – strain measurements.

Consequently, hydrogels consisting of the non-neutralized polymer and an acrylic acid amount of 25 wt% referred to the total mass seem not useful for core – shell applications. In case the non-neutralized polymer was chosen for the shell composition, the usage of low acrylic acid content is favorable.

Table 9. Young's -modulus, stress at break and strain at break for non-neutralized hydrogels with varying acrylic acid content at a swelling degree of 6 g/g

		Young's -modulus / kPa	Stress at break / kPa	Strain at break
Ref	AA 15 DN 0	16 ± 1	37 ± 2	4.2 ± 0.3
Ref	AA 25 DN 0	-	-	-
LiHec	AA 15 DN 0	20.9 ± 0.6	97 ± 9	7.7 ± 0.6
LiHec	AA 25 DN 0	-	-	-
PGV	AA 15 DN 0	22 ± 1	90 ± 8	6.6 ± 0.6
PGV	AA 25 DN 0	-	-	-

For the 75 mol% neutralized nanocomposites at a swelling degree of 3 g/g, only the samples with high acrylic acid content showed enhanced Young's -modulus, stress at break and strain at break in comparison to the reference sample. The hydrogels with low acrylic acid content showed no significant influence of filler incorporation on Young's -modulus and stress at break (Table 10). Enhancement was only found for strain at break.

Table 10. Young's -modulus, stress at break and strain at break for 75 mol% neutralized hydrogels with varying acrylic acid content at a swelling degree of 3 g/g

		Young's -modulus / kPa	Stress at break / kPa	Strain at break
Ref	AA 15 DN 75	16 ± 1	73 ± 7	8.0 ± 0.4
Ref	AA 25 DN 75	32 ± 2	57 ± 7	3.1 ± 0.6
LiHec	AA 15 DN 75	15 ± 1	89 ± 13	13 ± 2
LiHec	AA 25 DN 75	41 ± 8	149 ± 41	8 ± 1
PGV	AA 15 DN 75	13.3 ± 0.4	69 ± 16	8.7 ± 0.9
PGV	AA 25 DN 75	52 ± 1	137 ± 16	5.2 ± 0.7

Comparing samples with either low or high acrylic acid content, again an increase of Young's -modulus increasing acrylic acid content was observed. For both AGM composites, additionally an increase of stress at break was found. However, the elasticity was dramatically decreased with higher acrylic acid content for both nanocomposites and the reference samples. This result suggested a preference for low acrylic acid contents.

Again, Young's -modulus, stress at break and strain at break were also investigated at a higher degree of swelling, which was 6 g/g (Table 11).

Table 11. Young's -modulus, stress at break and strain at break for 75 mol% neutralized hydrogels with varying acrylic acid content at a swelling degree of 6 g/g

		Young's -modulus / kPa	Stress at break / kPa	Strain at break
Ref	AA 15 DN 75	9 ± 1	27 ± 5	4.7 ± 0.5
Ref	AA 25 DN 75	19 ± 1	18 ± 5	1.3 ± 0.3
LiHec	AA 15 DN 75	(nd)	(nd)	(nd)
LiHec	AA 25 DN 75	30 ± 3	52 ± 15	3.3 ± 1.0
PGV	AA 15 DN 75	8.24 ± 0.02	74 ± 8	9.6 ± 0.3
PGV	AA 25 DN 75	26 ± 2	48 ± 6	2.9 ± 0.4

Results for higher swollen hydrogel samples resembled those observed at low swelling degree. The nanocomposite samples with low acrylic acid content revealed a slight, non-significant reduction of the Young's -modulus as compared to the reference while stress

and strain at break were enhanced. For the nanocomposites with high acrylic acid content enhancement of all three properties, namely Young's -modulus, stress and strain at break, was observed. With increasing acrylic acid amount, an increase of the Young's -modulus was observed. For both stress and strain at break a decrease was detected with raising acrylic acid content. This tendency matched the findings for non-neutralized polymers that at higher swelling degrees the samples with higher acrylic acid content were more brittle and ruptured more easily. Especially the stress at break was negatively affected. While at a swelling degree of 3 g/g still an enhancement of the stress at break was found comparing the low acrylic acid content with the high acrylic acid content, at 6 g/g the hydrogels with more acrylic acid exhibited lower stress at break. Hence, low acrylic acid content was recommended when using the 75 mol% neutralized polymer for the shell chemistry.

Low acrylic acid content turned out to be favorable independently of the degree of neutralization of the polymer. Comparing the samples with low acrylic acid content, a neutralization of the polymer to 75 % resulted in a decrease of both Young's -modulus and stress at break while the strain at break was slightly increased.

In summary, the results suggest that the usage of low acrylic acid content in combination with a degree of neutralization of zero should be best for the composition of the shell.

4.3.1.3 Variation of filler content

Finally the amount of clay mineral added to the composites was varied and the materials were characterized by stress – strain measurements. For the investigations, 2.5 wt%, 5 wt%, 7.5 wt% and 10 wt% of clay mineral referred to the solid were chosen.

In this series of hydrogels the amount of acrylic acid was fixed at 15 wt% referred to the total mass. The acrylic acid was not neutralized. Although it was shown in section 4.3.1.1 that a high content of organic crosslinker is counterproductive when aiming for a high strain at break, an amount of organic crosslinker of 1 wt% was chosen. It was expected that by increasing the amount of filler the detrimental effect of the higher crosslinking level could be compensated. Labeling of the samples was done similar than above. The amount of each clay mineral was indicated by stating "2.5", "5", "7.5" or "10" for the corresponding amount of clay mineral. As an example, "LiHec 5" represents the lithium hectorite composite with 5 wt% clay mineral referred to the content of solids.

Table 12. Young's -modulus, stress at break and strain at break for hydrogels with varying clay mineral content at a swelling degree of 3 g/g

		Young's -modulus / kPa	Stress at break / kPa	Strain at break
Ref		55.7 ± 0.4	61 ± 10	1.6 ± 0.3
LiHec	2.5	52.5 ± 0.6	129 ± 10	3.7 ± 0.3
LiHec	5	63 ± 3	181 ± 28	4.6 ± 0.6
LiHec	7.5	76 ± 3	179 ± 14	3.4 ± 0.1
LiHec	10	82 ± 3	277 ± 91	5.4 ± 1.8
PGV	2.5	53.47 ± 0.01	94 ± 15	2.7 ± 0.5
PGV	5	68 ± 1	159 ± 11	3.4 ± 0.2
PGV	7.5	72 ± 2	101 ± 6	2.0 ± 0.1
PGV	10	90 ± 10	221 ± 11	3.0 ± 0.1

At a swelling degree of 3 g/g, the reinforcing effect caused by the incorporation of clay minerals as indicated by increasing Young's -modulus was observed with clay amounts of 5 wt% or higher (Table 12). Both stress and strain at break could be significantly enhanced already with the lowest clay content of 2.5 wt%. The highest values for stress at break were observed for the highest clay content of 10 wt% for both type of clay. Interestingly, optimum values for strain at break were observed at different clay loadings depending on the type of clay. Furthermore, no clear trend could be found for stress and strain at break in dependency of the filler content.

The effects were even more pronounced at 6 g/g (Table 13). Already small clay amounts caused an increase of the Young's -modulus. Stress at break was tremendously enhanced already at the lowest clay content for both clay AGM composites. Like before, the optimum values for stress at break for found at the highest clay content for both types of clay. Again the optimum values for strain at break were observed at different clay loadings depending on the type of clay. No clear trend for stress and strain at break in dependency of the filler content could be identified.

Table 13. Young's -modulus, stress at break and strain at break for hydrogels with varying clay mineral content at a swelling degree of 6 g/g

		Young's -modulus / kPa	Stress at break / kPa	Strain at break
Ref		35 ± 1	37 ± 12	1.5 ± 0.6
LiHec	2.5	40 ± 3	109 ± 6	4.1 ± 0.3
LiHec	5	46. ± 3	109 ± 9	3.6 ± 0.1
LiHec	7.5	51 ± 2	92 ± 5	2.6 ± 0.1
LiHec	10	67 ± 3	133 ± 3	3.31 ± 0.01
PGV	2.5	46 ± 1	99 ± 23	3.1 ± 0.7
PGV	5	55 ± 1	138 ± 18	3.4 ± 0.3
PGV	7.5	63 ± 2	92 ± 41	1.9 ± 0.8
PGV	10	70 ± 1	226 ± 40	4.2 ± 0.6

Liu et al. incorporated Laponite® clays in poly (*N*-isopropyl acrylamide) gels and found an increase of Young's -modulus and tensile stress at break with increasing filler content.[117] Haraguchi et al. and Haraguchi and Li presented comparable results for their Laponite® containing poly (*N*-isopropyl acryliamide) hydrogels in respect of Young's -modulus and stress at break. At the same time strain at break was reduced with increasing clay content.[110,121] Xiong et al. observed that tensile stress at break of their poly (acrylamide) – Laponite® nanocomposites increases dramatically with increasing Laponite® concentration.[112] Haraguchi and Song confirmed the enhancing effect of clay incorporation on the Young's -modulus of the poly (*N*-isopropyl acrylamide) hydrogel and observed increasing values for increasing clay content. They furthermore showed that the reinforcement always occurs independently of the amount of additionally added organic crosslinker, however the extent of reinforcement decreases with increasing crosslink content.[114] Wang et al. confirmed the findings of Haraguchi et al. for Laponite® incorporated poly (*N*-isopropyl acrylamide) hydrogels. They also found an increase of tensile stress at break and a decrease of strain at break with increasing Laponite® content and ascribe the effect to the increase of crosslinking density. Furthermore, Wang et al. demonstrated the occurrence of strain hardening which increases with increasing amount of clay mineral in their nanocomposite.[120] Also for gelatin – montmorillonite nanocomposites a dependency of the enforcement on the

content of clay was demonstrated. Both tensile stress at break and Young's -modulus were found to increase with increasing clay content.[122]

The results presented in literature would suggest that despite some fluctuations seen in the presented results Young's -modulus and stress at break would improve while the strain steadily decreases with increasing clay content. Comparing the two types of clay the overall performance of montmorillonite PGV® was found superior to lithium hectorite regarding the composite gels with high clay content.

As stated earlier, the relevant thresholds are 400 % of strain and an Young's -modulus of > 100 kPa. At the higher investigated swelling level of 6g/g the threshold value for strain was met by PGV 10 despite the high amount of organic crosslinker. Possibly the clay content could even by increased beyond that level. Unfortunately, the loss of strain at break caused by the high amount of organic crosslinker could not be fully compensated by the increasing filler amounts. Consequently, the amount of organic crosslinker in the shell composition should be kept low while the clay content has to be chosen at high levels.

4.3.2 Fine-tuning of the shell hydrogel

Systematic variation of the different parameters expected to influence the mechanical properties defining the performance of the shell material (Young's -modulus, stress at break and strain at break) suggested the following optimal composition:

- Acrylic acid: 15 wt% referred to total mass
- Degree of neutralization: 0 %
- Amount of organic crosslinker: low, ≤ 0.3 mol% referred to acrylic acid
- Clay content: high, ≥ 10 wt% referred to solid content
- Clay type (aspect ratio): montmorillonite PGV®

For two parameters the optima were observed at extreme values. In a final attempt to locate the best settings for high performance shell materials the variation range for these two parameters was further extended.

The amount of acrylic acid was fixed to 15 wt% referred to the total mass of the sample and the acrylic acid was not neutralized. The amount of organic crosslinker was further reduced to 0.2 wt% referred to acrylic acid while the clay content was maximized. Any drying of the clay minerals will unequivocally induce irreversible aggregation. The clay minerals therefore have to be handled continuously in suspension. The maximum clay mineral content that could be achieved in the nanocomposites was hence limited by the maximum solid content of the clay suspension in water added to the polymerization mixture. This in turn was mostly determined by the maximum viscosity of this suspension which could still be handled and which increased with increasing clay content until it finally got a paste-like texture. For lithium hectorite, this point was reached at a concentration of 5 wt% of clay mineral in water. Hence, the maximum concentration of clay mineral that could be chosen for the polymerization mixture was 20 wt% referred to the total solid content.

A reference sample and the composite hydrogels of the two types of clay minerals were prepared with above mentioned compositions. The samples were attempted to be swollen to the swelling degree of 6 g/g to investigate the performance of the shell. However, after equilibration for 10 days it was noticed that the AGM composite hydrogels were incapable to take up the saline completely. Thus the maximum swelling capacities of the investigated composite hydrogels were apparently below 6 g/g. Therefore the real maximum swelling degree was determined for each sample by drying pieces of the fully swollen samples. The following maximum swelling capacities were found:

- Reference: 7.3 g/g
- Lithium hectorite composite: 3.4 g/g
- Montmorillonite PGV® composite: 5.6 g/g

The reference hydrogel was mechanically characterized at 6 g/g, while the composite hydrogels were investigated at their maximum swelling degrees.

Unfortunately the reference sample turned out to be mechanically too unstable and sticky to be handled and allow measurement in the stress-strain device due to its low cross-linking level. The bare fact that both composite materials could be handled already indicates that the hydrogels were significantly reinforced by incorporation of clay minerals and that Young’s -modulus, stress at break and strain at break could be

improved (Table 14). Comparing the two composite hydrogels, a higher Young's -modulus was found for the lithium hectorite composite. Stress at break was higher for the montmorillonite PGV® composite. Concerning strain at break, the value for the lithium hectorite composite was surprisingly low. Contrary to this the montmorillonite PGV® composite exhibited a very high elasticity, as the dog bone shaped sample could be expanded by more than 12 times of its original size.

Table 14. Young's -modulus, stress at break and strain at break of the investigated hydrogels

	Young's -modulus / kPa	Stress at break / kPa	Strain at break
Ref	-	-	-
LiHec	114 ± 13	123 ± 10	2.15 ± 0.06
PGV	68 ± 5	490 ± 70	12.1 ± 1.5

The dramatic difference between the two composite samples becomes even more intuitive when comparing typical stress-strain curves for the two composites (Fig. 44).

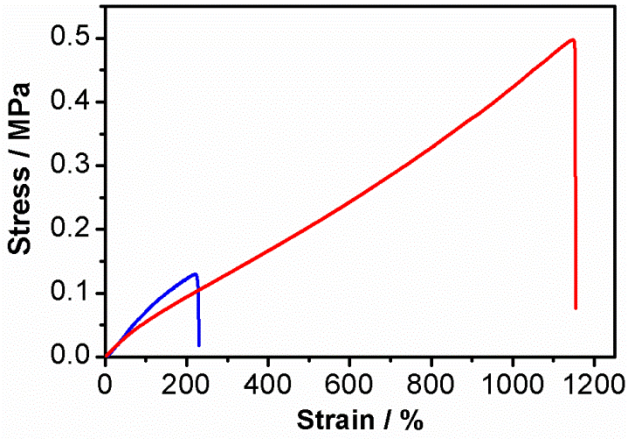

Fig. 44. Stress-strain progression of ─ lithium hectorite composite and ─ montmorillonite PGV® composite

Although at low elongation the strain of the lithium hectorite composite increases faster due to its higher Young's -modulus as compared to the montmorillonite PGV® composite, stress at break is much higher for the latter due to significant strain hardening as discussed before.

The observed differences concerning stress at break and strain at break between the two AGM composites were striking. While the general trends that were established in the literature applying Laponite® as filler were reproduced with the fillers tested here, these

results additionally suggest a very strong dependency on the dimensions and/or the aspect ratio of the filler which is more pronounced for clays with higher lateral dimension.

As discussed earlier (4.2.5) with the larger aspect ratio of the lithium hectorite two potential disadvantages are connected that might explain the different performances: 1. The larger lithium hectorites might hamper formation of a homogeneous crosslinking network and this way foster failure of the matrix in more brittle areas of higher cross-linking density. 2. For the much larger lithium hectorite at the same weight content of filler much fewer platelets are incorporated at which the same total stress has to be dissipated and where therefore failure might occur more easily.

Contrary to the lithium hectorite composites, for the montmorillonite PGV® composite the required threshold for the shell composition in respect of strain at break (> 400%) was surpassed by a factor of 3. The requirements (> 100 kPa) in respect of Young's -modulus (68.2 kPa) were however not met yet. Young's -modulus can, however, be easily increased in two ways which are either increasing the amount of organic crosslinker or increasing the amount of acrylic acid in the polymerization mixture. Both means will of course decrease the materials strain at break for which the benchmark was surpassed by far.

Since the impact of high crosslinker content on the strain at break was found to be more severe than the reduction induced by increasing the content of acrylic acid, the latter parameter was chosen to be increased to improve the Young's -modulus. An AGM composite was synthesized with the following parameters:

- Acrylic acid: 25 wt% referred to total mass
- Degree of neutralization: 0 %
- Amount of organic crosslinker: 0.2 mol% referred to acrylic acid
- Clay content: 18 wt% referred to solid content

Reference sample and montmorillonite PGV® AGM composite were left to swell to a x-load of 6 g/g for 10 days. Since as expected the swelling capacity of the composite material was insufficient to completely adsorb this amount of saline, the realized capacity was determined:

- Reference: 5.2 g/g
- Montmorillonite PGV® composite: 2.6 g/g

Consequently, stress – strain measurements were carried out on these swollen samples.

Table 15. Young's -modulus, stress at break and strain at break of the reference and montmorillonite PGV® composite

	Young's -modulus / kPa	Stress at break / kPa	Strain at break
Ref	32 ± 2	64 ± 5	3.8 ± 0.4
PGV	141 ± 1	606 ± 90	8 ± 1

Increasing the acrylic acid content in the hydrogel to 25 wt% referred to the total mass showed the desired effect (Table 15). Both Young's -modulus and stress at break were increased compared to the AGM composite with lower acrylic acid content of 15 wt%. As expected the strain at break occurred at lower elongation. However the threshold of 400 % elongation is still clearly outperformed with the observed strain at break of about 800 %. Furthermore for this composition also the Young's -modulus of 140 kPa fulfills the requirement of a value higher than 100 kPa.

5 Conclusion and Perspective

Superabsorbent polymers are known for their excellent swelling behavior. AGM can absorb more than 20 times amount of liquids referred to the dry weight. Upon swelling, polymer grains are desired to retain their shape. However, highly swollen AGM often exhibit low Young's -moduli and are easily deformable when exposed to pressure. The deformability upon load causes gel blocking. For usage in agricultural or hygiene products gel blocking dramatically restricts the overall performance of the AGM. This work focuses on AGM based on acrylic acid for the application in hygiene products. Consequently high pressure resistance of shape is desired in order to avoid gel blocking, while at the same time the maximum swelling capacity of the AGM particle should be sustained. The decisive features of AGM, which are swelling capacity and pressure resistance of shape represented by the gel strength, result from the structure of the polymer network, more precisely from crosslinking density and distribution of crosslinking points. The most common polymerization route for the synthesis of AGM, which was also applied in this work, is free radical crosslinking polymerization. Free radical crosslinking polymerization always causes heterogeneities in the polymer network like for example loose ends or loops, which reduces both swelling capacity and gel strength compared to samples with ideal network structure. Studies introduced by Haraguchi et al. claim that implementing inorganic fillers, specifically clay minerals, will improve the homogeneity of the polymer network and consequently performance of the hydrogels.[35,37] This approach was picked up and transferred to AGM chemistry with all corresponding development needed. Additional advantage was taken of the reinforcing effect induced by incorporation of stiff and anisometric clay platelets into the polymer. Two different clay minerals with different aspect ratios were chosen, namely montmorillonite PGV® with an aspect ratio of approximately 30 and lithium hectorite with an aspect ratio higher than 1000. By incorporating both types of clay minerals homogeneously into the AGM polymer it was possible to compare the effect of the different aspect ratios.

Incorporating clay minerals into the given AGM based on acrylic acid was by far not trivial as the polymerization mixture exhibits acidic pH and high ionic strength. Under these given conditions clay minerals agglomerate due to their structural features and surface chemistry. The basal planes of clay minerals are negatively charged, whereas the

pH-dependent charge of the edges is positive at the pH of 5 defined by the polymerization mixture. This causes the formation of house of cards structures by attraction of positive edge and negative basal plane. House of cards formation can be avoided either by charge neutralization of the clay edge or charge inversion of either the edge charge or the basal charge. High ionic strength of the suspension medium causes lamellar agglomeration of the clay minerals. It can be prevented by electrosterical stabilization by modification of the negatively charged basal plane with sterically demanding polycations.

Initially, modification of the clay edges was attempted as the utilized amount of modifier in this case could be kept small and its influence on the AGM properties minimal. Before modifying the clay edges, their acidity was investigated. Therefore, first the charge of the basal plane was covered by binding a polycation to avoid spillover effects of the electrostatic potential of the basal plane to the clay edge as well as cation exchange reactions that would adulterate the result. Then the PZNPC of the clay mineral was determined by pH titrations. The PZNPC of montmorillonite PGV® was found at pH 5. The PZNPC of Laponite® used as a model for lithium hectorite was found at pH 7.9.

Charge neutralization was attempted by anion exchange of hydroxyl by fluorine and charge reversion of the clay edge was attempted by complexation of poly anionic pyrophosphate to octahedral cations located at the clay edge. While the degree of agglomeration of montmorillonite PGV® in polymerization mixtures could be reduced by edge modification, analysis of the particle size distributions via static light scattering revealed remaining agglomerates in both fluorinated and phosphorylated clay suspensions.

The remaining agglomeration in the clay suspension after edge modification was attributed to the formation of lamellar agglomerates caused by the high ionic strength of the dispersion medium and was tackled by modification of the basal plane of the clay minerals. Two modifiers were identified that are capable to establish visually stable clay suspensions. The modifiers, OD and ODD, both exhibit a poly (ethylene imine) core which is protonized at pH = 5. For ODD, poly ethylene oxide chains are attached to the core. The quality of the stabilizing effect on clay mineral suspensions was quantified applying force sedimentation which allowed optimizing the amount of modifier needed. Force sedimentation also revealed that the additional sterical stabilization provided by ODD is beneficial for the suspension stability. The necessary amount of ODD to stabilize

the suspension of montmorillonite PGV® was determined at 45 wt% referred to clay. The same modifier level was subsequently applied for lithium hectorite stabilization in polymerization mixtures.

After establishing homogeneous suspensions of clay minerals bulk AGM composites were synthesized and compared with unfilled reference materials of the same composition in respect to their swelling capacity and gel strength as judged by VLRH measurements. By incorporation of surface-modified clay minerals it was attempted to cross the trade off line defined by the reference samples.

For both montmorillonite PGV® and lithium hectorite nanocomposites, a loss of the maximum swelling capacity was detected. Reasons for the reduction of the swelling capacity are the replacement of AGM by non-swelling inorganic filler plus modifier and possible restrictions of swelling induced by the clay mineral. Both types of nanocomposites showed an increase of the gel strength. For the montmorillonite PGV® nanocomposites, the increase of gel strength was sufficient to produce values for maximum swelling capacity and VLRH above the trade off line. The trade off line was, however, not crossed by the lithium hectorite composites.

Montmorillonite PGV® composite outperformed the unfilled reference material with identical amount of organic crosslinker at the full range of intermediate swelling degrees. For the lithium hectorite, a crossover the line defined by the reference samples was observed. At low swelling the nanocomposites of lithium hectorite as well as montmorillonite PGV® composites were slightly better as compared to the reference sample. At higher swelling and even more, as discussed in the previous paragraph, in the fully swollen state the lithium hectorites composites underperformed. With the larger aspect ratio of the lithium hectorite two potential disadvantages are connected that might explain the inferior performance: 1. The larger lithium hectorites might hamper formation of a homogeneous crosslinking network and this way foster failure of the matrix in more brittle areas of higher cross-linking density. 2. For the much larger lithium hectorite at the same weight content of filler much fewer platelets are incorporated at which the same total stress has to be dissipated and where therefore failure might occur more easily.

Among the possible failure mechanisms failure at the interface of modifier and polymer matrix was regarded the most probable. Therefore, the modifier was functionalized with a reactive double bond which could be incorporated into the polymer network during

polymerization. Covalently linking the modifier and thus the filler to the AGM was comparable to increasing organic crosslinking and the resulting composites were found on the trade off line.

In conclusion, even if montmorillonite PGV® composite improvements seem within ~ 10 % vs. reference, it is worthwhile to elucidate the effect on gel blocking in more detail and in particle AGM context.

Next the reinforcement of clay fillers on the performance of a potential shell in core – shell particles was studied. In this core – shell approach, the two competing functions of high maximum swelling capacity and high pressure resistance of shape were spatially separated. The core of the structure should provide high swelling ability, while the shell should grant high mechanical strength. As the main function of the core was delivering high swelling ability, the commercial bulk non surface crosslinked AGM would be chosen as core material. Previous studies examining other shell materials suggested that the Young's -modulus should be > 100 kPa to make a thin shell appropriate, while a minimum strain at break of 300 - 400 % elongation was required to break reference capacity/gel bed permeability tradeoff. With AGM composite materials applied as shells, compatibility of core and shell would be granted. As swelling ability would not be of big importance for the shell, the degree of neutralization of the polymer was irrelevant and was included in the systematic variation of polymerization parameters. Acrylic acid content, degree of neutralization, amount of organic crosslinker, clay content and type of clay were varied and the mechanical properties as characterized by stress-strain measurements were compared with unfilled reference materials. Low acrylic acid content, a degree of neutralization of zero, low content of organic crosslinker and high clay content were found to be favorable. As to the type of clay montmorillonite PGV® was superior over lithium hectorite.

As reported in literature with increasing clay content Young's -moduli and stress at break were found to increase while the composites become increasingly brittle and suffer a loss of strain at break. This latter effect is also strongly dependent on the aspect ratio and therefore for similar reasons as for bulk AGM performance, lithium hectorite composites failed to meet the above mentioned threshold criteria. In contrast, the best AGM montmorillonite PGV® composite outperformed the set thresholds and reached values of 800 % of elongation for the strain at break, a stress at break of 600 kPa and an Young's -

modulus of 140 kPa. The strain value leaves sufficient space to be rebalanced further to achieve even higher tensile modulus.

Next the performance of these core-shell particles with composite shells has to be studied in respect to its efficiency to prevent gel blocking. Appropriate processing has to be established that allows attachment of a composite shell to the AGM core, for example via spray coating. A parameter that needs to be intensively monitored in this context is the thickness of the shell and its influence on the performance of the core – shell particle. Gel blocking in dependence of the thickness of the shell should be analyzed.

While the larger aspect ratio of lithium hectorite as expected lead to the most pronounced improvements in the Young's -moduli, the overall performance of this type of clay was inferior both when applied as filler in bulk AGM and shell. Apparently for the overall performance in this particular polymer matrix, the number of particles per gram of filler and the possibly detrimental influence of the huge platelets on the homogeneity of the organic crosslinking points are more important factors. In this light, Laponite® modified with ODD should be reinvestigated.

6 Reference list

[1.] J. R. Gross, in *Studies in Polymer Science: Absorbent Polymer Technology* (Ed.: Lisa Brannon-Peppas and Ronald S.Harland), Elsevier, **1990**, 3-22

[2.] N. A. Peppas, J. Z. Hilt, A. Khademhosseini, R. Langer, *Adv. Mater.* **2006,** *18,* 1345-1360.

[3.] B. Jeong, Y. H. Bae, D. S. Lee, S. W. Kim, *Nature* **1997,** *388,* 860-862.

[4.] P. Gupta, K. Vermani, S. Garg, *Drug Discovery Today* **2002,** *7,* 569-579.

[5.] N. A. Peppas, P. Bures, W. Leobandung, H. Ichikawa, *European Journal of Pharmaceutics and Biopharmaceutics* **2000,** *50,* 27-46.

[6.] J. P. Gong, Y. Katsuyama, T. Kurokawa, Y. Osada, *Adv. Mater.* **2003,** *15,* 1155-1158.

[7.] J. L. Drury, D. J. Mooney, *Biomaterials* **2003,** *24,* 4337-4351.

[8.] B. K. Mann, A. S. Gobin, A. T. Tsai, R. H. Schmedlen, J. L. West, *Biomaterials* **2001,** *22,* 3045-3051.

[9.] K. T. Nguyen, J. L. West, *Biomaterials* **2002,** *23,* 4307-4314.

[10.] D. J. Beebe, J. S. Moore, J. M. Bauer, Q. Yu, R. H. Liu, C. Devadoss, B. H. Jo, *Nature* **2000,** *404,* 588-590.

[11.] J. H. Holtz, S. A. Asher, *Nature* **1997,** *389,* 829-832.

[12.] K. Lee, S. A. Asher, *J. Am. Chem. Soc.* **2000,** *122,* 9534-9537.

[13.] A. Heller, *Phys. Chem. Chem. Phys.* **2004,** *6,* 209-216.

[14.] N. Sahiner, *Colloid Polym Sci* **2006,** *285,* 283-292.

[15.] M. Liu, R. Liang, F. Zhan, Z. Liu, A. Niu, *Polym. Int.* **2007,** *56,* 729-737.

[16.] K. H. Liu, T. Y. Liu, S. Y. Chen, D. M. Liu, *Acta Biomaterialia* **2008,** *4,* 1038-1045.

[17.] P. S. K. Murthy, Y. Murali Mohan, K. Varaprasad, B. Sreedhar, K. Mohana Raju, *J. Colloid Interface Sci.* **2008,** *318,* 217-224.

[18.] N. Ravi, H. A. Aliyar, P. D. Hamilton, *Macromol. Symp.* **2005,** *227,* 191-202.

[19.] M. Kokabi, M. Sirousazar, Z. M. Hassan, *European Polymer Journal* **2007,** *43,* 773-781.

[20.] S. R. Sershen, G. A. Mensing, M. Ng, N. J. Halas, D. J. Beebe, J. L. West, *Adv. Mater.* **2005,** *17,* 1366-1368.

[21.] P. Li, Siddaramaiah, N. H. Kim, S. B. Heo, J. H. Lee, *Composites Part B: Engineering* **2008,** *39,* 756-763.

[22.] N. Sahiner, S. Butun, O. Ozay, B. Dibek, *J. Colloid Interface Sci.* **2012,** *373,* 122-128.

[23.] C. Mo, Z. Shu-quan, L. Hua-Min, H. Zhan-bin, L. Shu-qin, *J. Appl. Polym. Sci.* **2006,** *102,* 5137-5143.

[24.] M. J. Zohuriaan-Mehr, K. Kabiri, *Iranian Polymer Journal* **2008,** *17,* 451-477.

[25.] A. B. Kinney, A. B. Scranton, in *Superabsorbent Polymers*, American Chemical Society, **1994**, 2-26

[26.] K. Kabiri, H. Omidian, M. J. Zohuriaan-Mehr, S. Doroudiani, *Polym Compos* **2011,** *32,* 277-289.

[27.] F. L. Buchholz, *J. Appl. Polym. Sci.* **2006,** *102,* 4075-4084.

[28.] H. Wack, M. Ulbricht, *Ind. Eng. Chem. Res.* **2006,** *46,* 359-364.

[29.] L. Brannon-Peppas, in *Studies in Polymer Science: Absorbent Polymer Technology* (Ed.: Lisa Brannon-Peppas and Ronald S.Harland), Elsevier, **1990**, 45-66

[30.] F. L. Buchholz, in *Studies in Polymer Science: Absorbent Polymer Technology* (Ed.: Lisa Brannon-Peppas and Ronald S.Harland), Elsevier, **1990**, 23-44

[31.] J. Chen, Y. Zhao, *J. Appl. Polym. Sci.* **2000,** *75,* 808-814.

[32.] O. Okay, *Progress in Polymer Science* **2000,** *25,* 711-779.

[33.] K. Dušek, *Angew. Makromol. Chem.* **1996,** *240,* 1-15.

[34.] O. Okay, in *Hydrogel Sensors and Actuators* (Eds.: G. Gerlach, K. F. Arndt), Springer Berlin Heidelberg, **2010**, 1-14

[35.] K. Haraguchi, T. Takehisa, *Adv. Mater.* **2002,** *14,* 1120-1124.

[36.] M. Shibayama, J. Suda, T. Karino, S. Okabe, T. Takehisa, K. Haraguchi, *Macromolecules* **2004,** *37,* 9606-9612.

[37.] K. Haraguchi, H. J. Li, K. Matsuda, T. Takehisa, E. Elliott, *Macromolecules* **2005,** *38,* 3482-3490.

[38.] M. Zendehdel, A. Barati, H. Alikhani, *Polym. Bull.* **2011,** *67,* 343-360.

[39.] W. F. Lee, Y. C. Huang, *J. Appl. Polym. Sci.* **2007,** *106,* 1992-1999.

[40.] K. Shikinaka, Y. Koizumi, Y. Osada, K. Shigehara, *Polym. Adv. Technol.* **2011,** *22,* 1212-1215.

[41.] K. Kabiri, M. J. Zohuriaan-Mehr, *Macromol. Mater. Eng.* **2004,** *289,* 653-661.

[42.] W. F. Lee, L. G. Yang, *J. Appl. Polym. Sci.* **2004,** *92,* 3422-3429.

[43.] W. F. Lee, Y. C. Chen, *European Polymer Journal* **2005,** *41,* 1605-1612.

[44.] J. M. Lin, J. H. Wu, Z. F. Yang, M. L. Pu, *Macromolecular Rapid Communications* **2001,** *22,* 422-424.

[45.] W. Wang, Y. Zheng, A. Wang, *Polym. Adv. Technol.* **2008,** *19,* 1852-1859.

[46.] T. D. Fornes, D. R. Paul, *Polymer* **2003,** *44,* 4993-5013.

[47.] H. M. Smallwood, *J. Appl. Phys.* **1944,** *15,* 758-766.

[48.] Rao, J. M. Pochan, *Macromolecules* **2006,** *40,* 290-296.

[49.] J. C. Halpin, J. L. Kardos, *Polymer Engineering and Science* **1976,** *16,* 344-352.

[50.] R. Hill, *Journal of the Mechanics and Physics of Solids* **1964,** *12,* 199-212.

[51.] J. J. Hermans, *Koninklijke Nederlandse Akademie Van Weteschappen-Proceedings Series B-Physical Sciences* **1967,** *70,* 1-9.

[52.] E. Ruiz-Hitzky, A. Van Meerbeek, in *Developments in Clay Science: Handbook of Clay Science* (Eds.: F. Bergaya, B. K. B. Theng, G. Lagaly), Elsevier, **2006**, 583-621

[53.] K. Kabiri, M. J. Zohuriaan-Mehr, *Polym. Adv. Technol.* **2003,** *14,* 438-444.

[54.] S. Jockusch, N. J. Turro, Y. Mitsukami, M. Matsumoto, T. Iwamura, T. Lindner, A. Flohr, G. di Massimo, *J. Appl. Polym. Sci.* **2009,** *111,* 2163-2170.

[55.] S. Ma, M. Liu, Z. Chen, *J. Appl. Polym. Sci.* **2004,** *93,* 2532-2541.

[56.] W. H. Blackburn, L. A. Lyon, *Colloid Polym Sci* **2008,** *286,* 563-569.

[57.] C. D. Jones, L. A. Lyon, *Macromolecules* **2000,** *33,* 8301-8306.

[58.] V. Lapeyre, C. Ancla, B. Catargi, V. Ravaine, *J. Colloid Interface Sci.* **2008,** *327,* 316-323.

[59.] J. W. Gilman, *Appl. Clay Sci.* **1999,** *15,* 31-49.

[60.] Y. Yang, Z. K. Zhu, J. Yin, X. Y. Wang, Z. E. Qi, *Polymer* **1999,** *40,* 4407-4414.

[61.] W. J. Boo, L. Sun, J. Liu, E. Moghbelli, A. Clearfield, H. J. Sue, H. Pham, N. Verghese, *J. Polym. Sci. B Polym. Phys.* **2007,** *45,* 1459-1469.

[62.] F. Bergaya, B. K. G. Theng, G. Lagaly, *Handbook of Clay Science*, **2006**.

[63.] H. v. Olphen, *An Introduction to Clay Colloid Chemistry*, second edition ed. John Wiley & Sons, **1977**.

[64.] M. Onikata, M. Kondo, N. Hayashi, S. Yamanaka, *Clays Clay Miner.* **1999,** *47,* 672-677.

[65.] W. Loyens, P. Jannasch, F. H. J. Maurer, *Polymer* **2005,** *46,* 915-928.

[66.] Y. Xi, R. L. Frost, H. He, *J. Colloid Interface Sci.* **2007,** *305,* 150-158.

[67.] E. Manias, A. Touny, L. Wu, K. Strawhecker, B. Lu, T. C. Chung, *Chem. Mater.* **2001,** *13,* 3516-3523.

[68.] M. F. Brigatti, E. Galan, B. K. G. Theng, in *Developments in Clay Science: Handbook of Clay Science* (Eds.: F. Bergaya, B. K. G. Theng, G. Lagaly), Elsevier, **2006**, 19-86

[69.] M. Kosmulski, *J. Colloid Interface Sci.* **2004,** *275,* 214-224.

[70.] M. Benna, N. Kbir-Ariguib, A. Magnin, F. Bergaya, *J. Colloid Interface Sci.* **1999,** *218,* 442-455.

[71.] M. Delhorme, B. Jonsson, C. Labbez, *Soft Matter* **2012,** *8,* 9691-9704.

[72.] S. Tazi, B. Rotenberg, M. Salanne, M. Sprik, M. Sulpizi, *Geochim. Cosmochim. Acta* **2012,** *94,* 1-11.

[73.] M. Duc, F. Gaboriaud, F. Thomas, *J. Colloid Interface Sci.* **2005,** *289,* 148-156.

[74.] E. Tombácz, M. Szekeres, *Appl. Clay Sci.* **2004,** *27,* 75-94.

[75.] C. Tournassat, J. M. Greneche, D. Tisserand, L. Charlet, *J. Colloid Interface Sci.* **2004,** *273,* 224-233.

[76.] M. Delhorme, C. Labbez, C. Caillet, F. Thomas, *Langmuir* **2010,** *26,* 9240-9249.

[77.] A. M. L. Kraepiel, K. Keller, F. M. M. Morel, *Environmental Science & Technology* **1998,** *32,* 2829-2838.

[78.] E. Tertre, S. Castet, G. Berger, M. Loubet, E. Giffaut, *Geochim. Cosmochim. Acta* **2006,** *70,* 4579-4599.

[79.] C. Tournassat, E. Ferrage, C. Poinsignon, L. Charlet, *J. Colloid Interface Sci.* **2004,** *273,* 234-246.

[80.] I. C. Bourg, G. Sposito, A. C. M. Bourg, *J. Colloid Interface Sci.* **2007,** *312,* 297-310.

[81.] S. Kaufhold, H. Stanjek, D. P. Ner, R. Dohrmann, *Clay Miner.* **2011,** *46,* 583-592.

[82.] M. Duc, F. Gaboriaud, F. Thomas, *J. Colloid Interface Sci.* **2005,** *289,* 139-147.

[83.] R. B. Secor, C. J. Radke, *J. Colloid Interface Sci.* **1985,** *103,* 237-244.

[84.] F. R. C. Chang, G. Sposito, *J. Colloid Interface Sci.* **1996,** *178,* 555-564.

[85.] M. Rozalén, P. V. Brady, F. J. Huertas, *J. Colloid Interface Sci.* **2009,** *333,* 474-484.

[86.] H. Wanner, Y. Albinsson, O. Karnland, E. Wieland, P. Wersin, L. Charlet, *Radiochim. Acta* **1994,** *66-7,* 157-162.

[87.] G. E. Christidis, *Appl. Clay Sci.* **2008,** *42,* 1-7.

[88.] E. M. Pecini, M. J. Avena, *Langmuir* **2013,** *29,* 14926-14934.

[89.] www.lum-gmbh.com, 29-8-2013.

[90.] www.bareiss.de, 29-8-2013.

[91.] H. Kalo, M. W. Möller, D. A. Kunz, J. Breu, *Nanoscale* **2012,** *4,* 5633-5639.

[92.] L. Ammann, F. Bergaya, G. Lagaly, *Clay Miner.* **2005,** *40,* 441-453.

[93.] M. Ziadeh, B. Chwalka, H. Kalo, M. R. Schütz, J. Breu, *Clay Miner.* **2012,** *47,* 341-353.

[94.] O. P. Mehra, M. L. Jackson, *Clays Clay Miner.* **1958,** 317-327.

[95.] J. Breu, K. J. Range, E. E. Kohler, U. Wagner, *Appl. Clay Sci.* **1993,** *8,* 313-320.

[96.] M. Segad, B. Jönsson, B. Cabane, *J. Phys. Chem. C* **2012,** *116,* 25425-25433.

[97.] M. Segad, S. Hanski, U. Olsson, J. Ruokolainen, T. Åkesson, B. Jönsson, *J. Phys. Chem. C* **2012,** *116,* 7596-7601.

[98.] C. Tournassat, M. Bizi, G. Braibant, C. Crouzet, *J. Colloid Interface Sci.* **2011,** *364,* 443-454.

[99.] N. Öztekin, A. Alemdar, N. Güngör, F. B. Erim, *Materials Letters* **2002,** *55,* 73-76.

[100.] E. Fuente, A. Blanco, C. Negro, M. A. Pelach, P. Mutje, J. Tijero, *Ind. Eng. Chem. Res.* **2005,** *44,* 5616-5621.

[101.] A. Alemdar, N. Öztekin, N. Güngör, Ö. I. Ece, F. B. Erim, *Colloids and Surfaces A: Physicochemical and Engineering Aspects* **2005,** *252,* 95-98.

[102.] G. Sposito, N. T. Skipper, R. Sutton, S. H. Park, A. K. Soper, J. A. Greathouse, *Proceedings Of The National Academy Of Sciences Of The United States Of America* **1999,** *96,* 3358-3364.

[103.] H. Kalo, W. Milius, J. Breu, *Rsc Advances* **2012,** *2,* 8452-8459.

[104.] D. A. Kunz, J. Erath, D. Kluge, H. Thurn, B. Putz, A. Fery, J. Breu, *ACS Appl. Mater. Interfaces* **2013,** *5,* 5851-5855.

[105.] E. A. C. Follett, W. J. McHardy, B. D. Mitchell, B. F. L. Smith, *Clay Miner.* **1965,** *6,* 23-34.

[106.] H. Hayashi, M. Yamada, *Clays Clay Miner.* **1990,** *38,* 308-314.

[107.] P. Komadel, J. Madejová, in *Developments in Clay Science: Handbook of Clay Science* (Eds.: F. Bergaya, B. K. G. Theng, G. Lagaly), Elsevier, **2006**, 263-287

[108.] W. H. Huang, W. D. Keller, *Amer. Mineral.* **1971,** *56,* 1082-&.

[109.] C. J. Wu, A. K. Gaharwar, B. K. Chan, G. Schmidt, *Macromolecules* **2011,** *44,* 8215-8224.

[110.] K. Haraguchi, H. J. Li, *Macromolecules* **2006,** *39,* 1898-1905.

[111.] M. Shibayama, T. Karino, S. Miyazaki, S. Okabe, T. Takehisa, K. Haraguchi, *Macromolecules* **2005,** *38,* 10772-10781.

[112.] L. Xiong, X. Hu, X. Liu, Z. Tong, *Polymer* **2008,** *49,* 5064-5071.

[113.] L. Xiong, M. Zhu, X. Hu, X. Liu, Z. Tong, *Macromolecules* **2009,** *42,* 3811-3817.

[114.] K. Haraguchi, L. Song, *Macromolecules* **2007,** *40,* 5526-5536.

[115.] W. C. Lin, W. Fan, A. Marcellan, D. Hourdet, C. Creton, *Macromolecules* **2010,** *43,* 2554-2563.

[116.] R. O. Ritchie, *Nat Mater* **2011,** *10,* 817-822.

[117.] Y. Liu, M. Zhu, X. Liu, W. Zhang, B. Sun, Y. Chen, H. J. Adler, *Polymer* **2006,** *47,* 1-5.

[118.] O. Okay, W. Oppermann, *Macromolecules* **2007,** *40,* 3378-3387.

[119.] S. Abdurrahmanoglu, V. Can, O. Okay, *J. Appl. Polym. Sci.* **2008,** *109,* 3714-3724.

[120.] T. Wang, D. Liu, C. Lian, S. Zheng, X. Liu, Z. Tong, *Soft Matter* **2012,** *8,* 774-783.

[121.] K. Haraguchi, T. Takehisa, S. Fan, *Macromolecules* **2002,** *35,* 10162-10171.

[122.] J. P. Zheng, P. Li, Y. L. Ma, K. D. Yao, *J. Appl. Polym. Sci.* **2002,** *86,* 1189-1194.

7 Acknowledgements

I would like to thank Prof. Dr. Josef Breu for giving me the opportunity to accomplish my PhD thesis at his chair, for his guidance and advice during my work on a highly interesting subject and for the great change work on a project in cooperation with an industry partner.

I also would like to thank Dr. Mattias Schmidt, Dr. Peter Dziezok and Dr. Arsen Simonyan from Procter & Gamble for the pleasant, constructive collaboration and the inspiring and motivating discussions.

Furthermore, I want to express my gratitude to Wolfgang Milius, Bernd Putz, Beate Bojer, Sonja Lutschinger, Dieter Will, and Lena Geiling. Thank you for your help with every day lab problems, for the scientific advice and the provided support in the laboratory. Great thanks also to Petra Seidler and Iris Raithel for their assistance with bureaucratic paperwork of any kind.

Thanks to my students Sabrina Eller, Christina Wagner, Daniel Forberg, Andreas Schedl, Raphael Kunz and Laura Schwinger for assisting me with the lab work and bringing some diversion to the daily routine.

Special thanks go to my colleagues who accompanied during my work:

Thanks guys of the “rotes Labor”: Michael Möller, Bettina Chwalka, Thomas Lunkenbein, Evgeny Tsurko, Carina Bojer, Patrick Feicht, Mazen Ziadeh and Martin Schieder. Thank you for the fun we had together in the lab, for the numerous times you made me laugh and for all the interesting discussions and your advice.

I also would like to thank Markus Herling and Wolfgang Milius for not only supporting me during the working day but also for the running sessions we spent together many evenings. Thank you, Thomas Martin, for helping with and solving my computer problems. Bashar Diar Bakerly, thank you for always being ready to help and for all the scientific and non-scientific conversations we shared during our “15 minutes of break in the sun”.

Great thanks also to the rest of the group: Daniel Kunz, Jasmin Schmid, Josef Hausner, Matthias Stöter, Hussein Kalo, Andreas Edenharter, Christian Butterhof and Sebastian Koch for always having an open ear and helping hand and for the enjoyable atmosphere.

I also would like to thank everybody else who crossed my way and supported me in some way or another:

Thanks to our barbeque masters Paul Niemietz, Marko Schmidt and Dominik Greim for taking care of sufficient beer, meat, and - most important - coffee supply. Thank you Theresa Winkler, for pushing me on early working days and for all the nice conversations we had while doing our rounds in the "Hofgarten".

Furthermore I would like to thank my friends and housemates from Jean-Paul Str. Sebastian, Niklas, Anne and Andi, thank you for the cooking events, the barbecues, the lazy relaxing moments enjoying the sun in our garden, the parties and all fun we had together.

Thank you, Sven Kochmann, for our daily "conversations", the countless you tube videos that made me laugh, and for your endless creativity when it came to motivate me to finish my work.

I especially would like to thank you, Ricard, for motivating me, for your patience and your continuous support. Thank you for always finding the right words to cheer me up in hard times and for always being there for me.

Finally, I would like to sincerely thank my family for their love and support. Your help and advice made it possible for me to grow the person I am right now and reach this important step in my life.

Thanks also to Procter & Gamble for financial support.

(Eidesstattliche) Versicherungen und Erklärungen

(§ 5 Nr. 4 PromO)

Hiermit erkläre ich, dass keine Tatsachen vorliegen, die mich nach den gesetzlichen Bestimmungen über die Führung akademischer Grade zur Führung eines Doktorgrades unwürdig erscheinen lassen.

(§ 8 S. 2 Nr. 5 PromO)

Hiermit erkläre ich mich damit einverstanden, dass die elektronische Fassung meiner Dissertation unter Wahrung meiner Urheberrechte und des Datenschutzes einer gesonderten Überprüfung hinsichtlich der eigenständigen Anfertigung der Dissertation unterzogen werden kann.

(§ 8 S. 2 Nr. 7 PromO)

Hiermit erkläre ich eidesstattlich, dass ich die Dissertation selbständig verfasst und keine anderen als die von mir angegebenen Quellen und Hilfsmittel benutzt habe.

Ich habe die Dissertation nicht bereits zur Erlangung eines akademischen Grades anderweitig eingereicht und habe auch nicht bereits diese oder eine gleichartige Doktorprüfung endgültig nicht bestanden.

(§ 8 S. 2 Nr. 9 PromO)

Hiermit erkläre ich, dass ich keine Hilfe von gewerblichen Promotionsberatern bzw. -vermittlern in Anspruch genommen habe und auch künftig nicht nehmen werde.

…….

Ort, Datum, Unterschrift